Age-dependent cannabinoid CB_1 receptor plasticity and search for histamine H_4 receptors in the brain

Dissertation

zur

Erlangung des Doktorgrades (Dr. rer. nat.)

der

Mathematisch-Naturwissenschaftlichen Fakultät

der

Rheinischen Friedrich-Wilhelms-Universität Bonn

vorgelegt von

Monika Wanda Feliszek

aus Morąg (Polen)

Bonn 2016

Angefertigt mit Genehmigung der Mathematisch-Naturwissenschaftlichen Fakultät der
Rheinischen Friedrich-Wilhelms-Universität Bonn

1. Gutachter: Prof. Dr. Eberhard Schlicker
2. Gutachter: Prof. Dr. Klaus Mohr

Tag der Promotion: 21.04.2016
Erscheinungsjahr: 2016

Education is the most powerful weapon which you can use to change the world.

Nelson Mandela

List of Abbreviations

% (m/V)	mass/volume percentage
% (V/V)	volume percentage
Δ^9-THC	Δ^9-tetrahydrocannabinol
µ	micro- (10^{-6})
$\bar{x}$	mean value
[x]	x concentration
°C	degree Celsius
2-AG	2-arachidonoylglycerol
^{35}S	sulphur isotope, mass number: 35
A	agonist
a.m.	Latin *ante meridiem*, before noon
AA	arachidonic acid
AC	adenylyl cyclase
ad	up to (Latin)
ADA	adenosine deaminase
AEA	anandamide
ANOVA	analysis of variance
ATP	adenosine triphosphate
A_x	absorbance by wavelength of x (see also: OD)
BCA	bicinchoninic acid
Bp	base pairs
BPB	bromophenol blue
BSA	bovine serum albumine
Ca^{2+}	calcium ion
cAMP	cyclic adenosine monophosphate
CB	cannabinoid
CB_x	cannabinoid receptor, subtype x (1 or 2)
cDNA	complementary DNA (DNA synthesized from a messenger RNA)
$CB_x^{-/-}$	cannabinoid receptor (subtype x) knockout (deficient) mouse
cpm	counts per minute
D_1/D_2	dopamine receptor 1 or 2 families
DAG(L)	diacylglycerol (-lipase)
DMSO	dimethyl sulfoxide
DNA	deoxyribonucleic acid
dpm	disintegrations per minute

e.g.	for example
EC_{50}	half maximal effective concentration
ECS	endocannabinoid system
ECs-dx	deutereted (x= 2, 4, 5 or 8) endocannabinoids analogues
EDTA	ethylenediaminetetraacetic acid
EGTA	ethyleneglycoltetraacetic acid
et al.	Latin et alii, and others
EtBr	ethidium bromide
FAAH	fatty acid amide hydrolase
$FAAH^{-/-}$	fatty acid amide hydrolase knockout (deficient) mouse
FV	functional validation
g	gram
g	gravitational acceleration (9,81 m/s^2)
GABA	gamma-aminobutyric acid
GAPDH	glyceraldehyde 3-phosphate dehydrogenase
GDP	guanosine diphosphate
GP	guinea pig
GPCR	G protein-coupled receptor
GPR 55	novel cannabinoid receptor
G-Protein	guanosine nucleotide – binding protein
GTP	guanosine triphosphate
GTPγS	guanosine 5'-O-[gamma-thio]triphosphate
GTPγS Li_4	guanosine 5'-O-[gamma-thio]triphosphate tetralithium salt
GTPase	GTP hydrolase
h	hour
H_2O	water
H_x	histamine receptor, Subtype x
Hz	Hertz
IC_{50}	half maximal inhibitory concentration
INCB	International Narcotics Control Board
i.p.	intraperitoneal injection
ISTDs	internal standards
i.v.	intravenous injection
k	kilo- (10^3)
k	reaction rate constant
K^+	potassium ion

K_D	dissociation constant
L	litre
LC-MRM	liquid chromatography – multiple reaction monitoring
LC-MS/MS	liquid chromatography – tandem mass spectrometry
log	logarithm
LTP	long-term potentiation
m	metre
m	milli- (10^{-3})
M	molar (mol/L)
MAEA	methanandamide
MAGL	monoacylglycerol lipase
MAPK	mitogen-activated protein kinase
MDB	membrane desalting buffer (NucleoSpin®)
min	minute
mol	mole
mRNA	messenger RNA
MS	Multiple Sclerosis
MT/DW 96	microtiter/deep well plate, 96-wells
MW	molecular weight (g/mol)
n	nano- (10^{-9})
n	number of experiments or measurements
NAAA	N-acylethanolamine-hydrolysing acid amidase
NAPE-PLD	N-acylphosphatidylethanolamine-hydrolysing phospholipase
NAT	N-acyltransferase
OD	optical density, absorbance (see also: A_x)
OEA	deuterated analogue of oleylethanolamide
OEA	oleylethanolamide
OFT	Open Field Test
p	negative logarithm
p	probability of error
p.m.	Latin *post meridiem*, after noon
PA	phosphatidic acid
pA_2	potency of antagonist
PBS	phosphate buffered saline
PC	phosphatidylcholine
PCR	polymerase chain reaction

PE	phosphatidylethanolaminde
PEA	palmitoylethanolamide
pH	*potentia Hydrogenii*, negative logarithm of the activity of the hydronium ion
P_i	inorganic phosphate
PI	phosphatidylinositol
PLC	phospholipase C
RA1	lysis buffer (NucleoSpin®)
RA3	wash buffer (NucleoSpin®)
RAW2	wash buffer (NucleoSpin®)
rDNase	recombinant deoxyribonuklease
RNA	ribonucleic acid
RNase	ribonuklease
rpm	rounds per minute
RT	reverse transcriptase
s	second
s	standard deviation (see also SD)
s.c.	subcutaneous injection
SD	standard deviation (see also s)
SEM	standard error of the mean
Taq	*Thermophilus aquaticus*
TBE	Tris/borate/EDTA buffer
TE	Tris-EDTA buffer
Tris	tris(hydroxymethyl)aminomethane
U	unit
UV	ultraviolet
V	volt
WHO	World Health Organisation
WT	wild type

Table of contents

A. Introduction

This thesis is dedicated to two G protein-coupled receptors (GPCRs), namely the cannabinoid CB_1 (A.1 – A.2) and the histamine H_4 receptor (A.3). The CB_1 receptor forms a part of the endocannabinoid system (A.2), which plays an important role in the brain and is activated by Δ^9-tetrahydrocannabinol (Δ^9-THC; A.1), one of the major constituents of hashish and marijuana. The H_4 receptor (A.3) mainly occurs in immune cells; whether it plays a role also in the brain is matter of debate.

1. Δ^9-THC

The main psychoactive ingredient of the *Cannabis sativa* plant is Δ^9-THC (for chemical structure see Table 2). Even though the cannabis plant and its effects have been known and used recreationally or curatively since ancient times, the compound responsible for its psychoactive effects, Δ^9-THC, remained undiscovered till the early 1960s (Greydanus et al. 2013). The other components of the endocannabinoid system were discovered two decades later and even to this day, the endocannabinoid system is not completely understood (Mechoulam and Parker 2013). The properties of cannabis and Δ^9-THC, including their therapeutic potential and negative effects, were described in hundreds of papers.

Briefly, the use of marijuana (*Cannabis sativa* plant preparation) by humans and in laboratory animals impairs cognition and working memory, causes euphoria or sedation, sleepiness, dizziness, mood alterations, tachycardia and immune modulation; its analgesic, anti-emetic, appetite-stimulant and muscle relaxant effects were considered as therapeutic actions (Hollister 1986). Due to its antispastic and analgesic activity Δ^9-THC is used therapeutically in several countries under the trade name *Sativex* (international non-proprietary name: nabiximols; an oromucosal spray consisting of Δ^9-THC and cannabidiol) against neuropathic pain and spasticity in *Multiple Sclerosis* patients (Vermersch 2011; Robson 2014). The use of Δ^9-THC or its synthetic derivative nabilone was reported to be effective in the clinic against nausea and vomiting, especially when associated with chemotherapy. Other possible applications of “medicinal marijuana” are still discussed (Di Marzo and Petrocellis 2006; Grotenhermen and Müller-Vahl 2012; Greydanus et al. 2013; Robson 2014).

The common therapeutic use of marijuana is hindered by many facts such as its adverse effects which, especially in adolescent, chronic users, include an increased risk to develop a mental illness or cognitive disorder (Di Forti et al. 2007; Boyce and McArdle 2008; Rubino et al. 2012;

Renard et al. 2014; Lubman et al. 2015), its addictive potential (Hall and Degenhardt 2013), its possible role as a "gateway drug" (Volkow et al. 2014) and the fact that marijuana is the most commonly used illicit drug in the world mainly in young people (Greydanus et al. 2013; Renard et al. 2014). Hence, cannabis and its preparations are subject to the Single Convention on Narcotic Drugs and are listed in the Yellow List, a strict international regulatory agreement to prohibit and control drugs of abuse (INCB 2013). Nevertheless, the investigation of the effects of Δ^9-THC was a driving force for the development of indirect ways to activate the endocannabinoid system.

1.1 Δ^9-THC tolerance development

The abuse potential of Δ^9-THC observed in humans and confirmed in animals is one of the major issues speaking against the therapeutic use of cannabinoids (Ramesh et al. 2011; Volkow et al. 2014). Tolerance development after long-term Δ^9-THC treatment is known to occur in humans and was investigated in detail in animal studies in terms of brain region, dose and time-course (Zhuang et al. 1998; Bass and Martin 2000; McKinney et al. 2008). The mechanism of cannabinoid tolerance which is CB_1 receptor-dependent (Martin et al. 2004) still needs to be better understood; however, several signalling pathways and biological processes involved in tolerance development are already known. Chronic exposure of GPCRs to an agonist can result in several receptor adaptations: GPCR desensitization which occurs as a consequence of receptor phosphorylation resulting in uncoupling of G protein and receptor. Further adaptive processes comprise receptor down-regulation (decrease of receptor number) with receptor degradation (Tsao and von Zastrow 2000) and sequestration of the receptor from the cell surface, a mechanism termed internalization (Ferguson and Caron 1998; Roth et al. 1998). All these mechanisms may occur depending on the brain region and treatment model, hence, the regional differences of receptor changes may explain different behavioural responses to cannabinoids of laboratory animals (Martin et al. 2004; González et al. 2005). As described in section B.2.3.1 below, the ^{35}S-GTPγS binding assay directly measures the G protein response to receptor activation, which makes it an optimal method to measure receptor desensitization after chronic cannabinoid treatment.

1.2 Does aging influence Δ^9-THC tolerance development?

The age of the subject exposed to Δ^9-THC is an essential factor which influences the acute Δ^9-THC effects as well as tolerance phenomena both in humans and animals (for research

reports see Cha et al. 2006; Schramm-Sapyta et al. 2007; Swartzwelder et al. 2012; for reviews see: González et al. 2005; Rubino and Parolaro 2008; Realini et al. 2009; Renard et al. 2014; Lubman et al. 2014). Adolescence in humans (the lifetime period from 12 to 17 years) is characterized by strong neurobehavioural plasticity and represents a critical period for brain development. Numerous maturation processes in the central nervous system take place, e.g. neuronal maturation, synaptic pruning, myelination, volumetric growth and changes in receptor distribution; many of these processes are influenced by the endocannabinoid system (Renard et al. 2014). Therefore, particularly during this period of dynamic neurological changes intensified activation of the cannabinoid system e.g. through cannabinoid consumption, can lead to alterations in the brain and long-lasting consequences (Renard et al. 2014; Lubman et al. 2015).

Further examples of differential responses of the endocannabinoid system depending on age were provided by experiments on animals. As shown by Cha et al. (2006), adult rats chronically treated with Δ^9-THC and tested for spatial and non-spatial learning in the water maze, performed better than adolescent animals treated in the same manner. Accordingly Schramm-Sapyta et al. (2007) from the same laboratory argue that this difference is related to the strong addictive potential of Δ^9-THC at a young age. Anxiety and aversion, known as undesirable effects of marijuana (and acute Δ^9-THC treatment), were decreased in behavioural tests in adolescent rats whereas the inhibitory effect of Δ^9-THC on locomotion was stronger in adult than in adolescent animals. Further analysis regarding the differential effects of Δ^9-THC treatment in adolescent and adult rats in behavioural tests and receptor level measurement was provided by Moore et al. (2010). In this research report, the functional coupling of CB_1 receptors to $G_{\alpha i/o}$ protein was lower in adult than in adolescent rats after chronic Δ^9-THC treatment although CB_1 receptor number and distribution did not differ. In harmony with these data, ^{35}S-GTPγS binding activated by the cannabinoid CB_1 receptor agonist WIN 55,212-2 indicated lower receptor desensitization in adolescent than in adult animals.

This thesis focuses on Δ^9-THC tolerance development in adolescent and aged mice using behavioural and ^{35}S-GTPγS receptor-binding experiments and provides further evidence for age-dependent differential responses of the endocannabinoid system.

2. Endocannabinoid system

2.1 Introduction to the endocannabinoid system

Components of the endocannabinoid system

The endocannabinoid system is a dynamic complex of cannabinoid receptors, their endogenous lipid ligands and the enzymes involved in production and degradation of these ligands (Battista et al. 2012) as schematically presented in Figure 1. The two cannabinoid receptors, CB_1 and CB_2, belong to the G protein-coupled receptor superfamily and interact with endogenous ligands. These ligands are lipophilic substances of which anandamide and 2 AG are the best characterized ones (Mechoulam et al. 1998). The dynamic character and homeostasis of the endocannabinoid system is provided by the enzymes involved in the biosynthesis (Wang and Ueda 2009) and degradation (Basavarajappa 2007; Chanda et al. 2010) of the endogenous ligands.

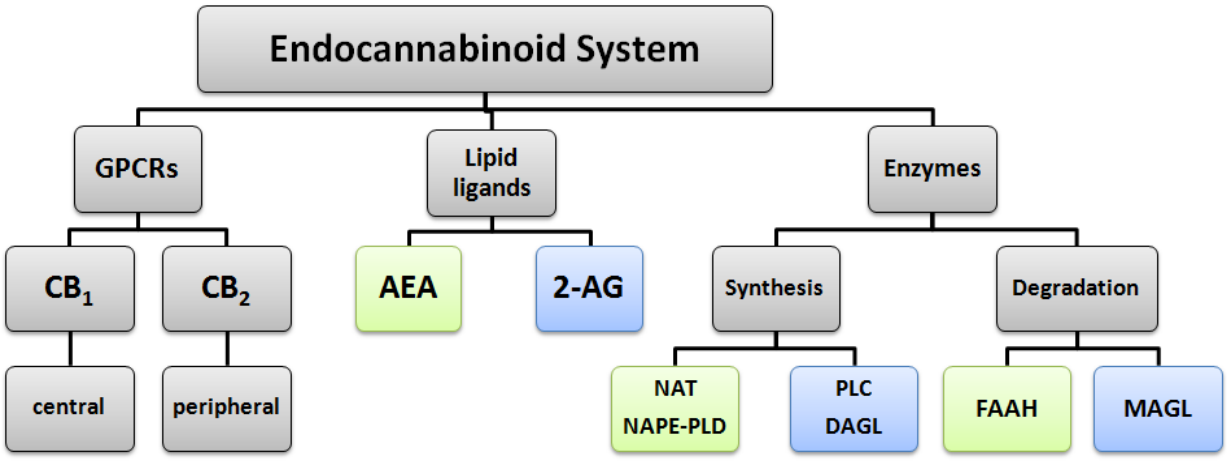

Figure 1. The main components of the endocannabinoid system. The same background colour (green and blue) has been used for the lipid ligands and the respective enzymes involved in their synthesis and degradation. 2-AG – 2-arachidonoylglycerol, AEA - anandamide, DAGL – diacylglycerol lipase, FAAH – fatty acid amide hydrolase, GPCRs – G protein-coupled receptors, MAGL – monoacylglycerol lipase, NAPE-PLD – N-acylphosphatidylethanolamine-hydrolysing phospholipase D, NAT – N-acetyltransferase, PLC – phospholipase C.

2.1.1 Cannabinoid receptors

Cannabinoid receptor types

The two cannabinoid receptors CB_1 and CB_2 were characterized in detail over the past decades. The CB_1 receptor cloned by Matsuda et al. (1990) and the CB_2 receptor cloned by Munro et al. (1993) exhibit 48 % of genetic homology. Both receptors are coupled to $G_{i/o}$ protein, thereby inhibiting the conversion of ATP to cAMP by adenylyl cyclases and activating mitogen-activated protein kinase (MAPK) pathways. The CB_1 receptor also influences some types of potassium and calcium channels (as shown in Figure 2; for review see: Howlett et al. 2002). The resemblance of the cannabinoid receptor type 1 and 2 results in responses with similar potency to exogenous ligands, such as Δ^9-THC, WIN 55,212-2, CP 55 940 or the endogenous agonists anandamide (AEA) and 2-AG (see Felder et al. 1995; for structures see Table 2). In addition to the differences in amino acid sequence, the CB_1 and CB_2 receptors have different tissue distributions and different signalling mechanisms. While CB_1 receptors are expressed presynaptically at terminals of the central and peripheral nervous system causing inhibition of neurotransmitter release (Schlicker and Kathmann 2001; Szabo and Schlicker 2005), the CB_2 receptors are located mainly on the cells of the hematopoietic system and modulate the immune response by modulation of cytokine release and migration of immune cells (Malfitano et al. 2014). Although the CB_1 receptor is one of the most widely expressed GPCRs in the CNS (Herkenham et al. 1990), its expression in non-neuronal tissues, such as spleen, was also described (Howlett et al. 2002). On the other hand, contradictory results were published regarding the expression of the CB_2 receptor in the CNS and this issue remains controversial (Gong et al. 2006; Ashton et al. 2006; Atwood and Mackie 2010; Onaivi 2011; Onaivi et al. 2012; Baek et al. 2013). Due to its expression in the immune system, the CB_2 receptor is investigated as a potential target for the treatment of inflammatory diseases and pain (Klein 2005).

There may be further, non-CB_1/CB_2 cannabinoid receptors. The orphan G protein-coupled receptor GPR55 was discovered in human striatum and other brain regions by Sawzdargo et al. (1999) and later classified as a novel cannabinoid receptor (Ryberg et al. 2007) based on its ^{35}S-GTPγS binding activation by the cannabinoids. On the other hand, the fact that GPR55 is not activated by the potent cannabinoid agonist WIN 55,212-2 (Ryberg et al. 2007) casts some doubt on its classification as a cannabinoid receptor. The distribution and physiology of GPR55 remains to be further investigated.

Cannabinoid receptor agonists

The agonists of the cannabinoid receptors (for chemical structures see Table 2) are commonly classified in four main groups according to their chemical structures (Childers and Breivogel 1998) as listed in Table 1.

Group	Chemical structure	Representative compound(s)	Origin
I – Classical cannabinoids	dibenzopyran	Δ^9-THC	plant-derived
II – Non-classical cannabinoids	bi- and tri-cycle analogs of Δ^9-THC, without pyran ring	CP 55,940	synthetic
III – Aminoalkylindoles	aminoalkylindoles	WIN 55,212-2	synthetic
IV– Eicosanoid group (endocannabinoids)	derivatives of arachidonic acid	2-AG, AEA	endogenous

Table 1. Classification of the cannabinoid receptor ligands (agonists) based on their chemical structure (Childers and Breivogel 1998). For chemical structures of the five compounds, see Table 2.

The representative cannabinoid receptor agonist is Δ^9-THC, a partial agonist at both cannabinoid receptors (Pertwee et al. 2010). It belongs to the classical cannabinoid group and is the main psychoactive component of marijuana (*Cannabis sativa)*. Since Δ^9-THC was used in the experimental part of this thesis, a separate part of the introduction (see section A.1) was dedicated to Δ^9-THC and its activity, its medical and non-medical applications and risks.

The non-classical cannabinoid CP 55,940 and WIN 55,212-2, the representative of the group III, act as potent (but not selective) cannabinoid receptor agonists and are not clinically used as opposed to the active components of marijuana (Δ^9-THC or cannabidiol). Nevertheless, many of the synthetic cannabinoids have implications in experimental pharmacology. CP 55,940 and WIN 55,212-2 are widely used in animal models both *in vitro* and *in vivo* because of their affinity to CB_1 and CB_2 receptors in the low nanomolar range and their relatively high efficacy at both receptor types (Pertwee and Ross 2002). These synthetic ligands, as well as Δ^9-THC, produce characteristic, behavioural effects in animals, including the so-called tetrad test for cannabinoid activity. The tetrad includes hypothermia, analgesia, hypoactivity, and catalepsy (reviewed by Chaperon and Thiébot 1999).

The fourth class of cannabinoids, the eicosanoid group, consists of arachidonic acid derivatives which are endogenous, highly lipophilic substances. The most investigated ones are AEA and 2-AG (Mechoulam et al. 1998). AEA (anandamide) was primarily found in brain tissue and later also in other organs. It is a partial agonist of the CB_1 receptor and a partial agonist with very low intrinsic activity of the CB_2 receptor (Pertwee et al. 2010). AEA administered i.p. to rodents mimics the effects caused by Δ^9-THC administration (Fride and Mechoulam 1993). The second endocannabinoid, 2-AG (2-arachidonoylglycerol), was found in numerous tissues in significantly higher concentrations than AEA, with the highest concentration in the nervous system (Sugiura et al. 2002). It is a full agonist at both types of cannabinoid receptors with a slightly lower affinity to the CB_2 receptor (Pertwee et al. 2010). The biosynthesis and degradation of AEA and 2-AG, the key processes, that maintain the integrity of the endocannabinoid system, are discussed in the following sections.

Origin	Structure	MW [g/mol]	Function
Plant origin, exogenous	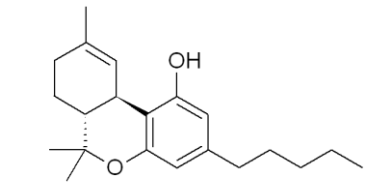 Δ^9-Tetrahydrocannabinol	314.47	Non-selective CB_1 and CB_2 partial agonist
Synthetic, exogenous	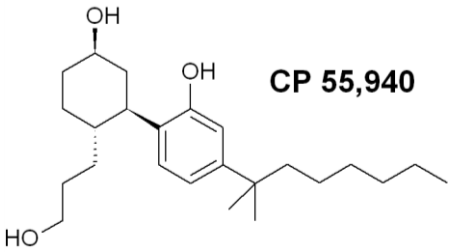 CP 55,940	376.57	Non-selective CB_1 and CB_2 full agonist
	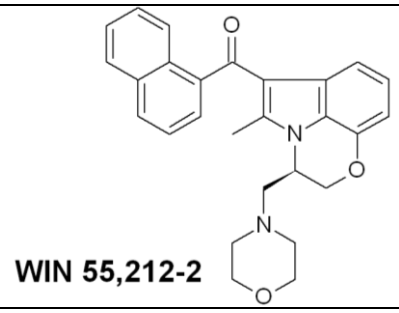 WIN 55,212-2	522.61	Non-selective CB_1 and CB_2 full agonist
Endogenous	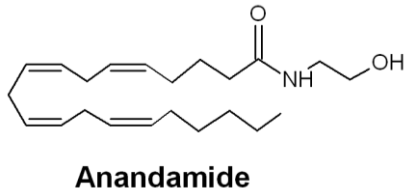 Anandamide	347.53	Non-selective CB_1 and CB_2 partial agonist
	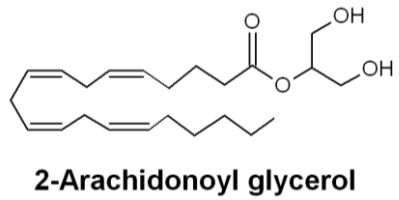 2-Arachidonoyl glycerol	378.6	Non-selective CB_1 and CB_2 full agonist

Table 2. Chemical structures, molecular weights and receptor interactions of five representative cannabinoid receptor agonists.

2.1.2 Enzymes involved in endocannabinoid synthesis and degradation

The optimal balance within the endocannabinoid system is provided by the enzymes involved in biosynthesis and degradation of the endocannabinoids. Figure 2 presents the main pathways of endocannabinoid metabolism in neuron. Although anandamide and 2-AG share numerous chemical and physiological properties and activate the same receptors, the biosynthesis and degradation of these lipid molecules is controlled by different enzymatic pathways, as described below in detail.

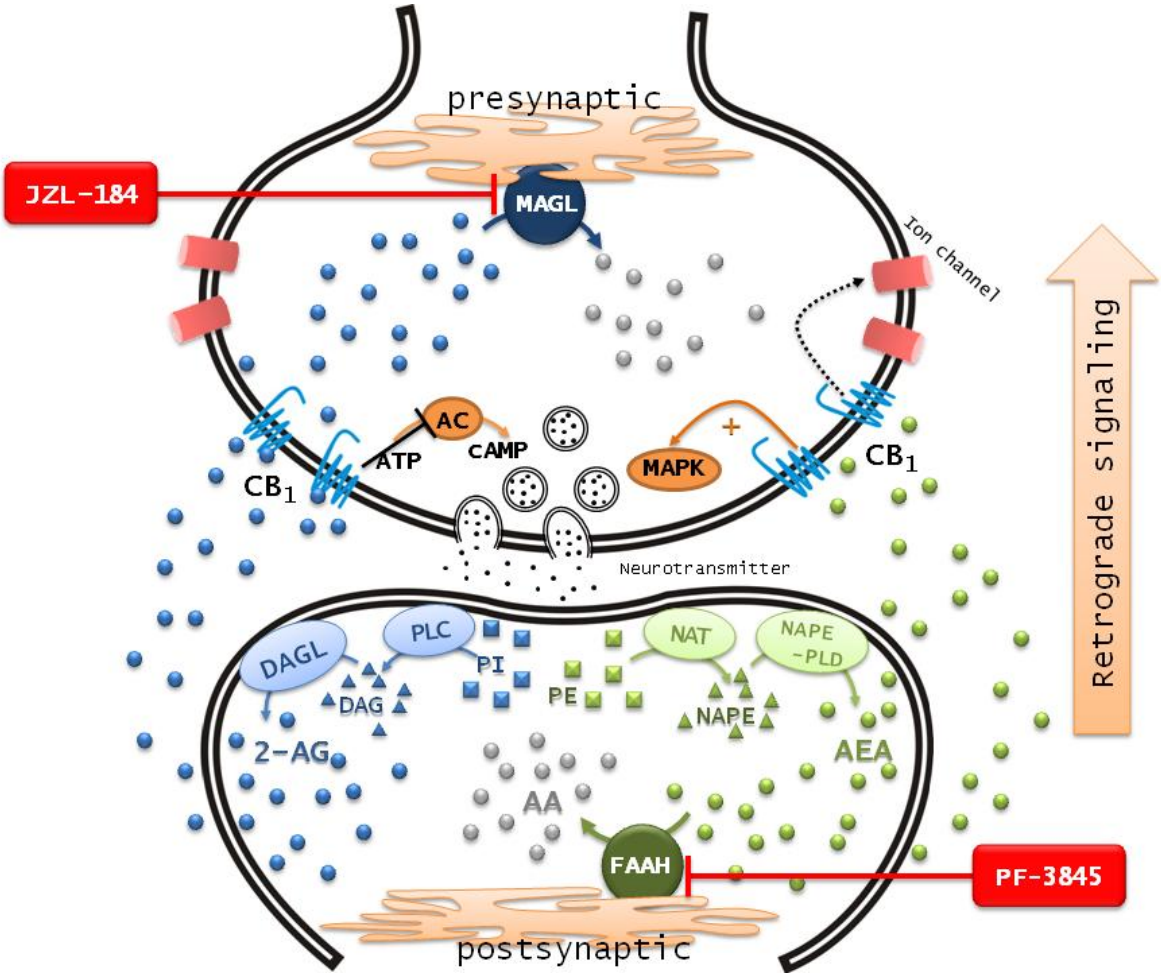

Figure 2. Mechanisms involved in retrograde signalling in neurons and CB_1 receptor functions. CB_1 receptor activation caused by the endocannabinoids AEA and 2-AG inhibits cAMP production by AC, regulates channels for K^+ and Ca^{2+} ions, inhibits neurotransmitter release to the synaptic cleft and activates MAPK (Howlett 2002). The concentration of AEA and 2-AG is controlled by "on demand" synthesis and degradation. The synthesis of AEA and 2-AG takes place in the postsynaptic neuron. Endocannabinoids are transported through the neuronal membrane and activate CB_1 receptors. The enzymes PLC and DAGL are involved in the synthesis of 2-AG whereas NAT and NAPE-PLD take part in the AEA production. FAAH (postsynaptic) and MAGL (presynaptic) hydrolyse AEA and 2-AG, respectively (Blankman et al. 2007). The FAAH inhibitor PF-3848 blocks the degradation of AEA and increases its concentration (Ahn et al. 2009) whereas JZL 184 is a potent and selective MAGL inhibitor which increases 2-AG levels (Long et al. 2009a; 2009b). 2-AG – 2-arachidonoylglycerol, AA – arachidonic acid, AC – adenylyl cyclase, AEA – anandamide, ATP – adenosine triphosphate, cAMP – cyclic adenosine monophosphate, DAG - diacylglycerol, DAGL – diacylglycerol lipase, FAAH – fatty acid amide hydrolase, MAGL – monoacylglycerol lipase, MAPK – mitogen-activated protein kinase, NAPE - N-acylphosphatidylethanolamine, NAPE-PLD – N-acylphosphatidylethanolamine hydrolysing phospholipase D, NAT – N-acetyltransferase, PE – phosphatidylethanolamine, PI - phosphatidylinositol, PLC – phospholipase C. Figure adapted and modified from Ahn et al. (2008).

Endocannabinoid synthesis – process "on demand"

Endocannabinoids are synthesized from membrane phospholipids at the moment of their intended action ("on demand"), contrary to neurotransmitters or neuropeptides which are stored in cell vesicles (Piomelli 2003; Ahn et al. 2008; Wang and Ueda 2009). More recent studies reported that endocannabinoids, mainly AEA, can be also stored in the lipid droplets in the cells (reviewed and discussed by Maccarrone et al. 2010; Min et al. 2010; Fezza et al. 2014), however, this hypothesis awaits further investigation.

As shown in Figure 3, the pathway of AEA formation (the so-called "transacylation-phosphodiesterase pathway") consists of two major steps. The enzymes involved in this process are N-acyltransferase (NAT) and N-acylphosphatidylethanolamine-hydrolysing phospholipase D (NAPE-PLD). In the first step, NAT catalyses the reaction of phosphatidylethanolamine (PE) with 1-arachidonoyl-phosphatidylcholine (PC); by this reaction N-arachidonoyl-PE (and lyso PC as by-product) are formed. In the second step, NAPE-PLD hydrolyses N-arachidonoyl-PE to AEA and phosphatidic acid (PA). Alternative routes of anandamide biosynthesis e.g. studied on NAPE-PLD knockout mice (NAPE-PLD$^{-/-}$), were also reported (for review see: Wang and Ueda 2009 and Ahn et al. 2008).

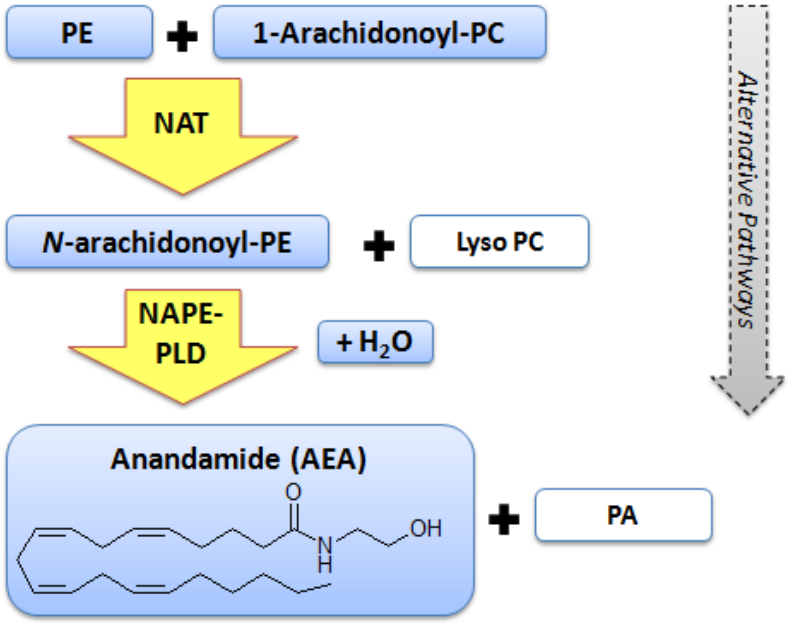

Figure 3. Biosynthesis of anandamide (AEA), "the transacylation-phosphodiesterase pathway". AEA is formed in two steps catalyzed by NAT and NAPE-PLD. NAPE-PLD – N-acylphosphatidylethanolamine-hydrolysing phospholipase D; NAT – N-acyltransferase; PA – phosphatidic acid; PC – phosphatidylcholine; PE- phosphatidylethanolamine. Modified from Wang and Ueda (2009).

The biosynthesis of 2-AG is presented in Figure 4. This process is mediated by the membrane enzymes phospholipase C (PLC) and diacylglycerol lipase (DAGL). PLC catalyses hydrolysis of phosphatidylinositol (PI) to give diacylglycerol (DAG) and inositol 1-phosphate. In the second step 2-AG and fatty acid are formed by DAGL (Ahn et al. 2008; Wang and Ueda 2009). The research on DAGL deficient mice provided evidence that DAGL activity and the 2-AG molecule are essential for retrograde signalling at synapses (Gao et al. 2010; Tanimura et al. 2010). Alternative biosynthesis pathways of 2-AG may also occur and are not described in detail (for reviews see Sugiura et al. 2006 and Murataeva et al. 2014).

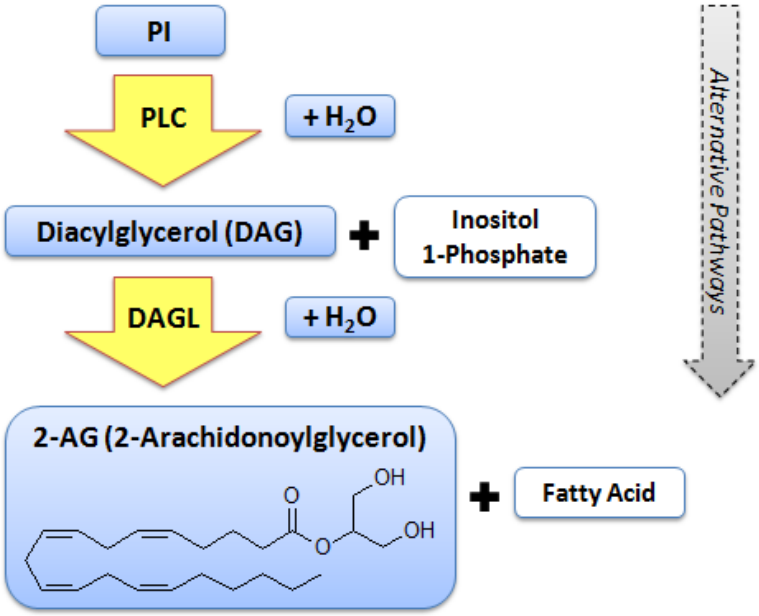

Figure 4. Biosynthesis of 2-arachidonoylglycerol (2-AG). In a two-step reaction catalyzed by the lipases PLC and DAGL, 2-AG is formed. PI – phosphatidylinositol; PLC- phospholipase C; DAGL – diacylglycerol lipase. Modified from Wang and Ueda (2009).

Endocannabinoid degradation

As illustrated in Figure 2, after biosynthesis in the postsynaptic neurons, endocannabinoids are released to the synaptic cleft and migrate to cannabinoid receptors. Complex processes are involved in the endocannabinoid transport mechanism (Ehehalt et al. 2006; Ahn et al. 2008). The cannabinoid receptors activated by the endocannabinoids trigger the signalling cascade and regulate ion channels and neurotransmitter release. After cellular uptake, two endocannabinoid-degrading enzymes, namely the postsynaptically located fatty acid amide hydrolase (FAAH) and the presynaptically located monoacylglycerol lipase (MAGL) hydrolyse anandamide and 2-AG, respectively, and terminate the retrograde signalling of the endocannabinoids (Piomelli 2003;

Ahn et al. 2008). The enzymes FAAH and MAGL play a crucial role as regulators of the endocannabinoid levels in the tissues.

The main enzyme involved in the degradation of anandamide is FAAH (recently re-named FAAH-1). Another two degrading enzymes with minor importance for the tissue levels of AEA, namely NAAA (reviewed by Ueda et al. 2010) and an isoform of FAAH-1 termed FAAH-2 (Cravatt et al. 2001) were described as well. The scheme of AEA degradation is presented in Figure 5. The major metabolic pathway involves FAAH-1 activity in which AEA is hydrolysed and arachidonic acid and ethanolamine are the degradation products. NAAA hydrolyses AEA to the same degradation products, however, its role is still poorly understood (Ueda et al. 2010).

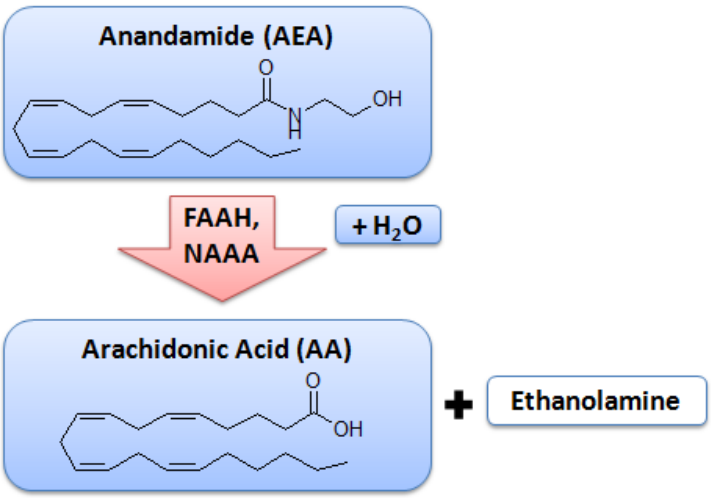

Figure 5. Degradation of anandamide by FAAH and/or NAAA. FAAH – fatty acid amide hydrolase; NAAA – N-acylethanolamine-hydrolysing acid amidase. Modified from Wang and Ueda (2009).

The chemical structures of AEA and 2-AG are similar and this led to the hypothesis that these two endocannabinoids could share the same enzyme during degradation. The involvement of FAAH in 2-AG hydrolysis *in vitro* was reported by Goparaju et al. (1998). Further investigation showed that 2-AG is not degraded by FAAH enzyme *in vivo* (Lichtman et al. 2002). Goparaju et al. (1999) investigated the potential involvement of MAGL in 2-AG degradation; the role of MAGL in 2-AG hydrolysis in the brain was reported by Dinh et al. (2002). The same authors described high levels of MAGL in the CNS and found decreased 2-AG levels in MAGL-overexpressing neuronal cells. MAGL inhibitors such as URB602 provide further evidence about the role of MAGL in the degradation process of 2-AG (Makara et al. 2005). Subsequently, JZL 184 (for chemical structure see Table 3) was reported as a potent and highly selective MAGL inhibitor (Long et al. 2009b) and finally, the development of the MAGL knockout mouse

(MAGL$^{-/-}$) confirmed the substantial role of MAGL in the regulation of the 2-AG levels (Chanda et al. 2010). Although further enzymes involved in 2-AG degradation were discovered (Blankman et al. 2007), the major role of MAGL is beyond any doubt (Murataeva et al. 2014).

The degradation of 2-AG by MAGL is presented in Figure 6. MAGL hydrolyses 2-AG to arachidonic acid and glycerol.

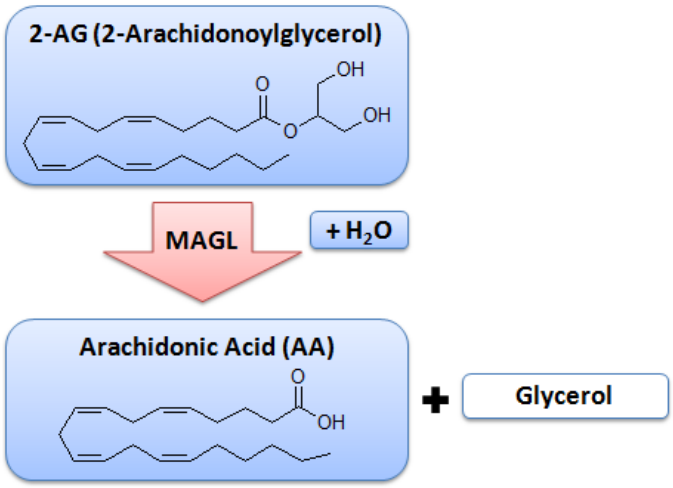

Figure 6. Degradation of 2-AG by MAGL (monoacylglycerol lipase). Modified from Wang and Ueda (2009).

Type	Structure	MW [g/mol]	Function
Synthetic	JZL 184	520.49	Non-competitive irreversible MAGL inhibitor

Table 3. Chemical structure and molecular weight of the MAGL inhibitor JZL 184.

The indirect activation of the endocannabinoid system - a potential therapeutic target

The use of Δ^9-THC as a therapeutic agent was discussed in section A.1. Targeting the receptor through its ligand seems to be the most direct and simple strategy in a search for new therapeutic agents. Nevertheless, the discovery of highly selective and potent inhibitors of the endocannabinoid degrading enzymes, such as PF-3845 for FAAH (Ahn et al. 2009;

Tchantchou et al. 2014) and JZL 184 for MAGL (Long et al. 2009a; 2009b), opened new horizons for the endocannabinoid system as a therapeutic target.

Since one of the subjects of this thesis is the effect of different doses of JZL 184 on endocannabinoid levels and CB_1 receptor adaptation in mouse hippocampus, the rest of this section will describe the effects of MAGL (but not of FAAH) inhibitors.

JZL 184 was developed in Cravatt's laboratory by Long et al. (2009a) using activity-based proteomic methods (for the chemical structure of JZL 184, see Table 3). The properties of JZL 184, such as its (i) high potency (causing significant elevation of 2-AG concentrations also *in vivo*), (ii) selectivity (no effect on AEA concentration), (iii) rapid and sustained action (elevation of 2-AG levels over at least 8 h) and (iiii) ability to evoke CB_1-dependent behavioural effects (as reported by Long et al. 2009a), made this compound a breakthrough in the research on MAGL and its role in the 2-AG mediated signalling.

MAGL may have a therapeutic potential for a number of diseases and disorders (Fowler 2012; Mulvihill and Nomura 2013; Pertwee 2014). Considering the regulatory functions of the endocannabinoid system on pain sensation, inflammation, memory and appetite (Di Marzo 2009), an increased 2-AG concentration through MAGL blockade may be useful for the treatment of pain and inflammation (Kinsey et al. 2009; 2010; Ghosh et al. 2013; Ulugöl 2014), neurodegenerative diseases (Centonze et al. 2007; Chen et al. 2012; Bilkei-Gorzo 2012; Aso and Ferrer 2014), anxiety-related disorders (Sciolino et al. 2011) or obesity and metabolic disorders (Silvestri and Di Marzo 2013; D'Addario et al. 2014). Moreover, MAGL blockade was shown to slow cancer cell migration, invasiveness and tumorigenicity in several cancer types (Mulvihill and Nomura 2013).

Although JZL 184 administration to mice induces endocannabinoid-mediated behavioural effects in the tetrad test for cannabinoid activity (analgesia, hypomotility, hypothermia and catalepsy; Chaperon and Thiébot 1999; Wiley and Martin 2003), the effects of long-term administration of JZL 184 were surprisingly different from those due to acute/single administration. The MAGL-deficient mouse ($MAGL^{-/-}$; Chanda et al. 2010) with permanent elevation of 2-AG levels did not show dramatic changes of the behaviour without treatment although the behavioural response after WIN 55,212-2 treatment was decreased. The density and agonist-mediated signalling of the CB_1 receptors were reduced in MAGL knockout mice, however, no changes in CB_1 receptor mRNA levels were found (Chanda et al. 2010). A further question in this context was, whether the effects of the long-term pharmacological blockade of MAGL activity in mice are comparable with the profile of $MAGL^{-/-}$ mice. Schlosburg et al. (2010) showed a functional

antagonism of the endocannabinoid system occurring after chronic JZL 184 treatment (40 mg/kg JZL 184, i.p. administration for 6 days). The mice exhibited tolerance to the CB_1 agonist-mediated effects in the behavioural pain assay. The *in vivo* experiments were confirmed by *in vitro* studies in which CB_1 receptor desensitization was observed, among others in radioligand [^{3}H]-SR141716A binding and in cannabinoid receptor-activated ^{35}S-GTPγS receptor binding and ^{35}S-GTPγS binding autoradiography.

Surprisingly, further experiments in MAGL$^{-/-}$ mice showed, that contrary to the administration of synthetic cannabinoid receptor agonists which cause deficits in memory, attention and cognition in human and in animals (Hall and Degenhardt 2009; Zanettini et al. 2011; Skosnik et al. 2012; Mechoulam and Parker 2013), the permanent increase in 2-AG occurring in MAGL$^{-/-}$ mice was associated with an improved performance in learning and cognition in behavioural tests (Pan et al. 2011). Additionally, the hippocampal long term potentiation (LTP) of synaptic transmission, supposed to be a cellular model of learning and memory (Bliss and Collingridge 1993), was enhanced in MAGL$^{-/-}$ mice, whereas synthetic cannabinoids caused suppression of the LTP in the hippocampus *in vitro* (Hoffman et al. 2007) and *in vivo* (Hill et al. 2004). The discrepancies point to a complex, dual nature of the endocannabinoid system (Sarne et al. 2011), which leaves an urgent need for further research to fully understand the character of this system.

In several diseases, up-regulation of the endocannabinoid system serves as an autoprotective mechanism which reduces unwanted pathological effects or even slows the disease progression (Pertwee 2014). Several pieces of evidence for the neuroprotective character of the endocannabinoids make indirect strategies of endocannabinoid system activation a promising target for the treatment of a number of diseases and disorders (Parolaro et al. 2010; Pertwee 2014). In this thesis, I investigated the influence of various doses of JZL 184 on endocannabinoid levels and CB_1 receptor function as determined in ^{35}S-GTPγS binding experiments.

2.2 Alterations of the endocannabinoid system with age

The involvement of the endocannabinoid system in aging was investigated among others by Bilkei-Gorzo and co-workers (reviewed by Bilkei-Gorzo 2012). They found that the lack of the CB_1 receptor is associated with an early onset of cognitive/learning impairment and neuronal loss and that the CB_1 receptors on GABAergic neurons protect against age-related neuronal degenerative changes and inflammation (Bilkei-Gorzo et al. 2005; Albayram et al. 2011; Albayram et al. 2012). Since the endocannabinoid system plays a neuroprotective role and most of the neurodegenerative diseases are related to old-age, targeting of this system could provide

new strategies in the prevention and treatment of neurodegenerative diseases (Marchalant et al. 2012; Sánchez and García-Merino 2012).

On the other hand, not only in the aging brain, but also in the developing adolescent brain, the endocannabinoid system plays a crucial role during dynamic neuronal changes and processes associated with adolescent behaviour and cognitive functions (Trezza et al. 2008; Mechoulam and Parker 2013). The proper functioning of the endocannabinoid system is necessary for mental health in the adulthood (Realini et al. 2009; Renard et al. 2014; Lubman et al. 2015). The differential response to the cannabinoid Δ^9-THC in adolescent when compared to adult animals (as described in section A.1.2) provides further confirmation of the fact that endocannabinoid system activity changes during ontogeny and aging.

As reviewed by Spear (2000) and Andersen (2003), there is a fundamental strategy in the development of the brain in mammals termed "functional validation". The functional validation is based on synapses and receptor overproduction and elimination and consists of two major phases, linked with two lifetime periods. The first phase, occurring just before birth after completion of the brain innervation, is characterised by the programmed cell death (cell apoptosis) of 50% of the neurons. At this point dramatic changes of the brain morphology take place and synaptic transmission efficiency is improved. The second phase is related to the periadolescent period and characterized by an immense overproduction of synapses and receptors, which are subsequently pruned or eliminated. The endocannabinoid system, which appears already in early prenatal stages in rats and in humans (for review see: Harkany et al. 2007), undergoes developmental changes different from those of the functional validation. Contrary to most of the neuroreceptor systems associated with functional validation, the central cannabinoid receptor (CB_1) density increases during the maturation from childhood through adolescence to adulthood to reach constant levels as reported by Belue et al. (1995). This mechanism of ontogeny was later confirmed by Verdurand et al. (2011) using the emission positron tomography in a study in adolescent and adult rats.

The dopamine receptor families D_1 and D_2 represent another example of the lack of functional validation in the development of central nervous system receptors. Expression of dopamine receptors increases until puberty; subsequently they are pruned to the adult level (Leslie et al. 1991; Teicher et al. 1995). Another transmitter of the central nervous system, the function of which changes during development/maturation, is γ-aminobutyric acid (GABA). Rivera et al. (1999) proved that GABA, known as an inhibitory neurotransmitter in adolescents and adults, acts excitatory in early developmental phases and switches from excitatory to

inhibitory activity during ontogenetic brain development. The alterations of some selected mechanisms during ontogeny in the CNS of rats are shown in Figure 7.

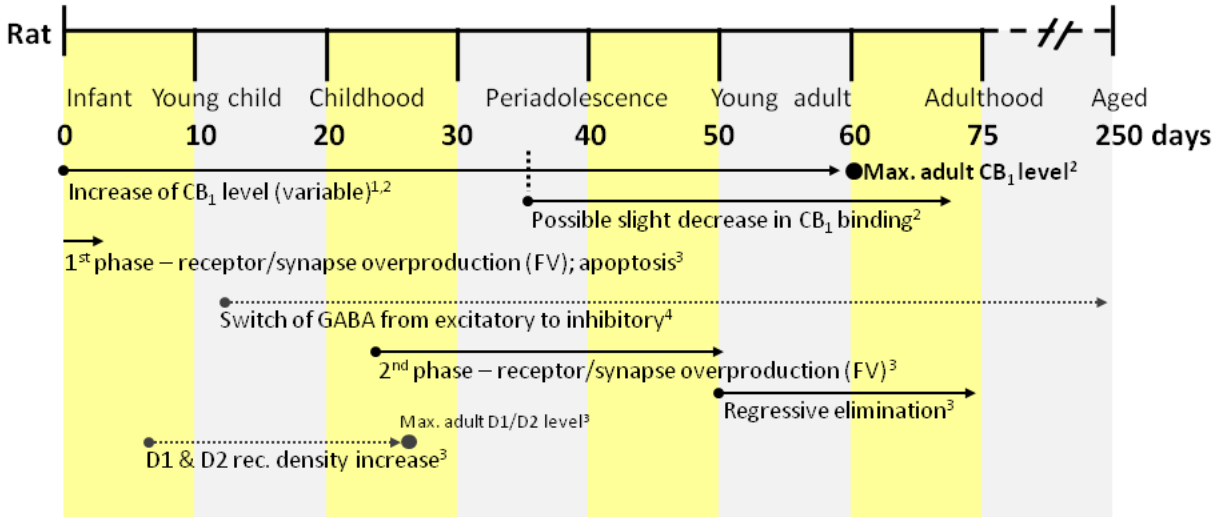

Figure 7. Comparison of the age periods and ontogeny events in rats. Adapted and extended from Spear (2000), Andersen (2003) and Verdurand et al. (2011). FV – functional validation.

[1]Belue et al. (1995); [2]Rodríguez de Fonseca et al. (1993); [3]Andersen (2003); [4]Rivera et al. (1999)

With respect to the endocannabinoid system, Trezza et al. (2008) and Lubman et al. (2014) reported strong behavioural consequences to cannabinoid exposure during the adolescence of humans and animals. However, in humans, research is restricted due to ethical reasons and several experimental limitations, such as limited participant number, heterogeneity of the groups, limited behavioural and *in vitro* methods affect the comparability and reproducibility of results. Despite these difficulties, numerous studies confirm the negative effects of adolescent cannabis use in humans (Rubino and Parolaro 2008; Realini et al. 2009; Rubino et al. 2009; 2012; Renard et al. 2014; Lubman et al. 2014). For instance, the review of Trezza et al. (2008) stated that the marijuana use in adolescence results in increased incidence of psychotic disorders (increased risk of the early schizophrenia onset or depression; Bossong and Niesink 2010) and impaired cognitive behaviour and memory. Lubman et al. (2014) identified synaptic pruning and white matter development as two crucial processes that may be impaired by cannabis consumption in adolescence. However, the mechanisms underlying the adolescence as a period of particularly high risk have still to be better understood. The latter problems, further risks, such as abuse and addictive potential of cannabinoids and their numerous adverse effects hinder their broader therapeutic use (Hall and Degenhardt 2009; Volkow et al. 2014; Filbey et al. 2014).

3. Other GPCRs – histamine H_4 receptor

Histamine is a biogenic amine involved in numerous physiological and pathological processes in mammalian organisms. The regulation of gastric secretion, inflammatory processes and pathological allergic responses are associated with histamine. Moreover, histamine acts as a neurotransmitter in the CNS (Schwartz 1975). At present, four histamine receptor subtypes, H_1, H_2, H_3 and H_4, are known (Haaksma et al. 1990; Leurs et al. 1995; Parsons and Ganellin 2006). All these receptors belong to the G protein-coupled receptor superfamily (Alexander et al. 2013). H_1 receptor antagonists are known as antiallergic drugs. H_1 receptor antagonists of the first generation and single antagonists of the second generation possess strong sedative effects which point to the presence of H_1 receptors in the brain (Parsons and Ganellin 2006; Simons and Simons 2011). Besides histamine H_1 also H_2 and H_3 receptors are found in the brain (Arrang et al. 1983; Haas et al. 2008). Although no histamine H_3 receptor ligands have been introduced to the market yet, the H_3 inverse agonist pitolisant is currently in an advanced stage of clinical trials as a potential medicine against neurological disorders like narcolepsy or epilepsy (Gemkow et al. 2009; Schwartz 2011; Kasteleijn-Nolst Trenité et al. 2013; Dauvilliers et al. 2013).

The H_4 receptor is the most recent addition to the histamine receptors. It is mainly expressed in hematopoietic cells and plays a role in immune response and inflammatory processes (Zhang et al. 2006; Walter et al. 2011). Although the expression of the histamine receptor subtypes H_1, H_2 and H_3 the brain is well defined (Arrang et al. 1983; Timm et al. 1998; Haas et al. 2008; Gemkow et al. 2009), the presence of the histamine H_4 receptor in the CNS is controversial as discussed by Schneider et al. (2015). Although H_4 receptor expression on the mRNA level was not found in the brain in the early study by Liu et al. (2001), it was detected later on by Strakhova et al. (2009). Moreover, research reports claiming the functional expression of the H_4 in the brain of mouse (Connelly et al. 2009) or rat (Desmadryl et al. 2012) were published (and reviewed by Marson 2011). In some studies, Western blots have been used to show the occurrence of H_4 receptor pattern in the brain; there is, however, much doubt whether really H_4 receptors were detected since the antibody used in those studies does not fulfil the strict specificity criteria (critically discussed by Schneider et al. 2015).

Since, H_4 receptor mRNA expression in human and mouse cerebral cortex tissue was detected using RT-PCR in Prof. Schlicker's laboratory (Schulte 2011), research on the H_4 receptor has been continued in this thesis. So an attempt has been made to detect H_4 receptor mRNA also in guinea pig cerebral tissue. Furthermore, I studied whether a functional readout of H_4 receptors in the brain can be identified, using the ^{35}S-GTPγS binding method.

4. Aim of this thesis

This thesis focuses on the ^{35}S-GTPγS binding assay combined with other experimental methods to investigate two G protein-coupled receptors. I examined whether adaptive changes of cannabinoid CB_1 receptors occur following their direct and indirect activation through appropriate drugs and whether functional histamine H_4 receptors occur in the brain.

The aim of the main part of this thesis related to the endocannabinoid system was: (i) to establish experimental conditions, including a selective agonist and appropriate groups, which were then used in the experimental series. Subsequently, (ii) in mice pre-treated chronically with Δ^9-THC, tolerance development to a challenge dose of Δ^9-THC was examined using a behavioural paradigm (Open Field Test), followed by agonist-stimulated ^{35}S-GTPγS binding studies. The functional changes in CB_1 receptor activity caused by chronic Δ^9-THC treatment were compared in adolescent and aged mice.

Furthermore, (iii) JZL 184, a selective MAGL inhibitor, was applied to mice in different doses and for different time periods to investigate an impact of these factors on the endocannabinoid levels in the brain (hippocampus). The endocannabinoids were detected and their concentration was measured using the LC-MS/MS (LC-MRM) method. The influence of the tested regimens on CB_1 receptor activity was measured in ^{35}S-GTPγS binding studies. The relationship between JZL 184 treatment regimen, endocannabinoid concentrations and CB_1 receptor activity in mouse hippocampus was analyzed. The goal of this part was to find a treatment schedule with JZL 184 which enhances endocannabinoid concentration in the brain without down-regulation of the CB_1 receptors.

Finally, I studied whether a functional H_4 receptor based on the ^{35}S-GTPγS binding assay can be shown in guinea pig brain (cerebral cortex).

B. Materials and Methods

1. Materials

1.1 Equipment

Analytical balance Extend ED124S, Sartorius, Göttingen, Germany

Analytical balance TE 610, Sartorius, Göttingen, Germany

ARE Heating Magnetic Stirrer, VELP Scientifica srl, Usmate, Italy

Cell Harvester IH 120, Inotech, Wohlen, Switzerland

Chromatographic columns: Phenomenex Luna 2.5-µm C18 (2)-HST column, 100 mm × 2 mm, combined with a SecurityGuard precolumn C18, 4 mm × 2 mm; Phenomenex, Aschaffenburg, Germany

CTC HTC PAL autosampler, CTC Analytics AG, Zwingen, Switzerland

Dispensette® Dispenser 2 ml and 5 ml, Brand, Wertheim, Germany

Dissecting set, Everhards, Meckenheim, Germany

Electrophoresis, Constant Power Supply 2297 MACRODRIVE 5 LKB Bromma, Sweden

Guillotine, self-made by Institute workshop artisan, Bonn, Germany

Homogeniser Potter-Elvehjem Braun 853302/4, B. Braun, Melsungen, Germany

Laboratory shaker Duomax 1030, Heidolph, Schwabach, Germany

LC system Agilent 1200 series, Agilent, Waldbronn, Germany

Liquid scintillation counter LS 6000 TA, Beckman Coulter, Fullerton, CA, USA

Mass spectrometer 5500 QTrap triple-quadrupole linear ion trap equipped with Turbo V Ion Source, AB SCIEX, Darmstadt, Germany

Microwave, Panasonic NN-E201WBGPG, France

Multipette Nr. 4710, Eppendorf, Hamburg, Germany

pH meter Five Easy, Mettler Toledo, Gießen, Germany

Pipettes Eppendorf Research, Eppendorf, Hamburg, Germany

Refrigerated centrifuge 5402, Eppendorf, Hamburg, Germany

Refrigerated centrifuge 5804, Eppendorf, Hamburg, Germany

Refrigerated centrifuge Type J2-21, Beckman, München, Germany

Spectrophotometer (RNA concentration), SmartSpec Plus Bio-Rad, München, Germany

Tabletop centrifuge Type 5415C, Eppendorf, Hamburg, Germany

Thermal cycler, MyCycler, Bio-Rad, München, Germany

ThermoMixer compact, Eppendorf, Hamburg, Germany

Tissue homogeniser/grinder Precellys 24, Berlin Technologies, Montigny-le-Bretonneux, France

Tissue Lyser, Qiagen, Hilden, Germany

TSE ActiMot System, Open Field Frames (42 cm x 42 cm x 28 cm), TSE Systems GmbH, Bad Homburg, Germany

UV chamber, Power Shot G5, Canon, Krefeld

UV/VIS Spektrophotometer BioPhotometer, Eppendorf, Hamburg, Germany

Vacuum Controller IH 195, Inotech, Wohlen, Switzerland

Vapotherm mikro 96, Barkey, Leopoldshoehe, Germany

Voltage source PowerPac 300, Bio-Rad, München, Germany

Vortexer ZX3, VELP Scientifica srl, Usmate, Italy

Waterbath and shaker 4010, Köttermann, Hänigsen, Germany

Waterbath, IKA IS2 IKA Laboratories Staufen, Germany

1.2 Software and databases

ACD/ChemSketch (freeware), Advanced Chemistry Development, Toronto, Canada

BLAST Basic Logical Alignment Tool and Nucleotide database, National Center for Biotechnology Information (NCBI), U.S. National Library of Medicine, Bethesda, MD, USA

GraphPad Instat 1.0 and Prism 5.0, GraphPad, San Diego, CA, USA

Mass spectrometry Software Analyst®, AB SCIEX, Framingham, MA, USA

Mendeley Desktop, Mendeley Ltd., London, United Kingdom

Microsoft Office 2007, Microsoft Corporation, Redmond, WA, USA

Photo edition: Irfan View 4.00 (freeware), http://www.irfanview.com

Photo documentation system, Power Shot G5, Canon, Krefeld, Germany

PubMed MEDLINE, http://www.ncbi.nlm.nih.gov/pubmed

Radioactivity Calculator QuickCalc, http://www.graphpad.com/quickcalcs/radcalcform.cfm

Sequence Manipulation Suite: PCR Primer Stats, http://www.bioinformatics.org, Paul Stothard, University of Alberta, Canada

TSE ActiMot System, software for Windows, TSE Systems GmbH, Bad Homburg, Germany

1.3 Disposables and chemicals

1.3.1 Disposables

Cannula disposable, Sterican G26 and G27, B. Braun Melsungen AG, Melsungen, Germany

Centrifuge tubes 15 ml and 50 ml, Sarstedt, Nümbrecht, Germany

Cuvettes 2 ml 67.741, Sarstedt, Nümbrecht, Germany

Folded filter 597½, Schleicher & Schuell, Dassel, Germany
Glass microfiber filters GF/B Nr. 1821915, Whatman, Maidstone, UK
Microcuvettes 100 µl, Sarstedt, Nümbrecht, Germany
Midi-Vials™ 8ml, Perkin-Elmer, Boston, MA, USA
MT/DW 96-well plates, Thermo Fischer Scientific, Braunschweig, Germany
Multipettes tips Combitips®, Eppendorf, Hamburg, Germany
Parafilm PM-956, Pechiney Plastic Packaging, Chicago, IL, USA
Pipette tips, Sarstedt, Nümbrecht, Germany
Pipette tips, sterile with filter, Axygen, Union City, CA, USA
Reaktion tubes 2 ml, Biozym, Oldendorf, Germany
Reaktion tubes Safe-Lock 0.5 ml, 1.5 ml and 5 ml, Eppendorf, Hamburg, Germany
Syringes 1 ml, BD Plastipak, Heidelberg, Germany

1.3.2 Chemicals

Chemical structures of all essential ligands used in ^{35}S-GTPγS binding studies or drugs administered to mice are presented in Table 2 (cannabinoid receptor ligands), Table 3 (JZL 184), and Table 4 (histamine receptor ligands).

β-Mercaptoethanol, Sigma Aldrich Chemie, Steinheim, Germany
Δ^9-Tetrahydrocannabinol, (100 mg/ml stock in ethanol 96 %), THC-Pharm GmbH, Frankfurt am Main, Germany
4-Methylhistamine dihydrochloride, Biotrend, Cologne, Germany
Absolute alcohol (ethanol 96%), KMF Laborchemie, Lohmar, Germany
Acetonitrile, LC-MS grade solvent, CHROMASOLV®, Sigma Aldrich, Munich, Germany
Adenosine deaminase, Roche, Mannheim, Germany
Agarose, Carl Roth, Karlsruhe, Germany
Boric acid, Roth, Karlsruhe, Germany
BSA (Bovine Serum Albumin), Sigma-Aldrich Chemie, Steinheim, Germany
Coomassie-Brilliant Blue G 250, Serva, Heidelberg, Germany
CP 55,940, Biotrend, Cologne, Germany
Cremophor, Sigma Aldrich Chemie, Steinheim, Germany
DMSO (dimethyl sulfoxide), Merck KGaA, Darmstadt, Germany
EDTA (ethylene diaminetetraacetic acid), Carl Roth, Karlsruhe, Germany
EGTA (ethylene glycol tetraacetic acid), Carl Roth, Karlsruhe, Germany

Endocannabinoids and related lipids, Cayman Chemicals, Ann Arbor, MI, USA:
2-AG (2-arachidonoylglycerol),
AEA (anandamide),
AA (arachidonic acid),
OEA (oleylethanoloamide),
PEA (palmitoylethanolamide),
and their deuterated analogues: 2-AG- d_5,
AEA-d_4,
AA- d_8;
OEA- d_2,
PEA- d_4

Ethidium bromide 10 mg/ml, Bio-Rad, Munich, Germany

Ethylacetate, LC-MS grade solvent CHROMASOLV®, Sigma Aldrich, Munich, Germany

Ficoll® PM 400, Sigma Aldrich Chemie, Munich, Germany

Formic acid, LC-MS grade solvent CHROMASOLV®, Sigma Aldrich, Munich, Germany

GDP (guanosinediphosphat sodium salt), Sigma Aldrich Chemie, Steinheim, Germany

GTPγS Li_4 (guanosine 5'-O-[gamma-thio]triphosphate tetralithium salt), Sigma Aldrich Chemie, Steinheim, Germany

Hexane, LC-MS grade solvent CHROMASOLV®, Sigma Aldrich , Munich, Germany

Hydrochloric acid 1 M, KMF Laborchemie, Lohmar, Germany

JNJ-7777120 – synthesized and kindly given by Prof. H. Stark and co-workers, Institute for Pharmaceutical and Medicinal Chemistry, Heinrich Heine University of Düsseldorf, Germany

JZL 184, Biotrend, Cologne, Germany

Lumagel-Safe® (scintillation liquid), Lumac LSC, Groningen, Netherlands

Magnesium chloride hexahydrate, Merck KGaA, Darmstadt, Germany

Ortho phosphoric acid 85%, Merck KGaA, Darmstadt, Germany

R(+)-WIN-55,212-2 mesylate salt, Sigma Aldrich Chemie, Steinheim, Germany

R-α-Methylhistamine dihydrogenmaleate – synthesized and kindly given by Prof. W. Schunack, Institute of Pharmacy, Free University in Berlin, Germany

Saline isotonic solution 0.9 % Braun, B. Braun Melsungen AG, Melsungen, Germany

Sodium bicarbonate, KMF Laborchemie, Lohmar, Germany

Sodium chloride, Carl Roth, Karlsruhe, Germany

ST-1006 – synthesized and kindly given by Prof. H. Stark and co-workers, Institute for Pharmaceutical and Medicinal Chemistry, Heinrich Heine University of Düsseldorf, Germany

Sucrose, Merck KGaA, Darmstadt, Germany

Thioperamide hydromaleate, Schering-Plough Reserch, Bloomfield, NJ, USA

Tracklt™ 100 bp DNA ladder, Invitrogen Life Technologies, Carlsbad, CA, USA

Tris-Base, Pufferan®, Carl Roth, Karlsruhe, Germany

Tris-HCl, Pufferan®, Carl Roth, Karlsruhe, Germany

Substances were dissolved depending on solubility and experimental conditions: in distilled water, DMSO, ethanol or reaction buffer or suspended in cremophore and saline. Dilution series for binding experiments were prepared with reaction buffer and, in the case of cannabinoids with reaction buffer with 0.5 % BSA.

Type	Structure	MW [g/mol]	Function
Synthetic	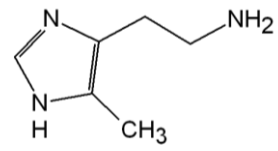 **4-Methylhistamine**	125.17	H_4 agonist
	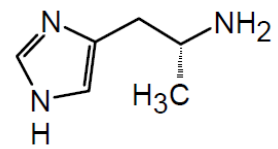 **R-α-Methylhistamine**	125.17	H_3 agonist
	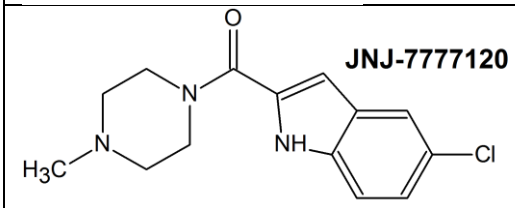 **JNJ-7777120**	277.75	H_4 (partial) agonist
	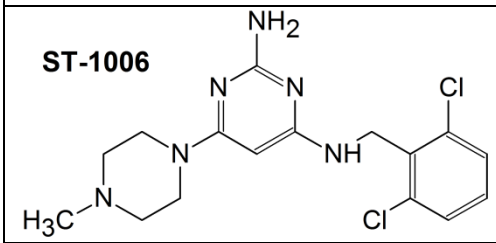 **ST-1006**	367.28	H_4 partial agonist
	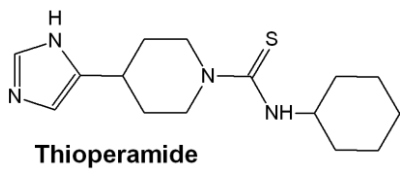 **Thioperamide**	292.44	H_3 antagonist

Table 4. Chemical structures of histamine H_3 and H_4 receptor ligands.

1.3.3 Injections

All injections were administered intraperitoneally (i.p.), in a volume of 0.1 ml per 10 g of mouse body weight.

Δ^9-THC injections:

Dose to mouse [mg/kg]	THC stock [100 mg/ml]	Cremophor [ml]	Saline [ml]
0 = Control (Vehicle)	(0.1 ml of ethanol)	0.5	9.4
10	0.1 ml (100 µl)	0.5	9.4

Table 5. Composition of Δ^9-THC solution.

JZL 184 injections:

Dose to mouse [mg/kg]	JZL-184 [mg]	Cremophor [ml]	Saline [ml]
0 = Control (Vehicle)	0	1	9
4	4	1	9
10	10	1	9
40	40	1	9

Table 6. Composition of JZL 184 solution.

1.3.4 Buffers and solutions

Buffers and solutions to work with tissues

Phosphate buffered saline (PBS)

NaCl	137 mM
Na_2HPO_4	8 mM
KH_2PO_4	1.4 mM
KCl	2.7 mM

Dissolved in H_2O and adjusted to pH 7.4 with HCl.

Buffers and solutions to work with protein

Tris-EDTA buffer (TE buffer)

Tris	50 mM
EDTA	5 mM

pH 7.5 at 4 °C

Tris-EDTA-sucrose buffer for membrane preparation (TE-sucrose buffer):

10.27 % sucrose, in TE buffer:

Sucrose	10.27 g
TE buffer	ad 100 g

Bradford stock solution

Coomassie Brilliant Blue G 250	0.1 g
Ethanol 50 % (V/V)	50 ml
Phosphoric acid 85 %	100 ml
Water bidest.	ad 250 ml

The stock solution has to be stored for four weeks at 4 °C before first use.

Bradford working solution

Bradford stock solution	1 volume fraction
Water bidest.	15 volume fractions

Bradford working solution has to be prepared fresh by just before use and filtrated through folded paper filter.

Buffers and solutions for ^{35}S-GTPγS binding experiments

Tris-EGTA reaction buffer

Tris	50 mM
EGTA	1 mM
$MgCl_2$	3 mM
NaCl	100 mM

pH 7.4 at 4 °C

Addition of 0.5 % BSA needed to dissolve lipophilic cannabinoids

Tris-EDTA wash buffer (TE buffer)

Tris	50 mM
EDTA	5 mM

pH 7.5 at 4 °C

Buffers and solutions to work with nucleic acids

The RNA isolation was conducted using NucleoSpin® kit. Following buffers were provided as a kit contents:

Lysis buffer RA1,

Wash buffer RAW2,

Lysis buffer RA3,

MDB (membrane desalting buffer),

Reaction buffer for rDNase,

rDNase, RNase-free.

rDNase reaction mixture (NucleoSpin®)

Reconstituted rDNase	10 µl
Reaction buffer for rDNase	90 µl

MasterMix for RT (reverse transcriptase) reaction

10 x buffer RT	2 µl
dNTP Mix 5 mM	2 µl
Oligo$(dT)_{18}$ Primer 10 µM	2 µl
RNase inhibitor 10 U/µl	0.5 µl
Omniscript RT	1 µl
Final volume	7.5 µl

Volumes listed above refer to a single sample. A volume of MasterMix for more samples was calculated using the formula: [µl] x (n+1), n=amount of samples.

RNase inhibitor 10 U/µl: RNase inhibitor Promega 40 U/µl was diluted to the concentration of 10 U/µl in ice-cold 1 x buffer RT. 1 x buffer RT was diluted 1:10 using 10 x buffer RT and RNase free water.

MasterMix for PCR

10 x PCR buffer (-$MgCl_2$)	5 µl
$MgCl_2$ 50 mM	1.5 µl
dNTP 10 mM each	1 µl
Primer sense 10 µM	2.5 µl
Primer antisense 10 µM	2.5 µl
Taq DNA Polymerase 5 U/µl	0.3 µl
Sterile water	ad 45 µl

Volumes listed above refer to a single sample. The amount of MasterMix for more samples was calculated using the formula: [µl] x (n+1,5), n=amount of samples.

For primer sequences, see Table 12**.**

5 x TBE (Tris borate EDTA) buffer

Tris	54.9 g
Boric acid	27.5 g
EDTA	4.65 g
Water bidest.	ad 1000 ml

To obtain 0.5 x TBE buffer, the 5 x TBE buffer was diluted 1:10 with water bidest.

Loading buffer for PCR (polymerase chain reaction)

Ficoll 400	1.5 g
1 % (w/v) BPB	2.5 ml
5 x TBE buffer	1 ml
Water bidest.	ad 10 ml

Solutions used for endocannabinoid extraction and quantification by LC-MRM (liquid chromatography-multiple reaction monitoring)

Tissue extraction:

Aqueous solvent / homogenisation buffer:

Formic acid	0.1 M

Organic solvent / extraction buffer:

Ethylacetate:	9 volume fractions
n-Hexan	1 volume fraction

Deuterated Mix, ISTDs (internal standards), final concentrations:

AEA-d4	4 ng/ml
2-AG-d5	2000 ng/ml
AA-d8	40000 ng/ml
MAEA (methanandamide)	2 ng/ml
OEA-d2	10 ng/ml
PEA-d4	20 ng/ml
1-AG-d5	100 ng/ml

Spike solution:

Deuterated Mix	1 volume fraction
Acetonitrile	19 volume fractions

LC-MRM solvents:

Solvent A:

0.1 % formic acid in water

Solvent B:

0.1 % formic acid in acetonitrile

1.3.5 Radiochemicals

^{35}S-GTPγS (guanosine 5-[γ-^{35}S]thiophosphate, triethylammonium salt, specific activity: 1250 Ci/mmol), Perkin Elmer, Boston, MA, USA (for chemical structure, see Table 9).

1.3.6 Kits

NucleoSpin ® RNA, Macherey-Nagel, Düren, Germany

Omniscript Reverse Trancriptase Reaction kit, Quiagen, Hilden, Germany

Pierce BCA protein assay kit, Pierce Biotechnology, IL, Rockford, USA

1.4 Animals

Animal care and conduction of experiments followed all applicable international and institutional guidelines. Permission number: Az 87-51.04.2011.A038 (obtained from the local ethical committee (Bezirksregierung Köln).

Animals were kept in the House of Experimental Therapy, University of Bonn.

$CB_1^{-/-}$ knockout and $CB_1^{-/-}/CB_2^{-/-}$ double knockout mice, Prof. A. Zimmer, Institute of Molecular Psychiatry, Bonn, Germany

C57BL/6J wild type mice, Charles River Laboratories, Sulzfeld, Germany

CD-1 mice, male, Charles River Laboratories, Sulzfeld, Germany

Guinea pig, Dunkin-Hartley, male, 8-16 weeks, Charles River Laboratories, Sulzfeld, Germany

Age or weight of mice used for experiments was specified in the relevant sections in chapter "Methods" (B.2).

2. Methods

2.1 Mouse treatment

2.1.1 Δ^9-THC treatment

Male C57BL/6J wild type mice of two age groups:

- adolescent (6-8 weeks old, 8 animals per group / n=8) and
- old (12 months old, 8-10 animals per group / n=8-10)

were treated with i.p. injections of Δ^9-THC or its vehicle (for composition of solutions, see Table 5), twice a day, approximately at 8.00 a.m. and about 16.30 p.m. Animals were treated with 10 mg/kg Δ^9-THC or vehicle, as shown in Table 7. On "Day 4" animals were treated only once in the morning; 24 h later ("Day 5"), they were challenged with Δ^9-THC or received vehicle instead. The Open Field Test was conducted 40 min after injection to measure the effect of the challenge dose on mice motility. The treatment schedule was modified from Bass and Martin (2000) and is presented in Table 7 below.

Treatment group	Day 1- Day 3	Day 4	Day 5	adolescent and old
Control	a.m.: vehicle p.m.: vehicle	a.m.: vehicle 24 h break	a.m.: vehicle Open Field Test	
Acute	a.m.: vehicle p.m.: vehicle	a.m.: vehicle 24 h break	a.m.: 10 mg/kg Δ^9-THC Open Field Test	
Chronic	a.m.: 10 mg/kg Δ^9-THC p.m.: 10 mg/kg Δ^9-THC	a.m.: 10 mg/kg Δ^9-THC 24 h break	a.m.: 10 mg/kg Δ^9-THC Open Field Test	
	P r e - t r e a t m e n t		**Challenge dose**	

Table 7. Induction of Δ^9-THC tolerance in C57BL/6J mice. Adolescent or old mice received one ("Acute") or repeated i.p. injections of 10 mg/kg Δ^9-THC ("Chronic"). Control groups ("Control") were treated with vehicle only.

2.1.2 JZL 184 treatment

Male CD-1 mice weighing about 30 g (8 animals per group / n=8) were treated once a day with 4, 10 or 40 mg/kg body weight JZL 184 or with vehicle by i.p. injections (for composition of solutions, see Table 6). Treatment lasted for 1, 3 or 14 days (for treatment schedule, see Table 8). Animals were killed 24 h after the last injection by decapitation and each hemisphere

of the hippocampus was frozen separately on dry ice and stored at -80 °C for ^{35}S-GTPγS binding studies (left hemisphere) and LC-MS/MS (LC-MRM) (right hemisphere).

Treatment	1 Dose	3 Doses	14 Doses
Vehicle	8 mice	8 mice	8 mice
JZL 184 4 mg/kg	8 mice	8 mice	8 mice
JZL 184 10 mg/kg	8 mice	8 mice	8 mice
JZL 184 40 mg/kg	8 mice	8 mice	8 mice
	Decapitation 24 h after last injection		

Table 8. JZL 184 treatment of CD-1 mice. Four, 10 or 40 mg/kg JZL 184 was administered i.p. to mice (n=8 per group) for 1, 3 or 14 days.

2.2 Behavioural studies: Open Field Tests

The Open Field experiments were conducted in collaboration with PD Dr. A. Bilkei-Gorzo, PD Dr. I. Rácz and K. Michel from the Institute of Molecular Psychiatry, University of Bonn within the DFG (Deutsche Forschungsgemeinschaft) Research unit FOR 926 (Forschergruppe 926).

2.2.1 Experimental procedure

The Open Field Test provides information about motor activity and exploratory behaviour of mice (Walsh and Cummins 1976). In this study, adolescent and old C57BL/6J wild type mice were treated according to Table 7 and as described in section B.2.1.1. Forty min after injection of the challenge dose, animals were placed in the middle of the open field frame and their motor activity was tracked by an automatic monitoring system (ActiMot) for 10 min in the darkness (infrared). Animals were tested in the Open Field Apparatus in a random order.

2.2.2 Experiment evaluation

Three parameters, i.e., distance travelled [m], rearing number and resting time [s], were measured by the ActiMot System. Using the GraphPad Prism 5 software means ± SEM were determined and presented as columns; the effect of age and treatment schedule was analyzed as well.

Furthermore, to simplify comparison of the data, the results obtained with the ActiMot System were normalized to "% of activity suppression" values. First, the performance of the Δ^9-THC-treated mice was expressed in % of the vehicle treated mice (control group) (see Equation 1).

$$\%\ Activity\ = \frac{100 \times Open\ Field\ Test\ parameter\ after\ \Delta^9\text{–}THC\ challenge\ dose}{Open\ Field\ Test\ measurement\ after\ vehicle\ treatment}$$

Equation 1. Calculation of percentage value of activity (% activity) of acute and chronically Δ^9-THC treated mice.

Subsequently, the "% activity suppression" was calculated as the difference between vehicle (100 %) and analyzed treatment group (as shown in Equation 2). However, Equation 2 corresponds only to the parameters "Distance travelled" and "Rearing number", which measure animals' activity.

$$\%\ Activity\ suppression_{by\ distance\ and\ rearing}\ =\ 100\ \%\ -\%\ activity\ after\ treatment$$

Equation 2. Calculation of the suppression of activity (% activity suppression), relevant for "Distance travelled" and "Rearing number".

In case of the parameter "Resting time", which directly corresponds to the inhibition of activity (% activity becomes % inhibition), the "% of activity suppression" was calculated as shown in Equation 3.

$$\%\ Activity\ suppression_{by\ resting\ time}\ =\ \%\ activity\ after\ treatment - 100\ \%$$

Equation 3. Calculation of the suppression of activity (% activity suppression), relevant for "Resting time".

The use of "% Activity suppression" simplifies analysis of behavioural tests. All conversions were conducted using GraphPad Prism 5 software. Mean values ± SEM of "% Activity suppression" were presented as column bar graphs for the two age and the two treatment groups.

2.3 Receptor binding experiments

2.3.1 Theoretical background

The ^{35}S-GTPγS binding assay provides information about activity and function of the G protein-coupled receptors (GPCRs) and is one of the most sensitive methods to determine the efficacy of the ligands interacting with GPCRs. The assay measures the earliest receptor-mediated events (Lazareno 1999; Harrison and Traynor 2003; Breivogel 2006; Strange 2010) and is based on the GPCR activation cycle (see Figure 8 and Figure 9).

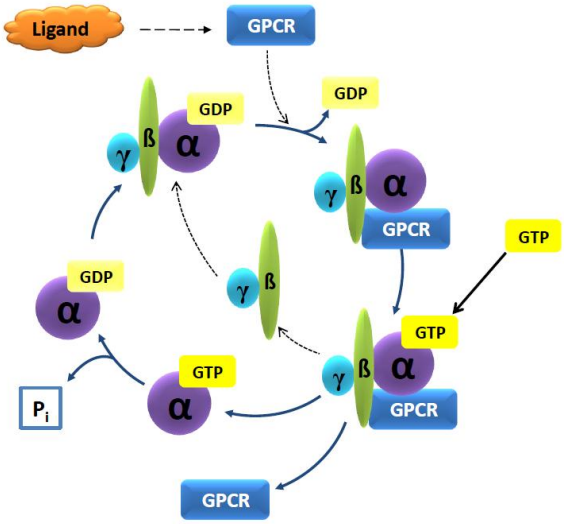

Figure 8. G protein-coupled receptor activation cycle.

The GPCR cycle starts with the activation of the GPCR by the agonist. Activation of the receptor causes that the inactive G protein, consisting of the Gα subunit and Gβγ heterodimer in which GDP is bound to the Gα subunit, changes its conformation and GDP is released and replaced by GTP. The GDP-GTP exchange is a crucial step which, depending on the G protein type, influences numerous signalling pathways such as cAMP production. The conformation change of the Gα subunit decreases the affinity of the receptor–Gα–Gβγ complex causing dissociation of these three components. Furthermore, the G protein possessing intrinsic GTPase activity hydrolyses GTP to GDP and inorganic phosphate (P_i) (see Figure 8, modified from Harrison and Traynor 2003 and Strange 2010). Then, the Gα subunit and Gβγ re-associate and the GPCR cycle is over.

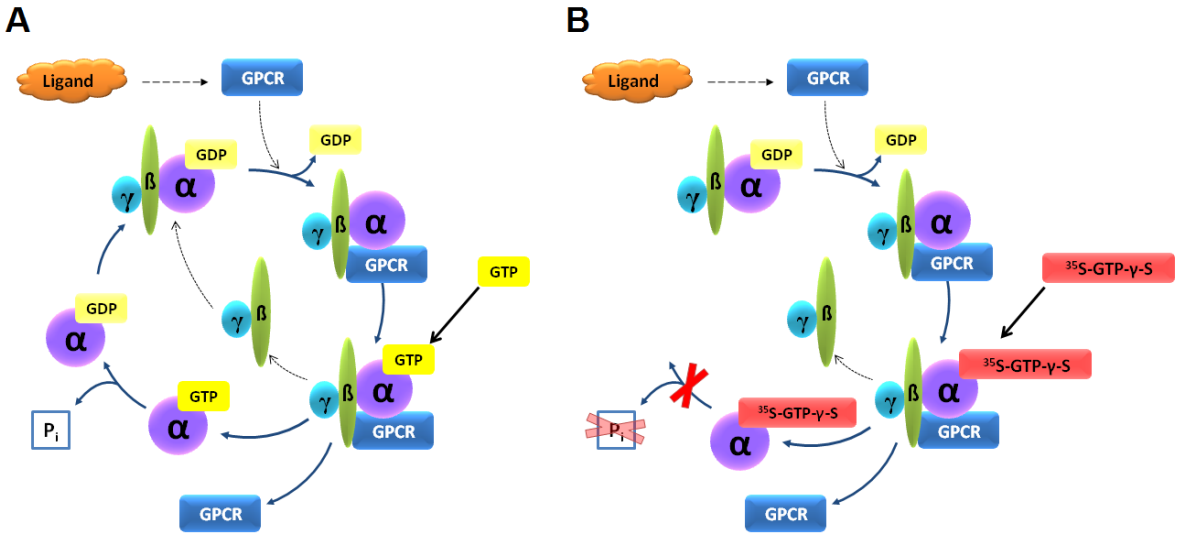

Figure 9. G protein-coupled receptor cycle under physiological conditions (A) and under the influence of ^{35}S-GTPγS (B).

When ^{35}S-GTPγS is added to the reaction mixture, it binds to the Gα subunit instead of non-radioactive GTP (Figure 9B). ^{35}S-GTPγS contains a sulphur instead of an oxygen atom at the γ phosphate group (for chemical structure, see: Table 9). So, this structure cannot be hydrolysed by the GTPase of the Gα subunit and the formed complex accumulates in the reaction mixture. Since the Gα remains associated with the cell membrane, the amount of the G protein-^{35}S-GTPγS complex can be measured and analyzed after filtration through a glass-fibre filter in which the cellular membrane, Gα and ^{35}S-GTPγS remain (Harrison and Traynor 2003).

Type	Structure	MW [g/mol]
Radiolabelled nucleotide	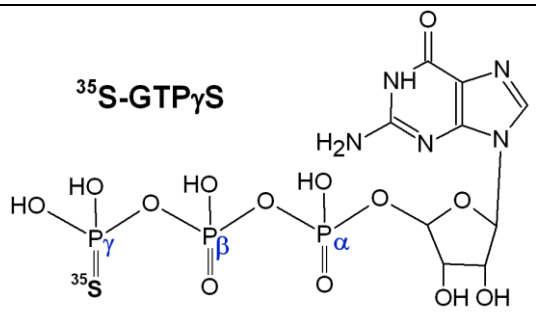	539.2

Table 9. Chemical structure of the ^{35}S-GTPγS, radiolabelled nucleotide used in binding experiments.

2.3.2 Experimental procedures

Membrane preparation

Animals were killed by decapitation. The brain was removed using a dissecting set, hippocampus or cortex was isolated on the cold (4 °C) block, frozen on dry ice in preconditioned ice-cold reaction tubes and stored at -80 °C or homogenized immediately after preparation. All procedures described below were conducted at 4 °C (centrifugation) or on ice.

For homogenization, frozen tissue (40 - 80 µg) was transferred into 1000 µl of ice-cold TE-sucrose buffer. Homogenization was conducted using a Potter-Elvehjem homogenizer (10 strokes per minute, 1200 rpm). The homogenate was transferred into a 1.5 ml reaction tube and the Potter vessel was rinsed with a further 500 µl of ice-cold TE-sucrose buffer. The tissue suspension was centrifuged for 10 min at 1500 x g. The supernatant was transferred into a new Eppendorf tube and centrifuged for 25 min at 20 000 x g. Subsequently, the supernatant was removed and the residual pellet re-suspended in 1000 µl TE buffer and centrifuged for 10 min at 20 000 x g (first wash step). The wash step was repeated, the supernatant discarded and the final pellet briefly homogenized in 500 µl Tris-EGTA reaction buffer using a Potter-Elvehjem homogeniser at 1200 rpm. Triplicates of 10 µl of protein suspension were used for determination of protein concentration (see below); the rest of the protein suspension was

frozen and stored at -80 °C. For ^{35}S-GTPγS binding experiments, the protein suspension was thawed and diluted to the needed protein concentration with Tris-EGTA reaction buffer.

Determination of protein concentration

Determination of the protein concentration using the Bradford assay (Bradford 1976) is based on the reaction of the Coomasie Brilliant Blue G-250 dye with protein contained in the analyzed suspension. The Coomasie Brilliant Blue G-250 dye in anionic form binds to positively-charged amino-groups (mainly: arginine, lysine and histidine) of the proteins causing a change in reagent colour (Compton and Jones 1985). The red-brown colour of the Bradford-stock solution changes to blue in the presence of protein and the intensity of this blue colour increases with an increasing amount of the protein in the tested sample. The intensity of the blue colour can be measured using a UV-photometer. The protein concentration was determined using a calibration curve.

As shown in Table 10, the calibration curve was prepared with BSA 0.1 µg/µl solution and distilled water to obtain standards of 1, 2.5, 5, 7.5, 10 and 15 µg of protein and distilled water as a control. To estimate the protein concentration, 10 µl of the test sample in Tris-EGTA buffer was added to 140 µl of distilled water; finally 2 ml of Bradford working solution were added to all sample and calibration curve cuvettes and mixed properly. The measurement of the absorbance (OD) was conducted at 595 nm, 5 to 30 min after addition of the Bradford working solution to the cuvettes.

The protein concentration was calculated using a calibration curve. The OD values of known standards were compared with the ODs of the samples.

BSA 0.1 µg/µl [µl]	Water dist. [µl]	BSA standard [µg]	
0	150	0	Calibration curve
10	140	1	
25	125	2.5	
50	100	5	
75	75	7.5	
100	50	10	
150	0	15	
*10**	140	x	Sample

Table 10. Calibration curve and sample preparation for the Bradford assay.

* - Here 10 µl of the sample was used instead, x – measured protein concentration [µg] in the sample.

^{35}S-GTPγS binding assay

Previously homogenized protein suspension, (diluted to the final concentration) was pre-incubated for 10 min at 30 °C with adenosine deaminase 0.004 U/ml to inactivate the endogenous adenosine. Removal of endogenous adenosine prevents the activation of adenosine receptors in the tissue. These receptors, expressed in many brain regions, among others in hippocampus or cerebral cortex, belong to the GPCR superfamily and activate G_i/G_o proteins causing an increase in the basal binding effect of the tissue. By inactivation of the adenosine, basal binding decreases and the signal : noise ratio is significantly improved (Moore et al. 2000).

All reagents were pre-diluted and/or solved in Tris-EGTA reaction buffer if not stated otherwise and pipetted into 2 ml reaction tubes in a 24-well plate to final volumes of 500 µl. Pipetting order, volumes and concentrations are shown in Table 11.

Reagent	Volume [µl]	Concentration	*Comment*
Tris-EGTA*	300	-	in all tubes
GDP	50	30 µM	in all tubes
Ligand	50	0.0003 µM - 30 µM	each concentration in triplicate
Ligand* solvent	50	-	control - total binding, in triplicate
^{35}S-GTPγS	50	0.5 nM	in all tubes
GTPγSLi_4	50	10 µM	unspecific binding, in triplicate
Protein homogenate	50	5-10 µg/50 µl	in all tubes
Final volume	**500**		

Table 11. Reagents used in the ^{35}S-GTPγS binding assay.

*Tris-EGTA buffer - if more than one ligand was used, the volume of reaction buffer was reduced accordingly;

*Ligand - cannabinoids – diluted and solved in Tris-EGTA + 0.5 % BSA

For the experiments with cannabinoids, Tris-EGTA reaction buffer with 0.5 % BSA has to be used. The lipophilic cannabinoids tend to adsorption to surfaces like glass or synthetic materials. Addition of 0.5 % BSA to the buffer prevents this effect. Washing the Cell-Harvester with Tris-EGTA with 0.5 % BSA just before filtration serves the same purpose.

Immediately after addition of the protein to the reaction mixture, the 24-well plate was covered with parafilm, briefly vortexed and placed into the water bath shaker for 1 h at 30 °C. One hour after the start of incubation, the reaction was stopped by rapid vacuum filtration of the reaction mixture through a GF/B Whatmann filter using an Inotech Cell-Harvester. The residual pressure

was 400 mbar. The filter was washed three times with ice-cold TE-wash buffer and round filters (diameter of 1 cm) were punched by the Cell-Harvester. The latter were placed into scintillation vials and 4 ml of scintillation liquid (LumaGel) was pipetted into each vial; vials were shaken for 12 h (overnight). The radioactivity (cpm) in the vials was determined using a Liquid Scintillation Counter (counting time of 5 min for each sample).

2.3.3 Calculation of results

A self-made Microsoft Excel spreadsheet was used to calculate unspecific and basal binding and GraphPad Prism 5 software served to calculate the effect of the ligand on the receptor. The results were presented in form of non-linear concentration-response curves as "% of specific ^{35}S-GTPγS binding" or "cpm over basal binding". All values were obtained in triplicate as cpm units and the mean values were used for calculations.

To determine the basal binding, the unspecific binding was subtracted from the total binding value (Equation 4):

$$basal\ binding\ [cpm] = \ \ total\ binding\ -\ unspecific\ binding$$

Equation 4. Calculation of the basal binding of the receptor.

To determine the effect of the ligand, unspecific binding was subtracted from the cmp value obtained for each concentration. To present the data in "cpm over basal", basal binding was subtracted from each cpm value (Equation 5) and a non-linear regression analysis was performed (Hill slope = 1). X axis: molar concentration [M] versus Y axis: cmp over basal values.

$$cmp\ over\ basal\ [cpm] = (ligand\ effect - unspecific\ binding) - basal\ binding$$

Equation 5. Calculation of cmp over basal.

To calculate "% of specific ^{35}S-GTPγS binding", basal binding (in cpm) was defined as 100% and the cpm value obtained for each ligand concentration was normalized to basal binding (Equation 6) followed by non-linear regression analysis (Hill slope = 1). X axis: concentration [M] versus Y axis: % of specific ^{35}S-GTPγS binding.

$$\%\ of\ specific\ ^{35}S\text{-}GTP\gamma S\ binding = \frac{ligand\ effect\ [cpm] * 100}{basal\ binding\ [cpm]}$$

Equation 6. Calculation of percent (%) of specific ^{35}S-GTPγS binding.

Recovery test

Due to the relative short half time of the ^{35}S isotope (87.6 days), the amount of radioactivity was adjusted before each experiment. The amount of radioactivity was calculated using GraphPad Radioactivity Calculator QuickCalcs; the recovery test was conducted in parallel.

2.3.4 Calculation of potencies

The potency of agonists was characterized using pEC_{50} values. The pEC_{50} is defined as the negative logarithm of the concentration of the agonist which induces the half-maximal effect. The pEC_{50} values were determined from the concentration-response curves using GraphPadPrism software.

The potency of a given antagonist was characterized by its pA_2 value, which is defined as the negative logarithm of the antagonist concentration at which the concentration-response curve of an agonist is shifted to the right by a factor of two (Arunlakshana and Schild 1997). The pA_2 value was determined according to the formula in Equation 7:

$$pA_2 = log\left(\frac{[A']}{[A]} - 1\right) - log[B]$$

Equation 7. Antagonist potency calculation: pA_2 value. [A'] and [A] are the EC_{50} values of the agonist obtained in the presence and absence of the antagonist, respectively; [B] is the antagonist concentration

2.4 Determination of endocannabinoids by liquid chromatography – multiple reaction monitoring

Detection and quantification of endocannabinoids using LC-MS/MS with MRM was conducted in collaboration with Dr. Laura Bindila and Claudia Schwitter at the laboratory of Prof. Dr. Beat Lutz, Institute of Physiological Chemistry, University Medical Center of the Johannes Gutenberg-University in Mainz within the DFG Research unit FOR 926.

Preparation, handling and measurement of the samples were conducted according to the recommendations published by Vogeser and Schelling (2007) and Vogeser and Seger (2010). For technical data, see section B.1.1. For chemicals and composition of solvents see section B.1.3.2 and B.1.3.4. Detailed LC and MS parameters were reported by Wenzel et al. (2013).

2.4.1 Sample preparation

Hippocampus samples (right hemisphere) of 96 CD-1 male mice pre-treated as described in section B.2.1.2, according to the Table 8, were isolated, rapidly frozen at dry ice in pre-cooled reaction tubes and stored at -80 °C.

For the analysis, tissue samples were transferred into preconditioned cold extraction tubes; ice-cold steel balls were placed into each tube, 50 µl of ice-cold spiking solution containing internal standards and 300 µl of aqueous solvent (0.1 M formic acid) were pipetted using a pipetting machine and homogenized using a Precellys 24 homogenizer. Subsequently, 300 µl of ice-cold organic solvent were added to each tube using a multistepper pipette and samples were run in Tissue lyser for 30 sec at 30 Hz to extract endocannabinoids.

To separate the organic and aqueous phase, the tubes were centrifuged for 10 min at 5000 x g and kept at -20 °C for 10-20 min to freeze the aqueous phase at the bottom of the extraction tube. The aqueous phase was stored for protein determination (Pierce BCA protein assay kit). The upper, organic phase (supernatant) was transferred into a MT/DW 96-well plate, evaporated to dryness in a Vapotherm to dryness and stored at – 20 °C until analysis. The samples were reconstituted in 50 µl of acetonitrile/H_2O (1:1) directly before loading to the chromatographic column.

2.4.2 Chromatographic conditions

Extracted endocannabinoids and AA were separated by injection of 20 µl samples (autosampler) on a Phenomenex Luna 2.5-µm C18 (2)-HST column, 100 mm × 2 mm, combined with a SecurityGuard precolumn C18, 4 mm × 2 mm with Solvent A and Solvent B (for composition see section B.1.3.4.).

2.4.3 Mass spectrometry - MRM

Endocannabinoids and AA separated using LC were analyzed by MRM on a 5500 QTrap triple-quadrupole linear ion trap mass spectrometer equipped with a Turbo V Ion Source (AB SCIEX) coupled to the LC system. Concentrations of AEA, 2-AG and AA were normalized to the protein content of each sample.

2.5 Detection of H_4 receptor mRNA expression

PCR experiments were conducted in collaboration with Margarita Fuhrmann and Prof. Dr. Kurt Racké from the Institute of Pharmacology and Toxicology, University of Bonn.

2.5.1 RNA purification from guinea pig cerebral cortex and spleen tissue

A male Dunkin-Hartley guinea pig was killed by decapitation. The cortex and spleen were dissected immediately after decapitation, frozen on dry ice and stored at -80 °C. The processing of the tissues was performed using the NucleoSpin® protocol, according to the manufacturer. Briefly, up to 30 mg of the tissue were thawed in the presence of 600 µl of RA1 buffer (RA1 buffer lyses the tissue and prevents RNA degradation by RNases) and disrupted using a Potter-Elvehjem homogenizer until a homogeneous tissue suspension was obtained. Subsequently, 3.5 µl of β-mercaptoethanol were added. Tissue was vortexed and filtrated through a NucleoSpin® filter-ring placed in the collection tube by centrifugation at 11 000 x g for 1 min. This step reduces the viscosity of the lysate. To adjust the RNA binding conditions, 600 µl of ethanol were added to the filtrate and mixed properly with the pipette. The succeeding centrifugation of the lysate through the silica membrane of the NucleoSpin® RNA column at 11 000 x g for 30 s resulted in RNA binding to the silica membrane. The addition of 350 µl of MDB and centrifugation at 11 000 x g for 1 min desalted the membrane. That step makes the rDNA digestion more effective. The DNA digestion was followed by applying of 95µl of rDNase reaction mixture onto the middle of the silica membrane of the column. The mixture was incubated for 15 min at room temperature.

Subsequent steps were conducted to wash and dry the silica membrane. First, 200 µl of the RAW 2 buffer (to inactivate the rDNase) were added to the column and centrifuged at 11 000 x g for 30 s. The column was transferred from the collection tube into another 2 ml tube. In a second wash step, 600 µl of RA3 buffer were added to the column and centrifuged at 11 000 x g for a further 30 s; the column was transferred again into the previous collection tube. Final wash by addition of 250 µl of RA3 buffer and centrifugation at 11 000 x g for 2 min caused complete drying of the silica membrane. The highly pure RNA was eluted from the membrane through addition of 60 µl of RNase-free water, followed by centrifugation through the membrane at 11 000 x g for 1 min. Gained RNA eluate was directly used for the reverse transcriptase reaction or stored at -80 °C.

2.5.2 Determination of RNA concentration

To determine the concentration of the RNA, the absorbance (A_{260}) of the solution was measured using a spectrophotometer at a wavelength of 260 nm. The calculation of the RNA concentration is based on the known absorbance value of A_{260} = 1, which corresponds to 40 µg/ml RNA.

To calculate the amount of the RNA, the A_{260} value of the measured RNA solution was multiplied by 40 µg/ml and by the dilution factor (Equation 8). The final RNA amount [µg] in the solution was calculated using Equation 9.

$$RNA\ concentration = 40\ \mu g/ml\ x\ A_{260}\ x\ dilution\ factor$$

Equation 8. Calculation of the RNA concentration.

$$Final\ RNA\ amount = concentration\ [\mu g/ml]\ x\ volume\ of\ the\ sample\ [ml]$$

Equation 9. Calculation of final RNA amount.

The purity of the RNA solution was estimated by calculation of the A_{260}/A_{280} ratio. An A_{260}/A_{280} value close to 2 indicates high purity of the RNA.

2.5.3 Reverse transcriptase reaction

Reverse transcriptase transcribes RNA to single-stranded cDNA (copy-DNA). The Omniscript Reverse Transcriptase Reaction kit was utilized to synthesize cDNA from the RNA of guinea pig spleen and cerebral cortex.

The mixture of:

Master mix	7.5 µl
RNA sample	1 µg
RNase free water	ad 20 µl

was incubated for 60 min at 37 °C, then for 5 min at 93 °C, shortly vortexed and immediately put on ice. Sterile water (80 µl) was added and samples were either directly used for PCR or stored at -20 °C. All procedures except incubation were conducted on ice and sterile equipment was used.

2.5.4 Polymerase chain reaction using *Taq* DNA Polymerase

During polymerase chain reaction, double-stranded DNA is synthesized from the cDNA template through the activity of the Taq DNA polymerase in the presence of the primers. Taq DNA polymerase is an enzyme isolated from *Thermophilus aquaticus YT1*.

All primers were designed using the primer designing tool "Primer-BLAST" (National Center for Biotechnology Information, National Library of Medicine). The properties and suitability of the primers were tested with the "Sequence Manipulation Suite – PCR Primer Stats" (www.bioinformatics.org/sms2) and verified (based on Mülhardt 2003) in terms of:

- Primer length (18-30 bases)
- Melting temperature (55-80 °C)
- GC content (40–60 %)
- GC clamp
- Self-annealing
- Product length (200-600 bp)

Primers were synthesized by Eurofins MWG Operon, Edersberg, Germany.
The sequences of the designed primers are listed in Table 12**.**

Guinea Pig:	H_4 Receptor	GAPDH
Forward	5' – AGA GAA ACT GAG CAG GTG CC – 3'	5' – TGA CCA CAG TCC ATG CCA TC – 3'
Reverse	5' – GAG CCC AGC AAA TGG CAA AA – 3'	5'– GCT TAG AGT GGG GCA GTG AC – 3'
Product length (bp)	344	567

Table 12. Sequences and product length of primers used for the polymerase chain reaction.

The reaction mixture was composed as follows:

Sample cDNA	*5 µl*
MasterMix for PCR	*45 µl*

A negative control, 5 µl of sterile water were used instead of sample cDNA. For composition of the MasterMix for PCR, see section B.1.3.2.

The reaction was performed in a thermo cycler according to the following program:

first denaturation	95 °C, 3 min	
denaturation	94 °C, 45 sec	35 cycles
primer annealing	(temperature - see Table 13), 30 sec	
extension	72 °C, 1 min	
final extension	72 °C, 10 min	
hold	4 °C	

Guinea Pig	Cortex	Spleen
H_4 Receptor	61.4 °C	61.4 °C
GAPDH	63 °C	63 °C

Table 13. Primer annealing temperatures.

PCR products were shortly centrifuged and directly used for agarose gel electrophoresis or frozen at -20 °C for later use.

2.5.5 Agarose gel electrophoresis

A 2 % (m/v) agarose gel was prepared as follows:

Agarose	2 g
0.5 x TBE buffer	ad 100 ml

Agarose was dispersed in a buffer; the mixture was heated in a microwave, avoiding boiling, till the agarose powder dissolved. To detect the DNA bands under UV light, addition of ethidium bromide is needed. Therefore, slightly cooled agarose solution was stained with 3.5 µl of EtBr and then uncongealed agarose gel was transferred into a cast with a comb placed inside of it. The comb is necessary to create the wells. The gel in the cast was cooled for about 1 h and used for electrophoresis.

The PCR reaction products were mixed with 5 µl of loading buffer (for buffer composition, see section B.1.3.2). A component of the loading buffer, Ficoll 400, enhances the density of the samples so that the samples sink into the well. The dye bromophenol blue in the loading buffer allows to observe how fast the sample is running through the gel between negative and positive

charge. The 100 bp ladder pipetted into one of the gel wells provides the template which enables sizing of the bands.

The gel was placed in the chamber filled with 0.5 x TBE buffer (running buffer) between negative and positive charge (wells on the side of negative charge). Pre-treated samples and the negative control (loading buffer only), each 45 µl, and the 100 bp DNA ladder in a volume of 15 µl were pipetted into the wells of the gel. The electrophoresis was conducted at room temperature, at constant voltage of 100 V for 40 – 50 min. Negatively charged DNA fragments pass through the gel towards the cathode, whereas the smaller fragments pass faster and further than the larger ones. After separation of the bands, the gel was placed inside of the UV-chamber and the bands were visually detected. Digital photography was made and pictures were saved (Photo documentation system, Power Shot G5, Canon). Comparison of the sample bands with the 100 bp ladder provides information about the detected fragments of genes.

2.6 Statistics

The statistical calculations were made using the GraphPad Prism 5 software.

All results are presented as arithmetic mean ($\bar{x}$) ± standard error of the mean (SEM) of n experiments. The mean value was calculated as shown in Equation 10:

$$\bar{x} = \frac{\sum_{i=1}^{n} x_i}{n}$$

Equation 10. Arithmetic mean calculation. x_i, single sample values; n, number of single values measured.

The standard deviation (SD), here designated as s, was calculated as shown in Equation 11:

$$s = \sqrt{\frac{\sum_{i}^{n}(x_i - \bar{x})^2}{n-1}}$$

Equation 11. Standard deviation calculation. x_i, single sample values; n, number of single values measured; $\bar{x}$, mean.

The standard error of the mean (SEM) was calculated using Equation 12:

$$SEM = \frac{s}{\sqrt{n}}$$

Equation 12. Standard error of the mean calculation. *s*, standard deviation; *n,* number of single values measured .

The Student's t-test was used to analyze *two* unpaired sets of values. To compare three and more groups, the one-way analysis of variance (ANOVA) was performed. The F-test was made to compare the standard deviations of two groups. The standard deviation was squared to obtain variances.

$$Variance = s^2$$

Equation 13. Calculation of variance. *s,* standard deviation.

The F ratio corresponds to:

$$F = \frac{larger\ variance}{smaller\ variance}$$

Equation 14. F ratio calculation.

The F ratio was calculated to compare variations among means of the analyzed groups. A large F value means that the variation between tested groups is higher than expected by chance. An F value close to 1.0 means that the groups do not differ. Furthermore, the P value was calculated to compare the groups and answer the question if the difference among analyzed data sets is significant. A large P value means that the differences between the groups are as expected by chance. A small P value means that the groups differ. In this thesis, P values less than 0.05 were considered significant (see Table 14).

P value	Meaning	Sign
≥ 0.05	not significant	ns
0.01 < 0.05	significant	*
0.001 < 0.01	very significant	**
< 0.001	extremely significant	***

Table 14. Significance levels.

ANOVA only allows to see if there is any difference between groups on some variable. In order to check whether this group differs from that, a post-hoc test is necessary. Here the Tukey test was used to compare all pairs of groups, whereas the Bonferroni correction was used to compare only certain pairs of data sets (Curtin and Schulz 1998).

C. Results

1. Effect of Δ^9-THC on CB_1 receptors

This thesis was prepared to answer the question: Does aging influence the tolerance development after chronic Δ^9-THC treatment in mice? For this purpose, both behavioural and biochemical experiments were conducted. The motor activity of the mice was measured using the Open Field Test. Subsequently CB_1 receptor activity in hippocampus was examined in ^{35}S-GTPγS binding experiments, post mortem.

In preliminary experiments, the proper dose of Δ^9-THC was determined; treatment with 3 mg/kg Δ^9-THC did not elicit significant behavioural and binding effects (results not shown) so, the dose of Δ^9-THC had to be increased to 10 mg/kg and the term "Δ^9-THC" corresponds to this dose in the rest of this section.

1.1 Behavioural test: Open Field Test

The effects of Δ^9-THC on numerous species, among others on mice, are discussed in section A.1, (Martin et al. 1991) of this thesis. The suppression of the spontaneous activity (hypoactivity), plus hypothermia, analgesia and catalepsy are known as the tetrad test for cannabinoid activity (Chaperon and Thiébot 1999). The intensity of the animal reaction to cannabinoids can be measured using these parameters. In this thesis, the Open Field Test was used to observe the activity suppression in mice and to detect the tolerance development to Δ^9-THC effects in mice chronically pre-treated with Δ^9-THC. The results were compared between adolescent and aged groups.

The results are presented as the distance travelled and the rearing number which are mouse activity markers (the higher the values, the higher the motor activity or exploring, respectively), whereas the resting time parameter illustrates the activity suppression (the higher the value, the lower the activity).

1.1.1 General

The Open Field Test is a behavioural test used to measure the activity (motility) of the rodents. The mouse is placed in the middle of an open space surrounded by a wall, which prevents escape. The measured behaviour of the mouse provides information about its condition. The Open Field Test is widely used in animal psychology e.g. in 'anxiety' models (Prut and Belzung 2003) and is a sensitive and relatively simple method to measure effects of pharmacological treatment (Choleris et al. 2001). A difficulty of this method is the reproducibility of the results, which depends on various parameters like housing of animals, transport of an animal to the open field frame from its home cage and many other immeasurable aspects (e.g. interaction of the animal with the experimenter) (Walsh and Cummins 1976).

In this study, motor activity of two age groups of mice (adolescent and old) was measured in three different treatment models (acute, chronic and control) according to Bass and Martin (2000) with modifications. Subsequently, the Open Field Test was performed. Details are given in section B.2.1.1; for composition of the injections see Table 5 and for the treatment schedule see: Table 7. Briefly, animals in the acute group were pre-treated with vehicle and challenged with Δ^9-THC, those in the chronic group were injected with Δ^9-THC as pre-treatment and challenged with Δ^9-THC, whereas the control group was injected with vehicle only. The parameters distance travelled [m], rearing number and resting time [s] were measured in an Open Field apparatus for 10 min in the darkness (infrared light) as described in section B.2.2.

The parameters indicating motor activity, i.e. distance travelled (Figure 10A) and exploratory behaviour expressed as rearing number (Figure 10B), were suppressed in animals challenged acutely with Δ^9-THC, compared to the control group. The repetitive pre-treatment with Δ^9-THC (chronic) resulted in a lower decrease of activity after the Δ^9-THC challenge dose than in the acutely treated group. However, Δ^9-THC pre-treatment did not completely prevent the effect of the Δ^9-THC challenge dose. The motor activity decrease in chronically treated animals compared to the vehicle treated controls was significant, but tended to be weaker than in mice after the acute Δ^9-THC dose. Furthermore, the difference between the acute and chronic treatment group was significant for rearing behaviour (Figure 10B), but not for distance travelled (Figure 10A). The rearing number parameter seems to be very sensitive to Δ^9-THC and points to tolerance development in mice after Δ^9-THC pre-treatment. However, a tendency towards a decreasing response to Δ^9-THC after chronic pre-treatment was also observed for "distance travelled".

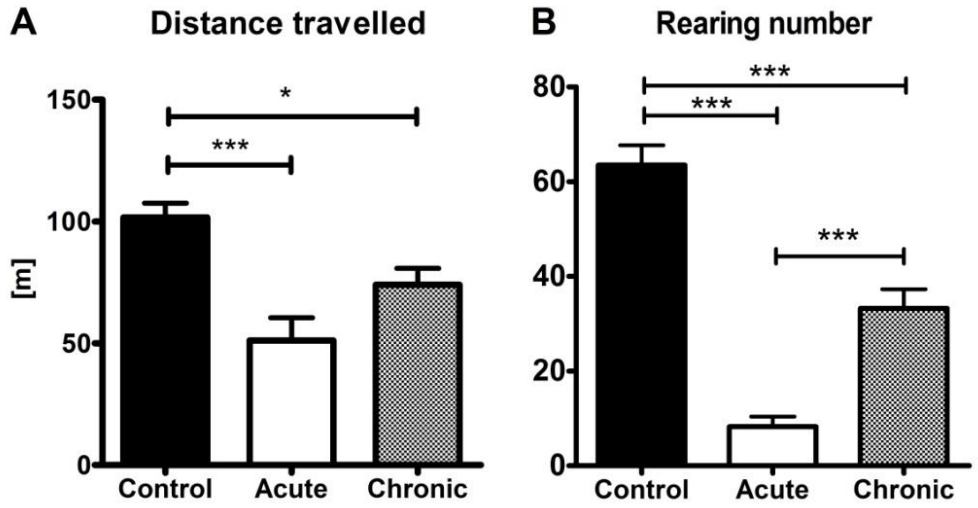

Figure 10. Open Field Test in C57BL/6J adolescent mice treated as shown in Table 7. Animal motor activity (distance travelled, A; rearing number, B) was tested in the Open Field apparatus for 10 min in the darkness (infrared). Treatment groups: Control – pre-treated and challenged with vehicle only; Acute – pre-treated with vehicle and challenged with 10 mg/kg Δ^9-THC, Chronic – pre-treated and challenged with 10 mg/kg Δ^9-THC. Means ± SEM from 8 mice. One-way ANOVA with Tukey multiple comparison post-test: *p<0.05, ***p<0.001.

The third parameter measured in the Open Field Test, resting time (that indicates a reduction of the motor activity of mice), was increased or tended to be increased in both groups challenged with Δ^9-THC, compared to the vehicle treated control, as shown in Figure 11. The acute administration of the Δ^9-THC to mice caused a significant increase in resting time compared to the vehicle-treated controls. The resting time of the mice pre-treated with Δ^9-THC did not differ from control or from the acutely Δ^9-THC treated group; however, there was a tendency towards tolerance development after chronic Δ^9-THC treatment.

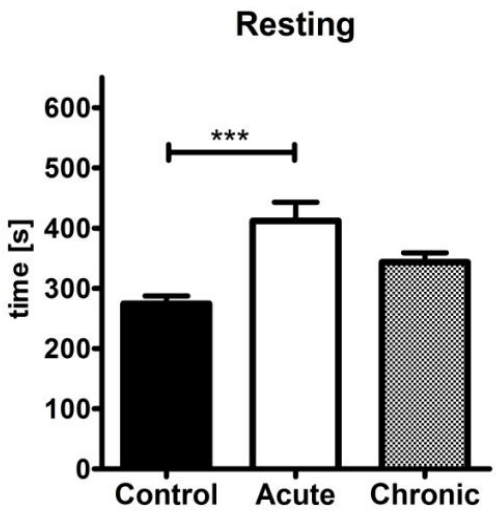

Figure 11. Open Field Test in C57BL/6J adolescent mice treated as shown in Table 7. The suppression of motor activity was tested in the Open Field apparatus for 10 min in the darkness (infrared). Treatment groups: Control – pre-treated and challenged with vehicle only; Acute – pre-treated with vehicle and challenged with 10 mg/kg Δ^9-THC; Chronic – pre-treated and challenged with 10 mg/kg Δ^9-THC. Means ± SEM from 8 mice. One-way ANOVA with Tukey multiple comparison post-test: ***$p<0.001$.

To sum up, pre-treatment of mice with Δ^9-THC resulted in tolerance to Δ^9-THC effects in rearing behaviour. A tendency towards tolerance development after chronic Δ^9-THC treatment was observed for the parameters distance travelled and resting time.

1.1.2 Comparison of adolescent and old mice

The next step in the experiments was the comparison of the activity level between adolescent and old mice, acutely and chronically treated with Δ^9-THC. To standardize the results and simplify the comparisons, all parameters measured were normalized to the percent of activity (% activity; calculated as explained in section B.2.2, Equation 1). Moreover, activity suppression of acutely and chronically treated mice was normalized to the control group of the age-matched animals (% activity suppression; calculated as explained in section B.2.2, Equation 2 and Equation 3).

The age had no influence on distance travelled and resting in control animals (not treated with Δ^9-THC) whereas the third parameter, rearing number, was reduced by ~ 50 % in old age (Figure 12).

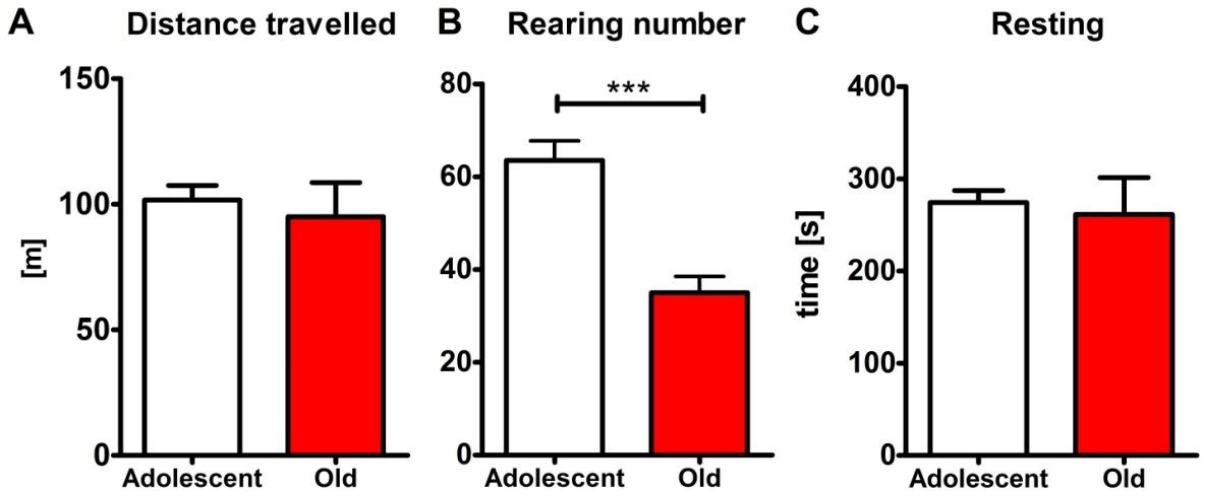

Figure 12. Open Field Test in untreated C57BL/6J adolescent and old mice. Parameters: A: Distance travelled [m], B: Rearing number and C: Resting time [s] measured in an Open Field apparatus for 10 min in the darkness (infrared). Means ± SEM from 8 mice. Student's t-test: ***p<0.001.

Acute treatment with Δ^9-THC suppressed activity also in old mice; the % activity suppression tended to be higher in old vs. adolescent mice for each of the three parameters (Figure 13). Chronic treatment led to a suppressed activity also in old mice; again, the activity suppression tended to be higher in old than in adolescent mice (Figure 13). The % activity suppression was lower for each of the three parameters after chronic than acute administration of Δ^9-THC, both in adolescent and old animals; however, this difference reached significance for the rearing number in adolescent animals only (Figure 13). Ageing does not alter tolerance development in the rearing number and resting time, i.e., activity suppression was attenuated by 40-50 % when compared to acute treatment (Figure 13B, C, Table 15). With respect to the distance travelled, tolerance development appears to be lower in old (by 21 %) than in adolescent mice (by 46 %); the difference does, however, not reach a significant level (Figure 13A, Table 15).

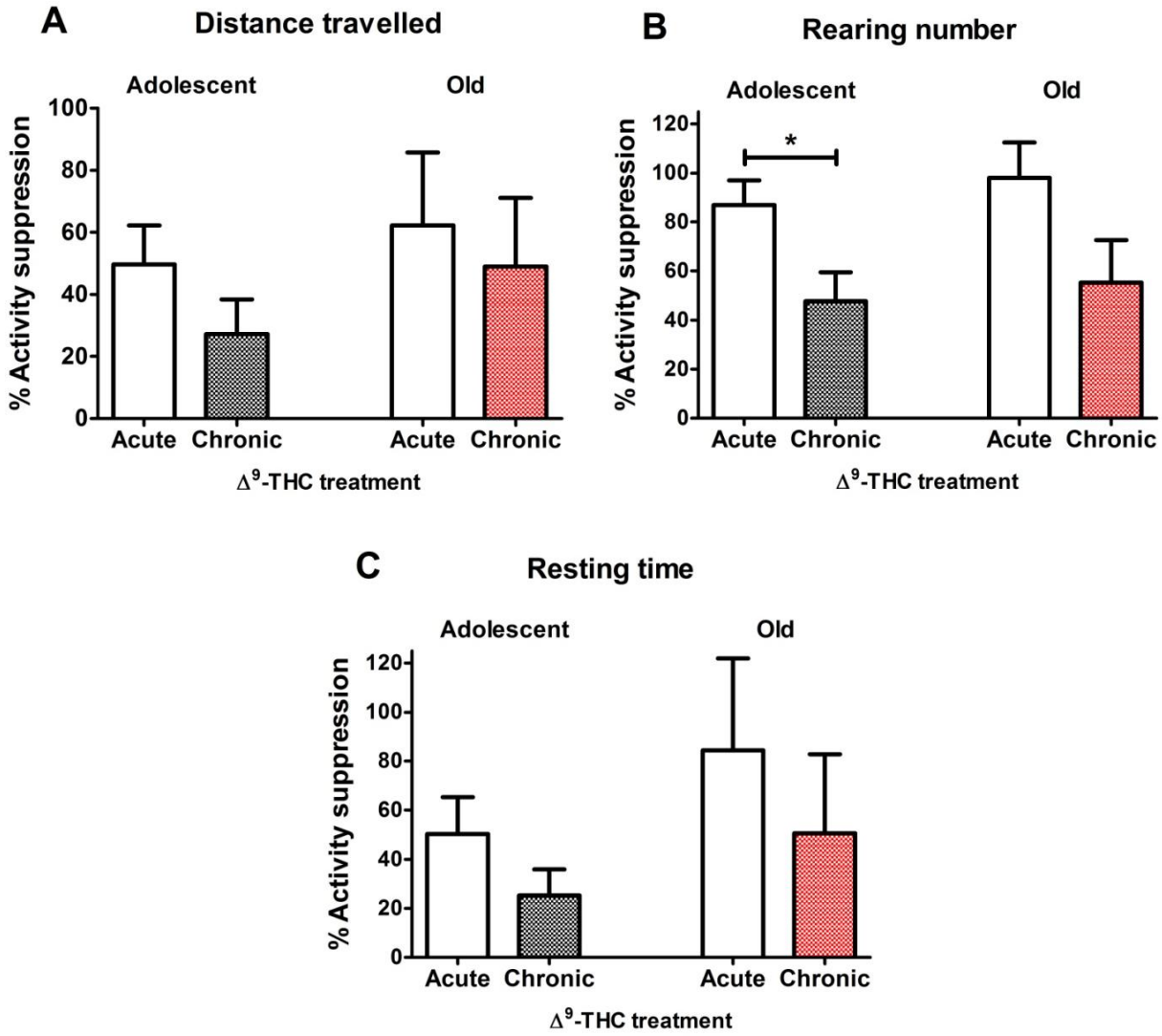

Figure 13. Open Field Test in Δ9-THC treated C57BL/6J adolescent and old wild type mice. Parameters measured: A: distance travelled, B: rearing number and C: resting time, normalized and expressed in percent of activity suppression. Treatment groups: Acute – pre-treated with vehicle and challenged with 10 mg/kg Δ9-THC, Chronic – pre-treated and challenged with 10 mg/kg Δ9-THC. Means ± SEM from 7-9 mice. Student's t-test: *p<0.05.

	Tolerance [%]		
	Distance travelled	Rearing number	Resting time
Adolescent	46	45	50
Old	21	44	39

Table 15. Comparison of tolerance development towards Δ9-THC in adolescent and old mice for the three parameters of the Open Field Test. Tolerance (%) was calculated as $(1 - \frac{\%\ Activity\ suppression\ Chronic}{\%\ Activity\ suppression\ Acute}) \times 100$.

1.2 Biochemical test: ^{35}S-GTPγS binding

1.2.1 General

To optimize the agonist-stimulated ^{35}S-GTPγS binding method for experiments on pharmacologically treated mice, numerous pre-tests were conducted to find an appropriate CB_1 receptor agonist.

One of the most potent synthetic CB_1 receptor agonists, WIN 55,212-2 (Griffin et al. 1998; Pertwee and Ross 2002; Childers 2006; Svízenská et al. 2008, described in section A.2.1.1; for structure see Table 2), was used in ^{35}S-GTPγS binding studies on wild type ($CB_1^{+/+}$) mouse hippocampal membranes. As shown in Figure 14, WIN 55,212-2 concentration-dependently stimulated specific ^{35}S-GTPγS binding; an increase of specific binding by 156 % was observed at 30 μM WIN 55,212-2, the highest concentration tested.

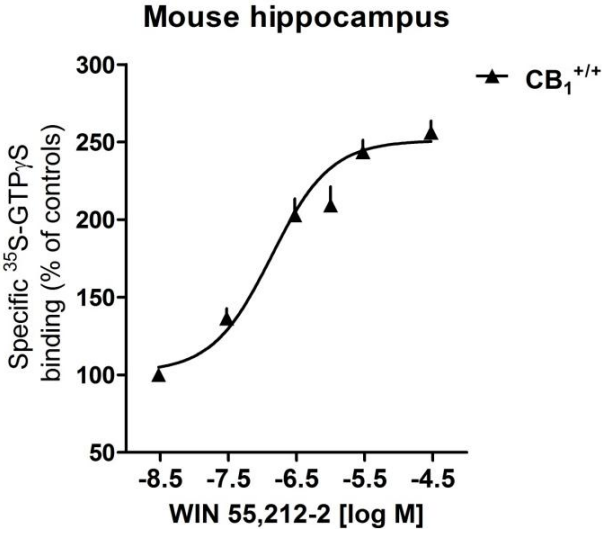

Figure 14. Effect of the CB_1 receptor agonist WIN 55,212-2 on the specific ^{35}S-GTPγS binding to C57BL/6J wild type mouse hippocampus membranes (6.5 μg/50 μl). Means ± SEM from 7 experiments. Unspecific binding (in the presence of GTPγS 10 μM): 27± 1 %.

Several references point to unspecific, non-cannabinoid receptor dependent effects of WIN 55,212-2 (Breivogel et al. 2001; Wiley and Martin 2002). To investigate whether this is relevant for the present experiments on hippocampus membranes, ^{35}S-GTPγS binding experiments were carried out on hippocampal membranes from CB_1 receptor knockout mice ($CB_1^{-/-}$). Since in hippocampal membranes from CB_1 receptor deficient mice WIN 55,212-2,

30 µM still increased binding by 43 %, (Figure 15) we were wondering whether this effect is related to CB_2 receptor activation. Since the expression of the CB_2 receptor in the central nervous system remains a controversial issue (Griffin et al. 1999; Gong et al. 2006; Atwood and Mackie 2010), further experiments on CB_1 and CB_2 double knockout mice ($CB_1^{-/-}/CB_2^{-/-}$) were conducted. As shown in Figure 15, the concentration-response curves of WIN 55,212-2 in membranes from $CB_1^{-/-}$ and $CB_1^{-/-}/CB_2^{-/-}$ mice were virtually identical. Again, an increase in specific binding by 43 % occurred at 30 µM. These findings indicate that the effects obtained with WIN 55,212-2 are related to an unknown, CB_1 and CB_2 receptor-independent mechanism.

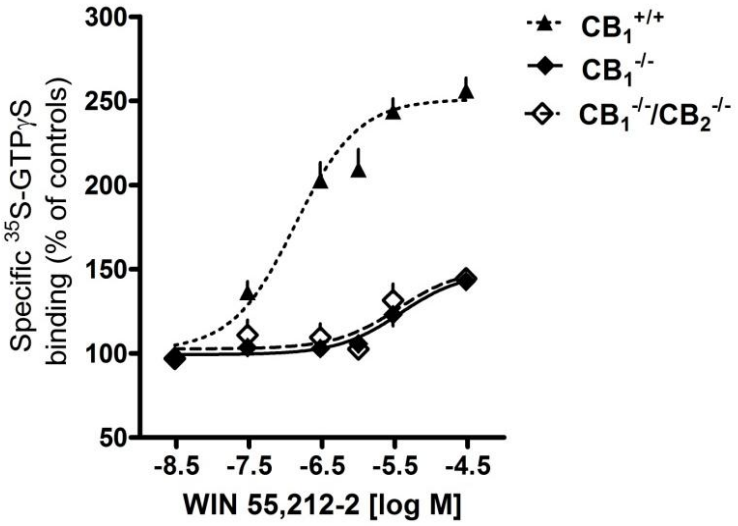

Figure 15. Effect of the CB_1 receptor agonist WIN 55,212-2 on the specific ^{35}S-GTPγS binding to C57BL/6J wild type ($CB_1^{+/+}$), CB_1 receptor knockout ($CB_1^{-/-}$) and CB_1 and CB_2 receptor double knockout ($CB_1^{-/-}/CB_2^{-/-}$) mouse brain hippocampus membranes (6.5 µg/50 µl). Means ± SEM from 3-7 experiments. Unspecific binding (in the presence of GTPγS 10 µM): 29 ± 2 %.

As already mentioned, the maximum effect of 156 % was decreased to 43 % in $CB_1^{-/-}$ and double knockout mice (Figure 15, Table 16). Moreover, the potency of WIN 55,212-2, expressed as the pEC_{50} value, was reduced by a factor of ~ 25 in membranes from knockout and double knockout mice (Table 16).

Mouse strain	pEC_{50} value	Maximal binding [%]
Wild type ($CB_1^{+/+}$)	6.87 ± 0.12	156 ± 7
CB_1 knockout ($CB_1^{-/-}$)	5.43 ± 0.20 ***	43 ± 3 ***
CB_1 and CB_2 double knockout ($CB_1^{-/-}$/ $CB_2^{-/-}$)	5.45 ± 0.34 **	43 ± 8 ***

Table 16. pEC_{50} values and maximal effects of WIN 55,212-2 for ^{35}S-GTPγS binding studies on wild type ($CB_1^{+/+}$), CB_1 receptor knockout ($CB_1^{-/-}$) and CB_1 and CB_2 receptor double knockout ($CB_1^{-/-}$/ $CB_2^{-/-}$) mice. The maximal binding of WIN 55,212-2 occurred at 30 µM. Means ± SEM from 3-7 experiments. One-way ANOVA with Bonferroni's multiple comparison test: **p<0.01, ***p<0.001.

The WIN 55,212-2-related increase in ^{35}S-GTPγS binding on membranes from CB_1 and CB_2 knockout mice (see Figure 15) speaks against the use of WIN 55,212-2 as an appropriate agonist for further experiments. Therefore, another potent cannabinoid receptor agonist, CP 55,940 (for structure see Table 2), was studied on membranes from wild type ($CB_1^{+/+}$) and CB_1 receptor deficient mice ($CB_1^{-/-}$).

As shown in Figure 16 and summarized in Table 17, CP 55,940 stimulated specific ^{35}S-GTPγS binding concentration-dependently; the maximum, obtained at a concentration of 30 µM, was 94 %. The same dilution series of CP 55,940 examined on hippocampal membranes from CB_1 receptor knockout mice ($CB_1^{-/-}$) failed to alter specific ^{35}S-GTPγS binding. Thus, further experiments on membranes from CB_1 and CB_2 double knockout mice were not necessary.

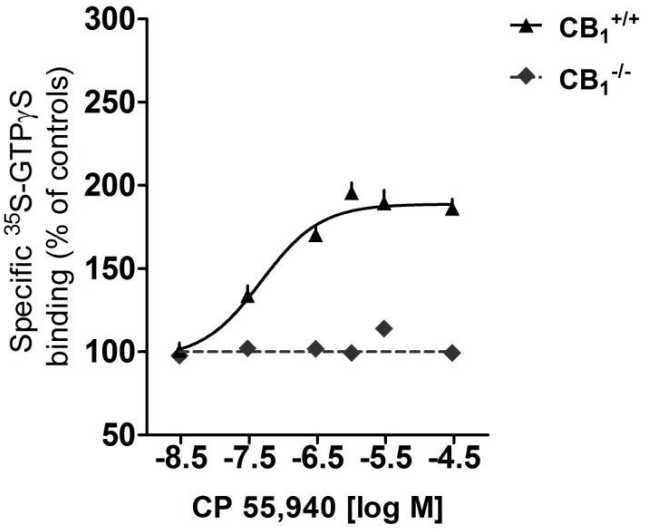

Figure 16. Effect of the CB_1 receptor agonist CP 55,940 on the specific ^{35}S-GTPγS binding on C57BL/6J wild type ($CB_1^{+/+}$), and CB_1 knockout ($CB_1^{-/-}$) mouse brain hippocampus membranes (6.5 µg/50 µl). Means ± SEM from 3-4 experiments. Unspecific binding (in the presence of GTPγS 10 µM): 26 ± 4 %.

Although the WIN 55,212-2-stimulated ^{35}S-GTPγS binding on wild type mouse hippocampus was stronger (maximal binding of 156%) than that of CP 55,950 (maximal binding of 94%), as shown in Table 17, the absence of a non-specific effect of CP 55,940 in CB_1 receptor knockout mice ($CB_1^{-/-}$) provides a sufficient reason to choose CP 55,940 as a standard agonist for further investigation of CB_1 receptor activity changes. Interesting enough, the potency (pEC_{50}) of CP 55,940 is 2.8-fold higher than that of WIN 55,212-2 (Table 17 and Table 16).

Mouse type	**pEC_{50} value**	**Maximal binding [%]**
Wild type ($CB_1^{+/+}$)	7.32 ± 0.24	94 ± 7
CB_1 knockout ($CB_1^{-/-}$)	-	-2 ± 6 ***

Table 17. pEC_{50} value in wild type mice and maximal binding effects of CP 55,940 in wild type ($CB_1^{+/+}$) and CB_1 receptor knockout ($CB_1^{-/-}$) mice in ^{35}S-GTPγS binding studies. The maximal binding effect obtained with CP 55,940 occurred at of 30 μM. Means ± SEM from 3-4 experiments. Student's t test: ***p<0.001.

1.2.2 Comparison of adolescent and old mice

The ^{35}S-GTPγS binding studies on mouse hippocampal membranes were conducted to investigate the activity of the CB_1 receptor after chronic Δ^9-THC treatment. For this purpose, the hippocampi of the mice repetitively treated with Δ^9-THC and their vehicle treated, age-matched controls were examined to detect adaptive receptor changes in ^{35}S-GTPγS binding experiments.

The adolescent and old mice pre-treated according to the scheme in Table 7 and tested in the Open Field Test were subsequently killed by decapitation; brains were removed and hippocampi isolated as described in section B.2.3.2. All ^{35}S-GTPγS binding experiments in this series were evaluated using "cpm over basal" values as the unit of the CB_1 receptor activation. The use of "% of controls" was inappropriate for presentation of this data, since surprisingly there were differences between the groups at the level of basal receptor binding (receptor binding in the absence of any agonist, see Figure 17). The unspecific binding was between 15 and 26 % of total binding.

As shown in Figure 17, basal ^{35}S-GTPγS binding of adolescent mice chronically treated with Δ^9-THC was significantly lower than basal binding of vehicle-treated age-matched mice. In other words, the basal binding of chronically Δ^9-THC treated adolescent mice was down-regulated. Basal binding to hippocampi of chronically Δ^9-THC and vehicle treated aged mice did not differ;

these values did not differ from basal binding of adolescent Δ9-THC treated mice, but were lower than basal binding of adolescent vehicle treated mice.

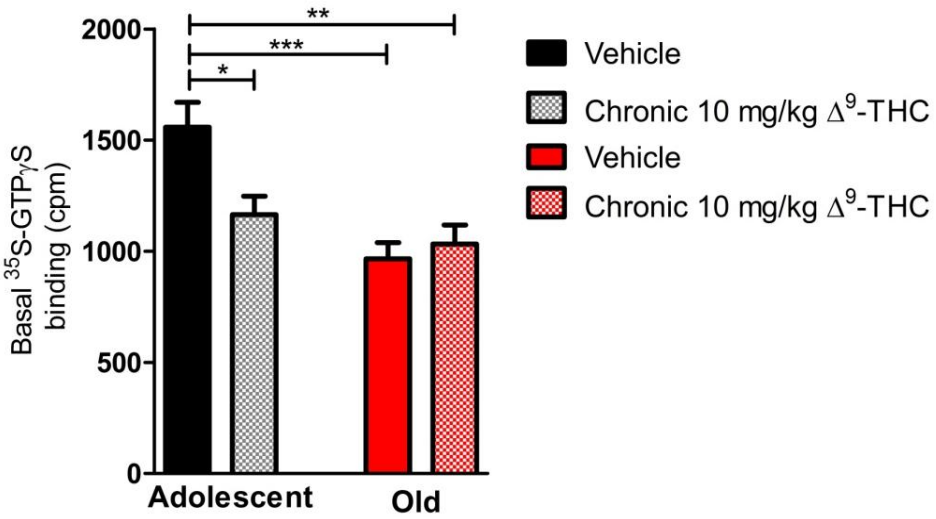

Figure 17. Basal ^{35}S-GTPγS binding (cpm) to adolescent and aged C57BL/6J wild type mouse hippocampal membranes (6.5 μg/50 μl). Vehicle – mice pre-treated and challenged with vehicle; Chronic – mice pre-treated and challenged with 10 mg/kg Δ9-THC. Means ± SEM from 7-9 experiments. Unspecific binding (in the presence of GTPγS 10 μM): 13.3 ± 1.8 % (adolescent) and 17 ± 0.4 % (old). One-way ANOVA with Tukey multiple comparison post-test: *p<0.05, **p<0.01, ***p<0.001.

The concentration-response curves of the CP 55,940-induced ^{35}S-GTPγS binding in adolescent mice (Figure 18A) strongly differed for membranes from Δ9-THC and vehicle treated mice (significant difference for CP 55,940 ≥ 0.03 μM). Membranes from Δ9-THC treated young animals showed a lower receptor binding, compared to vehicle treated mice. On the other hand, as shown in Figure 18B, chronic treatment with Δ9-THC did not affect the concentration-response curves of CP 55,940-induced ^{35}S-GTPγS binding within the aged mice.

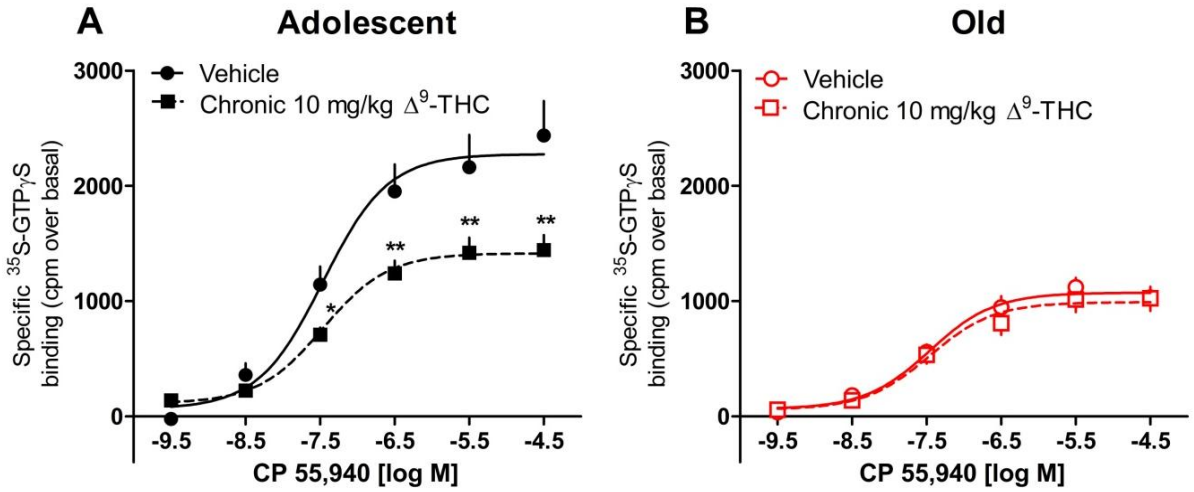

Figure 18. Effect of the CB_1 receptor agonist CP 55,940 on the ^{35}S-GTPγS binding (cpm over basal) to hippocampal membranes from adolescent (A) and old (B) C57BL/6J wild type mice (6.5 µg/50 µl). Vehicle – animals pre-treated and challenged with vehicle only; Chronic – pre-treated and challenged with 10 mg/kg Δ^9-THC. Means ± SEM from 7-8 (A) and 9 (B) experiments. Unspecific binding (in the presence of GTPγS 10 µM): 13.3 ± 1.8 % (A) and 17 ± 0.4 % (B). Student's t-test: *p<0.05, **p<0.01.

As shown in Figure 19 and Table 18, the maximal binding (binding stimulated by CP 55,940 at a concentration of 30 µM) was significantly down-regulated in adolescent, Δ^9-THC treated mice compared to their vehicle treated controls. In aged animals no significant differences in maximal binding occurred between the two treatment groups. The potency of CP 55,940 was identical for each of the four groups of animals (Table 18).

Treatment	Age	pEC_{50} value	Maximal binding [cpm over basal]
Vehicle (control)	Adolescent	7.48 ± 0.19	2440 ± 300
Δ^9-THC 10 mg/kg (chronic)		7.38 ± 0.15	1440 ± 130
Vehicle (control)	Old	7.49 ± 0.15	1030 ± 90
Δ^9-THC 10 mg/kg (chronic)		7.46 ± 0.19	1020 ± 110

Table 18. Maximal binding (obtained with 30 µM CP 55,940) and pEC_{50} values of the CP 55,940-stimulated ^{35}S-GTPγS binding in hippocampal membranes from vehicle and Δ^9-THC chronically treated adolescent and old C57BL/6J wild type mice. Vehicle – animals pre-treated and challenged with vehicle only, Chronic – pre-treated and challenged with 10 mg/kg Δ^9-THC. Means ± SEM from 7-9 experiments.

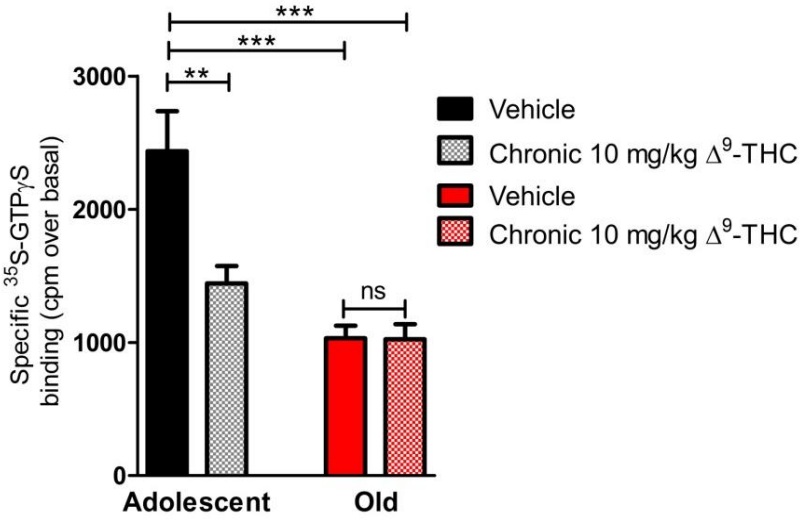

Figure 19. Maximal effect of the CB_1 receptor agonist CP 55, 940 for its stimulatory effect on ^{35}S-GTPγS binding (cpm over basal) to hippocampal membranes from adolescent and old C57BL/6J wild type mice (6.5 µg/50 µl). Vehicle – animals pre-treated and challenged with vehicle only; Chronic – pre-treated and challenged with 10 mg/kg Δ^9-THC. Means ± SEM from 7-9 experiments. Unspecific binding (in the presence of GTPγS 10 µM): 13.3 ± 1.8 % (adolescent) and 17 ± 0.4 % (old). One-way ANOVA with Tukey multiple comparison post-test: **p<0.01, ***p<0.001.

2. Effect of MAGL blockade on CB_1 receptors

It was reported in the literature that endogenous and exogenous cannabinoids can act neuroprotective (Centonze et al. 2007; Bilkei-Gorzo 2012). Activation of CB_1 receptors protects against age-related neuronal damage (Albayram et al. 2011; 2012), but on the other hand, long-term CB_1 receptor activation can lead to adaptive changes and receptor down-regulation, as shown in this thesis in adolescent mice chronically treated with Δ^9-THC and in numerous other reports (Martin et al. 2004). The indirect activation of the endocannabinoid system through degradation blockade as therapeutic target is attracting more and more attention (Di Marzo et al. 2007; Fowler 2012; Katz et al. 2014).

The goal of this part of the project was to find a JZL 184 dose and treatment period which enhance endocannabinoid levels, but do not elicit receptor down-regulation in mouse hippocampus. Briefly, the levels of the endocannabinoids (2-AG and AEA) and of their degradation product (AA) were determined and correlated with receptor activity changes.

In detail, male CD 1 mice were treated with JZL 184 once daily in doses of 4, 10 and 40 mg/kg or with vehicle during different periods of time (1 day, 3 days and 14 days), according to the scheme presented in Table 8. About 24 h after last treatment, animals were killed by

decapitation and each hemisphere of the hippocampus was isolated separately and rapidly frozen in pre-cooled reaction tubes. The left hemisphere of the hippocampus was used for ^{35}S-GTPγS binding studies whereas the right hemisphere was stored for endocannabinoid determination with the LC-MS/MS (LC-MRM) method.

2.1 Endocannabinoids determined by LC-MRM

As described in section A.2.1.2 and presented in Figure 5 and Figure 6, both main endocannabinoids AEA and 2-AG are hydrolysed by specific degrading enzymes. Although different enzymes are involved in the degradation of each endocannabinoid (FAAH for AEA and MAGL for 2-AG), one of the products of the hydrolysis reaction, namely arachidonic acid, is the same for both substrates.

As presented in Figure 20A, after a single dose of JZL 184 (treatment duration of 1 day), only the highest dose of 40 mg/kg JZL 184 caused a significant elevation in 2-AG concentration whereas both lower JZL 184 doses (4 and 10 mg/kg) failed to do so. After 3 days of treatment, the 2-AG level was still significantly affected only by 40 mg/kg JZL 184, however, the JZL 184 dose of 10 mg/kg tended to increase the 2-AG concentration. The chronic treatment with JZL 184 for 14 days resulted in a strong, significant increase in the 2-AG concentration at 10 and 40 mg/kg whereas 4 mg/kg JZL 184 did not affect the 2-AG level. Furthermore, after 14 days of JZL 184 administration, the AA concentrations were affected in the opposite way compared to the 2-AG levels (see Figure 20C). Since the AA is formed as one of the products of endocannabinoid degradation (see Figure 5 and Figure 6), JZL 184 at 40 mg/kg and surprisingly 4 mg/kg but not at 10 mg/kg given for 14 days was associated with AA concentrations significantly lower than control. The AEA concentrations were not affected by any dose of JZL 184, even after long-term treatment (Figure 20B).

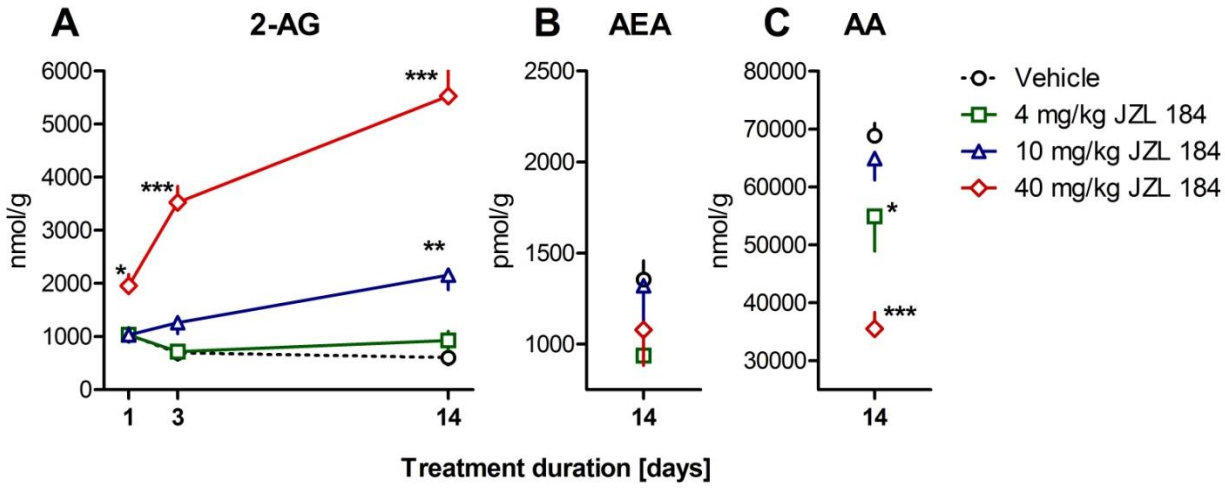

Figure 20. Concentrations of the endocannabinoids 2-AG and AEA and their degradation product AA in the hippocampus of JZL 184 treated CD-1 mice. 2-AG [nmol/g] levels after 1, 3 and 14 days of JZL 184 or vehicle treatment; AEA [pmol/g] and AA [nmol/g] after 14 days of JZL 184 or vehicle treatment. Means ± SEM from 7-8 mouse hippocampi. One-way ANOVA with Bonferroni multiple comparison post-test: *p<0.05, **p<0.01, ***p<0.001.

To sum up, the dose of 40 mg/kg JZL 184 was the most effective one and caused a significant elevation of the 2-AG concentration from the first day of administration onward, whereas 4 mg/kg JZL 184 failed to affect the 2-AG concentration regardless of the treatment duration. The dose of 10 mg/kg caused a significant increase in 2-AG level after 14 days of JZL 184 administration, but an upward trend was visible already after 3 days of administration.

2.2 CB_1 receptor activity determined by ^{35}S-GTPγS binding

As described in section A.2.1.2, the treatment with JZL 184 causes MAGL blockade and thus inhibition of the 2-AG metabolism. The elevated concentration of 2-AG causes enhanced cannabinoid receptor activation. The long-term activation of a given receptor can result in its desensitization and/or down-regulation (Martin et al. 2004). Studying the CP 55,940-stimulated ^{35}S-GTPγS binding, the functional changes of the CB_1 receptor through JZL 184 (administrated at different doses and over different time periods) were examined.

Basal ^{35}S-GTPγS binding, which was 947 ± 224 cpm in membranes from vehicle-treated mice (mean value ± SEM; n=6) was not affected by the JZL 184 treatment (not shown). As shown in Figure 21, the CP 55,940-stimulated ^{35}S-GTPγS binding to the hippocampus of mice treated with 4, 10 and 40 mg/kg JZL 184 and vehicle for 14 days did not differ significantly between

treatments. The concentration-response curves of the animals treated with 4 and 10 mg/kg JZL 184 coincided with the curve of the vehicle-control. However, the curve for the mice treated with 40 mg/kg JZL 184 showed a tendency (not significant) towards a down-regulation of the specific binding, compared to the control.

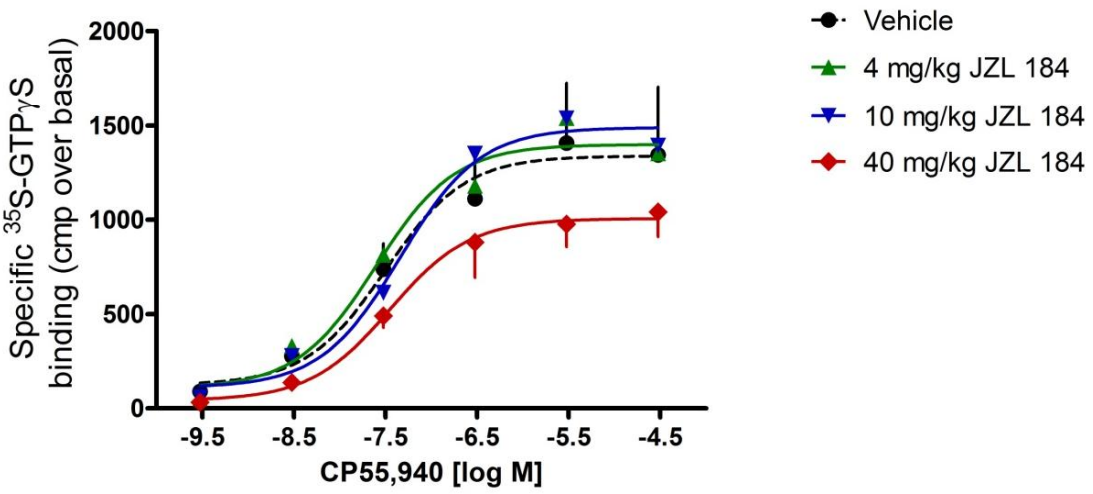

Figure 21. Effect of the CB_1 receptor agonist CP 55,940 on the specific ^{35}S-GTPγS binding (cpm over basal) to hippocampal membranes from CD-1 mice (6.5 µg/50 µl). Concentration-response curves of animals treated for 14 days with 4, 10 or 40 mg/kg JZL 184 or with vehicle. Means ± SEM from 5-6 experiments. Unspecific binding (in the presence of GTPγS 10 µM): 12.2 ± 0.8 %

The concentration-response curves for ^{35}S-GTPγS binding to hippocampal membranes did not differ between treatment regimens when JZL 184 at any dose was given for 1 day or 3 days only; therefore, the corresponding concentration-response curves are not shown here.

3. Searching for H_4 receptors

The presence of the H_4 receptor in the CNS has been a controversial topic for over one decade (Liu et al. 2001; Strakhova et al. 2009; reviewed by Marson 2011). In this thesis, I studied the mRNA expression of the H_4 receptor in guinea pig cerebral cortex and sought for a functional readout of this receptor in the CNS using the ^{35}S-GTPγS binding method.

3.1 Searching for mRNA: RT-PCR

Male Dunkin-Hartley guinea pigs were killed by decapitation and the cerebral cortex and spleen were isolated and directly frozen at -80 °C. Further procedures, such as tissue preparation, genetic material isolation, PCR and agarose gel electrophoresis were conducted as described in section: B.2.5. Primer sequences used for the PCR experiments are listed in Table 12.

The presence of H_4 receptor mRNA was previously detected in human and mouse cerebral cortex using the RT-PCR method (Schulte 2011). Therefore, detection of the H_4 receptor in the cortex tissue of the guinea pig was tried as well. The guinea pig spleen was examined for comparison, since it is well known that the H_4 receptor is expressed in this organ (Liu et al. 2001).

Figure 22 shows that the 344 bp products expected for the H_4 receptor sequence were found in cerebral cortex and spleen (positive control) of the guinea pig. The 567 bp GAPDH product (housekeeping gene) was also shown for both tested tissues.

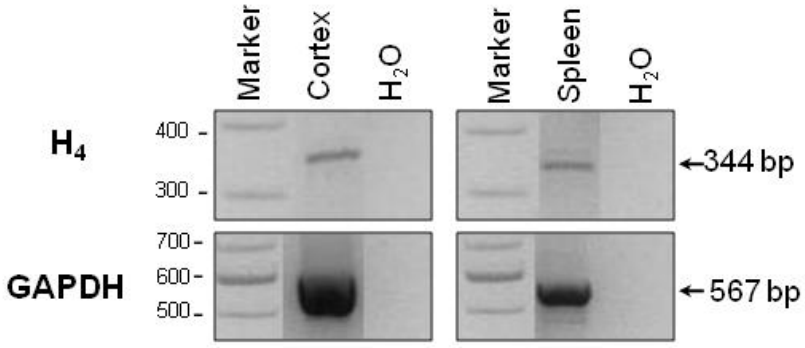

Figure 22. Detection of histamine H_4 receptor mRNA in the guinea-pig cerebral cortex and spleen by reverse transcriptase-polymerase chain reaction. The arrows in the upper panels (H_4) indicate the products expected for the guinea-pig H_4 sequence, whereas the arrows in the lower panels (GAPDH) refer to GAPDH, which was used as a housekeeping gene. Water was used instead of cDNA template as a negative control. The scale for the molecular weights of the amplicons (expressed in base pairs, bp) is given on the left of each panel (Marker). Representative picture chosen from n=3 experiments.

3.2 Searching for a functional readout: ^{35}S-GTPγS binding

To investigate the presence of functional histamine H_4 receptor on membranes of cerebral cortex of guinea pig and mouse, ^{35}S-GTPγS binding was studied in cortex homogenates. 4-Methylhistamine was chosen as H_4 receptor agonist. The H_3 agonist R-α-methylhistamine served as positive control to verify the functionality of the assay (for chemical structures of the histamine receptor ligands see Table 4).

On guinea pig cerebral membranes (Figure 23A), 4-methylhistamine did not have any effect up to 1 µM. Nevertheless, a further increase of the 4-methylhistamine concentration enhanced the ^{35}S-GTPγS binding (by 13 % at 100 µM). The addition of the H_4 receptor antagonist JNJ-7777120 in a concentration of 1 µM did not alter the effect of 4-methylhistamine on guinea pig cerebral cortex membranes. JNJ-7777120 1 µM, given alone, did not show any effect on ^{35}S-GTPγS binding in guinea pig cortex. The partial agonist of the H_4 receptor, ST-1006, also failed to cause any effect on the ^{35}S-GTPγS receptor binding, even at a concentration as high as 100 µM. The positive control is presented in Figure 23B. The H_3 receptor agonist R-α-methylhistamine 0.001 to 0.3 µM concentration-dependently enhanced ^{35}S-GTPγS binding with a maximal binding effect of 23 % which was induced by 0.1 µM R-α-methylhistamine. The addition of the H_3 receptor antagonist thioperamide at 0.1 µM caused a rightward-shift of the R-α-methylhistamine curve, which confirms the involvement of the H_3 receptor. Thioperamide, given alone (0.1 µM), did not affect the specific ^{35}S-GTPγS binding.

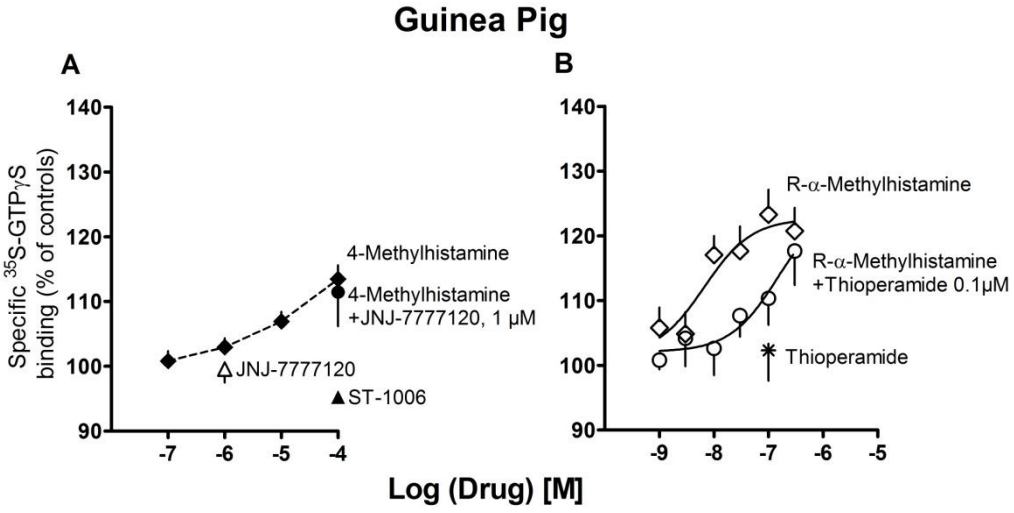

Figure 23. Effect of histamine H_4 (A) and H_3 (B) receptor ligands on the specific ^{35}S-GTPγS binding to guinea pig cortex membranes. The effect of (A) the H_4 agonist 4-methylhistamine, the partial H_4 agonist ST-1006, the H_4 antagonist JNJ-7777120 and (B) the H_3 agonist *R*-α-methylhistamine and the H_3 antagonist thioperamide (as positive controls) were studied. H_4 and H_3 receptor ligands were given alone or combined. Means ± SEM from 3 - 6 experiments. Unspecific binding (in the presence of GTPγS 10 µM): 22.3± 0.8 (A) and 13.3 ± 1.3 (B).

In experiments on mouse cortical membranes (C57BL/6J, wild type), 4-methylhistamine 3 nM to 30 µM failed to stimulate the specific ^{35}S-GTPγS binding (Figure 24A), whereas the H_3 receptor agonist R-α-methylhistamine caused a 23 % increase in ^{35}S-GTPγS binding (Figure 24B). The addition of 0.1 µM thioperamide resulted in the shift of the R-α-methylhistamine curve to the right, as expected. Thioperamide given alone failed to affect the binding (Figure 24B).

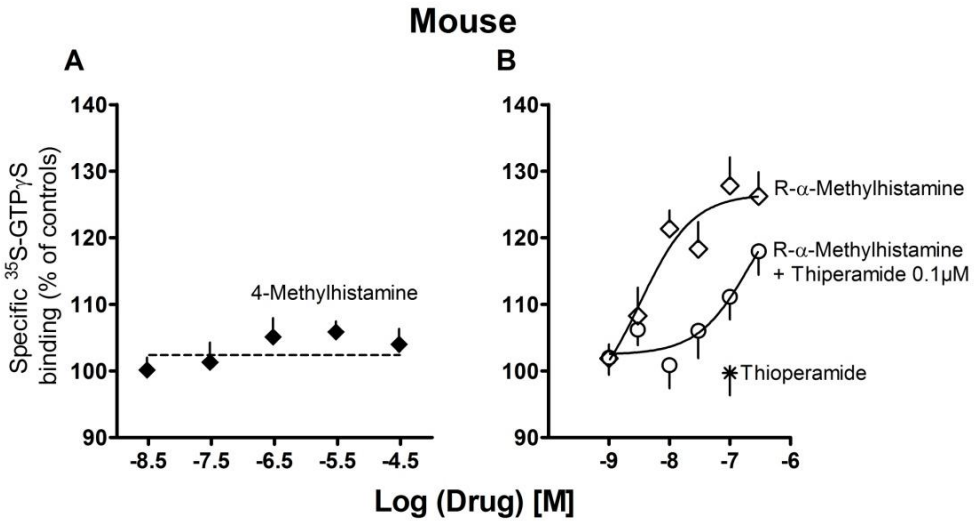

Figure 24. Effect of histamine H_4 (A) and H_3 (B) receptor ligands on the specific ^{35}S-GTPγS binding to C57BL/6J mouse cortex membranes. The effect of (A) the H_4 agonist 4-methylhistamine and (B) the H_3 agonist *R*-α-methylhistamine and the H_3 antagonist thioperamide (as positive control) were studied. The H_3 receptor ligands were given alone or combined. Means ± SEM of 3 - 6 experiments. Unspecific binding (in the presence of GTPγS 10 µM): 26.2± 2.8 (A) and 24.7 ± 0.7 (B).

The agonistic potency of R-α-methylhistamine (expressed as pEC_{50}) and the antagonistic potency of thioperamide (expressed as pA_2) are given in Table 19. The values for either ligand are virtually identical for guinea pig and mouse.

Ligand	Potency estimate	Guinea pig	Mouse (C57BL/6J)
R-α-methylhistamine	pEC_{50}	8.3	8.4
Thioperamide	pA_2	8.2	8.5

Table 19. Potencies of the H_3 receptor agonist R-α-methylhistamine and the H_3 receptor antagonist thioperamide in the ^{35}S-GTPγS binding assay in guinea pig and mouse hippocampal membranes. Values are based on the concentration-response curves in Figure 23B (guinea pig) and Figure 24B (mouse).

D. Discussion

1. Effects of Δ^9-THC on CB_1 receptors

The development of tolerance to 10 mg/kg Δ^9-THC was examined in two age groups of mice, adolescent and old, and the influence of aging on animal behaviour was compared with functional changes of CB_1 receptors in hippocampal membranes. Note that in this section the term "Δ^9-THC" corresponds to the dose of 10 mg/kg Δ^9-THC.

1.1 Behavioural test: Open Field Test

The analysis of behavioural tests is difficult because of the low reproducibility of the results between single experiments even in the same laboratory; comparisons between different laboratories are almost impossible. Numerous factors can affect the behaviour of an animal. Stress, which is strongly modulated by environmental factors, plays an indisputable role in behavioural experiments. Housing conditions, such as group or individual housing, long-term or short-term housing, the temperature, noise, light (Jähkel et al. 2000; Turner et al. 2005; Obernier and Baldwin 2006; Gonder and Laber 2007), human-animal interactions and pain have to be considered (Würbel 2002). All these exogenous factors as well as the individual health condition and individual activity of the mouse can affect the behaviour. In the Open Field Test procedure, each movement of the experimenter can increase the anxiety of the mice and thus influence their performance in the test.

1.1.1 General

The activity of Δ^9-THC was described in this thesis in section A.1. Briefly, Δ^9-THC interacts as a partial agonist with both cannabinoid receptors, CB_1 and CB_2, which are expressed in numerous tissues and organs in mammalian organisms. This interaction is responsible for the broad and complex effects of cannabinoids in animals and humans (Pertwee et al. 2010). Accordingly, a variety of models has been developed; moreover, the development of tolerance to Δ^9-THC was studied in rodents and other species as reviewed by González et al. (2005). The differential protocols to produce tolerance to Δ^9-THC provide numerous variables, which complicate the comparison of these studies and provide unclear and sometimes contradictory results. The ambiguity of the results can be related to the route of drug administration, the Δ^9-THC dose and the treatment duration. In addition, the tests used, the time between drug administration and

test conduction, experimental conditions, such as light, animal handling or acclimatization period and at last the way of data analysis influence the final results. These and other aspects will be discussed in this section.

The protocol used in this study to induce Δ^9-THC tolerance was based on that published by Bass and Martin (2000). They established the time course for the induction of Δ^9-THC tolerance in behavioural tests of antinociception (reduced pain sensitivity) and hypoactivity (suppression of spontaneous activity). Under numerous doses and treatment periods they tested, the regimen of seven single doses of 10 mg/kg Δ^9-THC twice a day (3.5 days of treatment) caused the strongest decrease in the potency of the challenge dose of 10 mg/kg Δ^9-THC in mice. In this thesis, I compared tolerance development between two age groups: adolescent (6 weeks) and old (12 months).

The main modifications adopted in our experiments, compared to the protocol of Bass and Martin (2000), are summarized in Table 20. Bass and Martin (2000) used ICR mice, as opposed to C57BL/6J mice used in this study. As reported in the literature (Hotchkiss et al. 2004; Daskalakis et al. 2014) differences in response between mouse strains are possible, however, the cited references correspond to different experimental parameters. The routes of administration of the drug or vehicle differed as well, as described in Table 20. To induce tolerance, Δ^9-THC was administered i.p. (Bass and Martin 2000: s.c.); the challenge dose of Δ^9-THC was again administered i.p. (Bass and Martin 2000: i.v.).

I.p. injections were chosen for the present experiments since they represent a common and quite simple laboratory technique of drug administration. However, a lower accuracy of administration may be associated with i.p. injections. The fluid may be erroneously injected into the urinary bladder, gastrointestinal tract or subcutaneously (Turner et al. 2011). Furthermore, after i.p. administration, a delay of the effect occurs, what I compensated for by a longer time interval between the injection of the Δ^9-THC challenge dose and the Open Field Test procedure (40 min after i.p. injection instead of 5 min after i.v. injection).

		Bass and Martin (2000)	This thesis
Mouse strain		ICR	C57BL/6J
Treatment groups		I. Chronic II. Acute III. Vehicle (control)	I. Chronic II. Acute III. Vehicle (control)
Age groups		No age groups	I. Adolescent (6 weeks) II. Old (12 months)
Induction of tolerance	**Dose of Δ⁹-THC**	10 mg/kg and other doses	(3 mg/kg, no effect) 10 mg/kg
	Route of administration	s.c.	i.p.
Challenge dose	**Dose of Δ⁹-THC**	10 mg/kg	10 mg/kg
	Route of administration	i.v. in the tail vain	i.p.
Time interval between Δ⁹-THC challenge dose and OFT		5 min	40 min
Behavioural test		Spontaneous activity in the Animal Activity Monitor	Distance travelled, rearing number and resting time in the Open Field Test using the ActiMot Software

Table 20. Differences between the protocols used by Bass and Martin (2000) and in this thesis. i.p. - intraperitoneal; i.v. - intravenous; s.c. – subcutaneous.

The way of analysis and presentation of the data is a key for understanding the changes between the tested groups. The "raw" data of the three parameters tested in the Open Field Test either represent activity of the mice (distance travelled and rearing behaviour) or suppression of the activity (resting time). To simplify the analysis and to standardize the data presentation, parameters were expressed as percentage values of activity suppression (% activity suppression; calculation method described in section B.2.2).

1.1.2 Comparison of adolescent and old mice

Three questions were considered. First, does aging influence the basal activity of the animals? The three parameters were affected differently (Figure 12). Although the rearing number (which is related to the exploratory behaviour of the mouse) decreased with age, the other parameters (distance travelled and resting time) did not show age-related differences. Second, does repeated administration of Δ^9-THC induce tolerance? Figure 13 shows that repeated injection of Δ^9-THC reduced the activity suppression elicited by a challenge dose of Δ^9-THC by ~ 20 – 50 %; the difference, however, reached significance for one of the 6 groups only, namely for the rearing number in the adolescent group. Third, is the development of tolerance age-dependent? A comparison of the three behavioural paradigms shows that the tolerance development does not show an age-dependent decline for the rearing number and the resting time (Figure 13, Table 15). With respect to the distance travelled, one might assume that the tolerance is marked in the adolescent but only slight in the old animals; however, the values are not significantly different.

Although greater behavioural effects were expected based on the data published by Bass and Martin (2000), the trends presented in the behavioural tests in this thesis confirm the current state of knowledge about the Δ^9-THC tolerance development.

1.2 Biochemical test: ^{35}S-GTPγS binding

1.2.1 General

An unspecific effect of WIN 55,212-2 on ^{35}S-GTPγS binding to hippocampal membranes from CB_1 knockout mice ($CB_1^{-/-}$) was shown by Breivogel et al. (2001). Moreover, such an unspecific effect was also found in other experimental methods (reviewed by Wiley and Martin 2002). Therefore, in this thesis, the effect of WIN 55,212-2 on ^{35}S-GTPγS binding was tested for CB_1 knockout ($CB_1^{-/-}$) and CB_1 and CB_2 receptor double knockout ($CB_1^{-/-}/CB_2^{-/-}$) mice. An identical unspecific binding was found in hippocampal membranes from both mice strains (Figure 15). Due to this finding, the cannabinoid receptor agonist CP 55,940, which by itself failed to activate ^{35}S-GTPγS binding on CB_1 knockout ($CB_1^{-/-}$) mice (Figure 16), was chosen as an appropriate agonist for further ^{35}S-GTPγS binding experiments.

1.2.2 Comparison of adolescent and old mice

In each ^{35}S-GTPγS binding experiment, the basal binding was measured in the absence of any exogenous agonist and for later data evaluation (the use of the basal binding values in data evaluation is described in section B.2.3.2; Equation 4 – 6). The basal binding value represents the activity of GPCRs expressed and acting spontaneously and/or interacting with their endogenous ligands in the tested tissue (here in the hippocampus), e.g. CB_1, opioid, dopamine or adenosine receptors (Marchese et al. 1999) and many more. The CB_1 receptors which are extremely highly expressed GPCRs in the CNS (Herkenham et al. 1991; Tsou et al. 1998) have a dominant impact on the basal binding value. As described in section B.2.3.2, the incubation of the hippocampus tissue homogenates with ADA serves to improve the basal binding signal through deactivation of the endogenously formed adenosine, thereby improving the detection of the agonist-induced CB_1 receptor binding.

As presented in Figure 17, the basal binding of vehicle treated adolescent mice was much higher than that of the vehicle treated old animals. As a matter of fact, the basal activity seems to decrease with age, e.g. due to a lower density and/or spontaneous activity of CB_1 receptors.

Basal binding was also influenced differently in hippocampal membranes from adolescent and aged mice by Δ^9-THC treatment. Although a down-regulation occurred in adolescent animals, no difference was obtained for aged mice. Those data may mean that the receptor density and/or spontaneous activity of CB_1 receptors is no longer susceptible to adaptive changes in aged animals.

The comparison of the CP 55,940-induced ^{35}S-GTPγS binding provided conclusions analogous to those reached for basal binding. As shown in Figure 18A, significant differences between the concentration-response curves occurred within the adolescent group. The hippocampal CB_1 receptor activity in adolescent animals pre-treated with Δ^9-THC was significantly decreased, compared to the age-matched vehicle treated controls (Figure 18A), indicating down-regulation of the CB_1 receptors through the long-term Δ^9-THC pre-treatment. On the other hand, as shown in Figure 18B, no differences in specific ^{35}S-GTPγS binding between treatments were observed within the old age group.

One finding, namely the decrease in basal ^{35}S-GTPγS binding after pre-treatment with Δ^9-THC in adolescent mice, has, to the best of my knowledge, not been reported previously and interferes with the interpretation of the data. Thus, one may argue that the decrease in the CP 55,940-induced ^{35}S-GTPγS binding after Δ^9-THC pre-treatment is solely due to the fact that basal binding

was lowered in parallel. To overcome this problem, additional experiments would be interesting in which an agonist facilitating ^{35}S-GTPγS binding via a non-CB_1 receptor is studied. If the maximum signal of such an agonist is unaffected by Δ^9-THC pre-treatment, this would lend further support to our view that CB_1 receptor activity and/or density is decreased. If, however, the maximum signal of the reference agonist is decreased as well, one has to be cautions with postulating a tolerance development of CB_1 receptors.

The question arises whether behavioural and binding data can be correlated. The age-related decline in rearing behaviour might be indeed correlated with the decrease in basal binding. On the other hand, the possibility has to be considered that the same direction of both parameters is an accidental event. Moreover, the other two behavioural paradigms (distance travelled; resting time) did not show an age-dependent alteration.

If one compares the CP 55,940-induced increase in ^{35}S-GTPγS binding and the alteration of behavioural parameters by a challenge dose of Δ^9-THC, the results are again only partially congruent. In adolescent animals, both binding and behaviour showed a tolerance after Δ^9-THC pre-treatment. If one, however, considers aged animals, behaviour shows tolerance development whereas binding fails to do so after repeated administration of Δ^9-THC. With respect to one behavioural parameter, distance travelled, the tolerance development in response to Δ^9-THC pre-treatment tended to be (but was not significantly) less marked in aged than in adolescent mice.

The discrepancy between behavioural effects and ^{35}S-GTPγS receptor binding could be among others due to the factors discussed in paragraph D.1.1 in this section. A longer treatment period should be chosen in the future to test if the behavioural tolerance increases with treatment duration. It would be interesting to investigate also other brain regions for ^{35}S-GTPγS receptor binding changes after Δ^9-THC chronic treatment. Furthermore, the investigation of additional age groups could provide more exact information with respect to the time-point at which receptor adaptation due to the Δ^9-THC chronic administration ceases to occur.

2. Effect of MAGL blockade on CB_1 receptors

CB_1 receptor have a protective effect against some age-dependent alterations in the brain (Albayram et al. 2011; 2012; Bilkei-Gorzo et al. 2012; Bilkei-Gorzo 2012) and the possibility has to be considered that drugs activating CB_1 receptors may be beneficial against the age-related decline in brain function. Although Δ^9-THC is not suited for this purpose due to its addictive properties, a compound like JZL 184, that inhibits the degradation of the endogenously formed cannabinoid 2-AG via MAGL, may be interesting and indeed beneficial effects of MAGL blockade have been shown in neurodegenerative diseases (Chen et al. 2012). The major challenge of such an approach is to find a treatment schedule under which endogenous 2-AG levels are increased but a concomitant down-regulation of CB_1 receptors is lacking (or weak). A high dose of JZL 184 (daily i.p. injections of 40 mg/kg over a time period of 6 days) indeed did not only increase 2-AG levels but also decreased the CB_1 receptor-mediated ^{35}S-GTPγS binding in the mouse brain (Schlosburg et al. 2010). In the present study, lower doses of JZL 184 than 40 mg/kg and an acute, subacute (3 days) and chronic (14 days) treatment schedule of this drug were examined (Table 21). This part of the study was restricted to adolescent mice since, as shown in the first part (C.1.2), CB_1 receptor-dependent alterations did not occur in binding studies on hippocampal membranes from aged animals.

For this purpose, endocannabinoid levels were determined in the hippocampi of the mice treated with JZL 184 using LC-MS/MS tandem mass spectrometry (LC-MRM). Furthermore, CP 55,940-stimulated ^{35}S-GTPγS binding was determined in the hippocampi of the treated mice to investigate the receptor activity changes caused by MAGL blockade. The CD-1 (and not the C57BL/6J) mouse strain was chosen. According to the mouse growth charts published on the website of the mouse provider company Charles Rivers (http://www.criver.com), the weight of the 6 week old male CD-1 mouse is 30 – 35 g whereas the age-matched C57BL/6J mouse weighs 20 – 25 g only. Since endocannabinoid level measurement and ^{35}S-GTPγS binding were conducted each on the opposite hippocampus hemispheres of the same mouse, extensive amounts of tissue were needed. The weight of the mouse and hence the expected larger brain size was crucial for planning of experiments. The CD-1 mouse strain with a higher body weight was therefore more appropriate for experiments with JZL 184.

	Schlosburg et al. (2010)	This thesis
Mouse strain	C57BL/6J	CD-1
JZL 184 dose i.p., once daily	40 mg/kg, vehicle	4 mg/kg, 10 mg/kg, 40 mg/kg, vehicle
JZL 184 treatment period	1 day (acute) or 6 days (chronic)	1 day (acute), 3 days (subacute) or 14 days (chronic)
Decapitation	2 h after last treatment	24 h after last treatment
Experimental methods	Endocannabinoid levels using LC-MS/MS CB_1 receptor function using ^{35}S-GTPγS binding and further *in vivo* and *in vitro* methods	Endocannabinoid levels using LC-MS/MS CB_1 receptor function using ^{35}S-GTPγS binding
Tissue used in experiments	Whole brain	Hippocampus hemispheres - right one in LC-MS/MS - left one in binding

Table 21. Procedural differences in the experimental models used by Schlosburg et al. (2010) and in this thesis.

2.1 Endocannabinoids determined by LC-MRM

As expected, the 2-AG, but not AEA concentration in mouse hippocampus increased with increasing JZL 184 treatment duration and with increasing JZL 184 dose (see Figure 20A and B). Moreover, the concentration of AA decreased with increasing JZL 184 dose. This alteration could be expected as well since AA is formed by the enzymatic reaction involved in 2-AG degradation (see section A.2.1.2, Figure 6).

Unlike in the study of Schlosburg et al. (2010) in which also a modest increase in AEA, the other major endocannabinoid, was shown after chronic JZL 184 treatment, even the highest JZL 184 dose (40 mg/kg) did not affect AEA in our experiments (Figure 20B). This discrepancy could be due to the time point of the measurement (2 h after injection in the study of Schlosburg et al. (2010) and 24 h after injection in this thesis). Indeed, the supplementary data of Schlosburg et

al. (2010) showed that 26 h after the final JZL 184 injection, the AEA level was no longer altered whereas the 2-AG level was still enhanced. Like in the study of Schlosburg et al. (2010), chronic treatment with 40 mg/kg JZL 184 elevated 2-AG concentration and decreased AA level in this thesis. The analysis of additional doses of JZL 184 and of various treatment periods showed that the lowest JZL 184 concentration, which effectively increased the 2-AG level, was 10 mg/kg (Figure 20A). After 3 days, an increasing trend after 10 mg/kg and a significant increase after 40 mg/kg JZL 184 occurred. JZL 184 at 4 mg/kg failed to affect the 2-AG level, irrespective of the duration of the treatment. However, surprisingly, the AA concentration was significantly decreased after chronic treatment with 4 mg/kg and not 10 mg/kg of JZL 184 (Figure 20C).

To sum up, in the LC-MRM experiments, the JZL 184 dose of 40 mg/kg effectively increased 2-AG at each time period, whereas 10 mg/kg of JZL 184 showed an increasing tendency in 2-AG level, which became significant only after 14 days.

2.2 CB_1 receptor activity determined by ^{35}S-GTPγS binding

Basal ^{35}S-GTPγS binding, which was decreased by repeated administration of Δ^9-THC (see C.1.2), remained unaffected after the increase in the endogenous level of 2-AG by JZL 184, irrespective of its dose and the treatment duration. This result is surprising since 2-AG is a full and Δ^9-THC a partial CB_1 receptor agonist (Pertwee et al. 2010). On the other hand, the data fit to the CP 55,940-induced facilitation of ^{35}S-GTPγS binding. Thus, no significant effects in ^{35}S-GTPγS receptor binding were observed here and the concentration-response curves of all treatments and doses did not differ significantly (curves for animals treated for 14 days are shown in Figure 21). The strongest treatment schedule, i.e., 40 mg/kg JZL 184 for 14 days, showed a decreasing trend in the 'cmp over basal' range of the concentration-response curve, compared to the lower JZL 184 doses and the vehicle treated control.

Schlosburg et al. (2010), who had treated mice with 40 mg/kg of JZL 184 for 6 days (Table 21), postulated a desensitization of the CB_1 receptor, although most of the ^{35}S-GTPγS receptor binding concentration-response curves only tended to be lower than the curves related to the vehicle-treated animals. However, comparison of the *Emax* (maximal effect) of the curves indeed showed a significant decrease of the binding after JZL 184 treatment. The autoradiography analysis confirmed this information. The lack of a significant effect in the present work in comparison with the ^{35}S-GTPγS receptor binding results on whole brain

homogenates published by Schlosburg et al. (2010) is surprising, especially due to the extremely high expression of the CB_1 receptor in the hippocampus.

In this context, two comments about the handling of the ^{35}S-GTPγS receptor binding data by Schlosburg et al. (2010) are necessary. In the work of Schlosburg et al. (2010) ^{35}S-GTPγS receptor binding was expressed as % stimulation of basal and not in absolute terms. If data are handled in such a manner, important information may be obscured. Second, they studied binding curves not only in JZL 184 (and vehicle) treated mice but also in mice chronically treated with the FAAH inhibitor PF3845 or its vehicle and in MAGL deficient mice ($MAGL^{-/-}$) compared to their wild type ($MAGL^{+/+}$) controls. Surprisingly, the maximal binding effect of the two vehicle treated controls and $MAGL^{+/+}$ mice showed different values of the % stimulation. The maximal effect was about 75 %, about 120 % and more than 150 %, respectively. Because of the large discrepancy between the three control groups, comparison of the three treatment schedules within the study of Schlosburg et al. (2010) and comparison between their and our results is questionable.

In summary, the CP 55,940-induced increase in ^{35}S-GTPγS binding upon repeated administration of 40 mg/kg JZL 184 underwent tolerance in the study by Schlosburg et al. (2010) but only tended to do so in the present one. Nonetheless, there is a common denominator of both studies, i.e., one can assume that the increased concentration of 2-AG is more or less cancelled out by a down-regulation of CB_1 receptor function or, in other words, this treatment schedule will not allow a long-term treatment e.g. of age-related cognitive deficits.

While our experiments were in progress, two papers appeared in which doses of JZL 184 lower than 40 mg/kg were examined. In the study of Kinsey et al. (2013) behavioural parameters (antinociceptive and gastroprotective effect), parameters of the CB_1 receptor function *in vitro* and the 2-AG level were considered (see Table 22 for a comparison of the methods used in the study of Kinsey et al. (2013) and for present thesis). Repeated administration of doses ≥ 16 mg/kg led to tolerance to the antinociceptive effects of JZL 184 and cross-tolerance to the effect of Δ^9-THC *in vivo* and to a decrease in density (determined by ^{3}H-SR141716A binding) and function of CB_1 receptors (determined by ^{35}S-GTPγS). On the other hand, JZL 184 doses ≤ 8 mg/kg retained their antinociceptive and gastroprotective effects after chronic MAGL blockade, without CB_1 receptor adaptation. Our finding that JZL 184 at a dose of 10 mg/kg enhances 2-AG and has no effect on ^{35}S-GTPγS receptor binding agrees with the results of Kinsey et al. (2013). On the other hand, although the MAGL inhibitor in our project was applied for 14 days (and not for 6 days as by Kinsey et al. 2013), the ^{35}S-GTPγS receptor binding concentration-response curves and maximal binding effects did not differ significantly

after JZL 184 at 40 mg/kg. Kinsey et al. (2013) stated that doses of JZL 184 ≤ 8 mg/kg caused beneficial effects whereas doses of ≥ 16 mg/kg caused tolerance-dependent effects. Unlike in this thesis, JZL 184 at 4 mg/kg significantly increased 2-AG levels in the study of Kinsey et al. (2013). This discrepancy may be due to the different time-point of mouse decapitation (2 h after the last injection by Kinsey et al. (2013) and 24 h after the last JZL 184 injection in this thesis). In this thesis JZL 184 at 10 mg/kg was considered to be the lowest effective dose causing 2-AG elevation without affecting CB_1 receptor function, even after 14 days of JZL 184 administration.

In the second study (Ghosh et al. 2013), behavioural experiments were performed only. JZL 184 reduces nociception in the carrageenan model of the mouse through a cannabinoid receptor mediated mechanism; the analgesic effect of JZL 184 undergoes tolerance after repetitive treatment with high doses (16 or 40 mg/kg) but not after a low dose (4 mg/kg). This data supports our findings that 10 mg/kg did not yet lead to tolerance development of ^{35}S-GTPγS binding.

To sum up, 10 mg/kg is an appropriate dose of JZL 184 which elevates 2-AG concentration without CB_1 receptor desensitisation after repetitive treatment (14 days). The doses between 10 mg/kg and 40 mg/kg should be further investigated to determine the highest possible dose of JZL 184 which increases 2-AG but does not affect CB_1 receptor function.

	Kinsey et al. (2013)	**This thesis**
Mouse strain	C57BL/6J	CD-1
JZL 184 treatment period	6 days	14 days
Decapitation	2 h after last injection	24 h after last injection
Experimental methods	Behavioural tests Endocannabinoid levels using LC-MS/MS ^{35}S-GTPγS receptor binding [^{3}H]SR141716A binding	Endocannabinoid levels using LC-MS/MS ^{35}S-GTPγS receptor binding
JZL 184 doses and alterations of ^{35}S-GTPγS receptor binding	≤ 8 mg/kg – no receptor alterations ≥ 16 mg/kg – significant decrease in receptor binding (no data for > 8 - 16 mg/kg)	4 mg/kg – no receptor alteration 10 mg/kg – no receptor alteration 40 mg/kg – tendency towards a decrease in receptor binding

Table 22. Differences in the experimental models used by Kinsey et al. (2013) and in this thesis.

3. Searching for H_4 receptors

3.1 Searching for mRNA expression: RT-PCR

H_4 receptors are primarily distributed in immune cells, e.g., mast cells, lymphocytes, eosinophils, NK cells (as reviewed by Tiligada et al. 2009). It is, however, also of interest to study whether they may occur in the brain. Although Liu et al. (2001) failed to detect histamine H_4 receptor mRNA in the brain of guinea pig and mouse, this thesis shows that H_4 receptor mRNA is detectable in the cerebral cortex of the guinea pig. Identification of H_4 receptor transcripts in the mouse cortex was shown before by our group (Schulte 2011). Although the findings made with the PCR method may seem meaningful, they must be discussed critically. Thus, H_4 receptor mRNA detection using the PCR method does not prove in which specific cell type the H_4 receptor occurs and the PCR signal may originate from immune cells in the brain. Other authors tried to detect the H_4 receptor on the protein level; Connelly et al. (2009) and Lethbridge and Chazot (2009) provided immunological evidence (immunoblotting) for the presence of H_4 receptors in the human and mouse brain. Nevertheless, also these results must be assessed critically since the H_4 receptor antibodies used in those studies did not fulfil the stringent criteria for antibodies against G protein-coupled receptors (Michel et al. 2009; Beermann et al. 2012; Seifert et al. 2013).

3.2 Searching for a functional readout: ^{35}S- GTPγS binding

Considering the PCR findings which pointed to the H_4 receptor presence in the brain and the problems encountered with H_4 receptor antibodies, we searched for H_4 receptors in the cerebral cortex of guinea pig and mouse in a functional model. For this purpose ^{35}S-GTPγS experiments with application of various histamine H_4 ligands (for chemical structures see Table 4) were performed. For the sake of comparison, H_3 receptor ligands were studied as well. The H_3 receptor ligands R-α-methylhistamine and thioperamide and the H_4 receptor ligands 4-methylhistamine, JNJ-7777120 and ST-1006 were investigated under the same experimental conditions on cortical membranes of two animal species, guinea pig and mouse. The ^{35}S-GTPγS binding assay was chosen since it allows the detection of many types of functional $G_{i/o}$ protein-coupled receptors (Strange 2010).

The H_4 receptor agonist, 4-methylhistamine (Lim et al. 2005), failed to enhance ^{35}S-GTPγS binding on cortical membranes from the mouse (up to 30 μM). By contrast, in guinea pig cortex, concentrations of 10 and 100 μM increased the specific ^{35}S-GTPγS binding. The activation of

^{35}S-GTPγS binding, however, occurred at concentrations markedly exceeding the K_i value of 50 nM of 4-methylhistamine at H_4 receptors (Lim et al. 2010). In order to provide further evidence, additional H_4 receptor ligands were studied. The H_4 receptor antagonist JNJ-7777120 (Jablonowski et al. 2003) at 1 µM (corresponding to its K_i value; Lim et al. 2010) failed to influence the ^{35}S-GTPγS binding, regardless of whether it was added to 4-methylhistamine or given alone. Moreover, the partial H_4 receptor agonist, ST-1006 (Sander et al. 2009), also failed to affect the ^{35}S-GTPγS specific binding in guinea pig cortex membranes even at 100 µM which is more than thousandfold higher than its K_i at human H_4 receptors. In conclusion, our data suggest that H_4 receptor activation does not lead to an increase in ^{35}S-GTPγS binding on guinea pig and mouse cortical membranes.

To confirm that proper experimental conditions were used in ^{35}S-GTPγS binding experiments with H_4 the receptor ligands, ^{35}S-GTPγS binding experiments with H_3 receptor ligands were conducted as positive control on cerebral cortex membranes from guinea pig and mouse. The H_3 receptor agonist, R-α-methylhistamine (Arrang et al. 1987), activated ^{35}S-GTPγS binding both in mouse and guinea pig cerebral cortex membranes. The binding experiments on mouse cerebral cortex membranes confirm the data previously published by our group (Nickel et al. 2001). Activation of ^{35}S-GTPγS binding by R-α-methylhistamine on guinea pig cortex is shown here for the first time. The addition of the H_3 receptor antagonist thioperamide (Arrang et al. 1987) caused a rightward shift of the concentration-response curve of R-α-methylhistamine, as expected. The potencies of R-α-methylhistamine and thioperamide (Table 19) are shown again in Table 23 together with values obtained in other functional H_3 receptor models of the same species.

Ligand	Potency estimate	Experimental model	Guinea pig	Mouse	
				NMRI	C57BL/6J
***Rα*MH**	pEC_{50}	^{35}S-GTPγS binding activation	8.3[1]	7.8[2]	8.4[1]
	pEC_{50}	Inhibition of noradrenaline release	7.8[3]	7.5[4]	ND
Thio-peramide	pA_2	^{35}S-GTPγS binding activation	8.2[1]	ND	8.5[1]
	pA_2	Inhibition of noradrenaline release	7.8[3]	8.7[4]	ND

Table 23. Potencies of the H_3 receptor agonist R-α-methylhistamine (*Rα*MH) and the H_3 receptor antagonist thioperamide for the activation of ^{35}S-GTPγS binding and the inhibition of noradrenaline release in guinea pig and mouse. Comparison of this study and the literature. C57BL/6J, NMRI – mouse strains; ND – not determined. [1] Figure 23B; [2] Nickel et al. (2001); [3] Timm et al. (1998); [4] Schlicker et al. (1992).

Considering the possibility that the H_4 like the H_3 receptor may serve as a presynaptic receptor leading to the inhibition of exocytotic noradrenaline release (Schlicker et al. 1994) superfusion experiments were performed on human, guinea pig and mouse cortex slices and the electrically induced ^{3}H-noradrenaline release was measured. In these experiments (data not shown), noradrenaline release was not affected by 4-methylhistamine although H_3 receptor-mediated inhibition of noradrenaline release occurred. The latter data are an additional argument that H_4 receptor do not occur in the brain.

E. Summary (Abstract)

This thesis focuses on two $G_{i/o}$ protein-coupled receptors, namely the cannabinoid CB_1 and the histamine H_4 receptor. In the first and second part of the study, the plasticity of CB_1 receptors in terms of age and of pre-treatment with an exogenous and endogenous cannabinoid was examined. In the third part, I searched for the occurrence of H_4 receptor mRNA and of functional H_4 receptors in the brain.

In the *first* project, CB_1 receptor plasticity was studied in the Open Field Test and in a biochemical paradigm (G protein activation quantified by the ^{35}S-GTPγS binding method) of adolescent (6-8 week-old) and aged (12-month-old) mice. Single administration of the exogenous cannabinoid Δ^9-tetrahydrocannabinol (Δ^9-THC) decreased the distance travelled and the rearing number and increased the resting time to about the same extent in adolescent and old animals. Pre-treatment of mice with Δ^9-THC (7 injections over a time period of 3.5 days) attenuated the effect of a challenge dose of Δ^9-THC by about 50 % in the rearing and resting time paradigm, independent of the age; with respect to the distance travelled, the attenuation of the effect tended to be slightly less pronounced in old when compared to adolescent mice. Basal ^{35}S-GTPγS binding was less pronounced in hippocampal membranes from aged when compared to adolescent mice. Δ^9-THC pre-treatment attenuated basal binding by about 50 % in membranes from adolescent but had no effect in membranes from old mice. The increase in ^{35}S-GTPγS binding elicited by the cannabinoid receptor agonist CP 55,940 was less marked in untreated old than in untreated adolescent mice. After pre-treatment with Δ^9-THC, the CP 55,940-related increase in ^{35}S-GTPγS binding was not affected in old but was reduced by about 50 % in adolescent mice. The results show that aging markedly affects basal and CP 55,940-induced ^{35}S-GTPγS binding and the tolerance development of both parameters to Δ^9-THC pre-treatment; in the behavioural paradigm, aging does not consistently influence tolerance development.

The *second* project was dedicated to the effect of an endogenous cannabinoid, i.e., 2-arachidonoyl glycerol (2-AG), on basal and CP 55,940-induced ^{35}S-GTPγS binding; formation of endogenous 2-AG was increased by blockade of its degrading enzyme by JZL 184. The question was whether a treatment schedule can be found under which 2-AG (determined by liquid chromatography tandem mass spectrometry) is increased but adaptive down-regulation of CP 55,940-induced ^{35}S-GTPγS binding is avoided. Adolescent mice were pre-treated with JZL 184 at 4, 10 or 40 mg/kg over a period of 14 days. JZL 184 at 4 mg/kg did not affect hippocampal 2-AG levels and the CP 55,940-induced ^{35}S-GTPγS binding in hippocampal membranes. The next higher dose (10 mg/kg) increased 2-AG without affecting

CP 55,940-induced ^{35}S-GTPγS binding. The highest dose (40 mg/kg) increased 2-AG but simultaneously also decreased the CP 55,940-induced ^{35}S-GTPγS binding. Basal ^{35}S-GTPγS binding was not affected by JZL 184 at 4 - 40 mg/kg. The data suggest that 10 mg/kg of JZL 184 when administered over a longer time period leads to a sustained increase in 2-AG. Since this dose does not cancel out the activation of CB_1 receptors by their simultaneous down-regulation, administration of JZL 184 10 mg/kg may be a strategy of long-term cannabinoid treatment.

The occurrence and role of the histamine H_4 as opposed to the CB_1 receptor in the brain is unclear. In the *third* project, I could show that H_4 receptor mRNA is detectable in the cerebral cortex of mice and guinea pigs, using the reverse transcriptase polymerase chain reaction. The search for a functional correlate was, however, negative; thus, I could not show a H_4 receptor-related facilitation of ^{35}S-GTPγS binding in cortical membranes of either species. As a positive control, histamine H_3 receptor activation did increase ^{35}S-GTPγS binding.

F. References

Ahn K, McKinney MK, Cravatt BF (2008) Enzymatic pathways that regulate endocannabinoid signaling in the nervous system. Chem Rev 108:1687–707.

Ahn K, Johnson DS, Mileni M, Beidler D, Long JZ, McKinney MK, Weerapana E, Sadagopan N, Liimatta M, Smith SE, Lazerwith S, Stiff C, Kamtekar S, Bhattacharya K, Zhang Y, Swaney S, Van Becelaere K, Stevens RC, Cravatt BF (2009) Discovery and characterization of a highly selective FAAH inhibitor that reduces inflammatory pain. Chem Biol 16:411–20.

Albayram Ö, Alferink J, Pitsch J, Piyanova A, Neitzert K, Poppensieker K, Mauer D, Michel K, Legler A, Becker A, Monory K, Lutz B, Zimmer A, Bilkei-Gorzo A (2011) Role of CB1 cannabinoid receptors on GABAergic neurons in brain aging. Proc Natl Acad Sci U S A 108:11256–61.

Albayram Ö, Bilkei-Gorzo A, Zimmer A (2012) Loss of CB1 receptors leads to differential age-related changes in reward-driven learning and memory. Front Aging Neurosci 4:34.

Alexander SPH, Benson HE, Faccenda E, Pawson AJ, Sharman JL, Spedding M, Peters JA, Harmar AJ (2013) The Concise Guide to PHARMACOLOGY 2013/14: G protein-coupled receptors. Br J Pharmacol 170:1459–581.

Andersen SL (2003) Trajectories of brain development: point of vulnerability or window of opportunity? Neurosci Biobehav Rev 27:3–18.

Arrang JM, Garbarg M, Schwartz J-C (1983) Auto-inhibition of brain histamine release mediated by a novel class (H3) of histamine receptor. Nature 302:832–7.

Arrang JM, Garbarg M, Lancelot JC, Lecomte JM, Pollard H, Robba M, Schunack W, Schwartz J-C (1987) Highly potent and selective ligands for histamine H3-receptors. Nature 327:117–23.

Arunlakshana O, Schild HO (1997) Some quantitative uses of drug antagonists. 1958. Br J Pharmacol 120:151–61; discussion 148–50.

Ashton JC, Friberg D, Darlington CL, Smith PF (2006) Expression of the cannabinoid CB2 receptor in the rat cerebellum: an immunohistochemical study. Neurosci Lett 396:113–6.

Aso E, Ferrer I (2014) Cannabinoids for treatment of Alzheimer's disease: moving toward the clinic. Front Pharmacol 5:37.

Atwood BK, Mackie K (2010) CB2: a cannabinoid receptor with an identity crisis. Br J Pharmacol 160:467–79.

Baek J-H, Darlington CL, Smith PF, Ashton JC (2013) Antibody testing for brain immunohistochemistry: brain immunolabeling for the cannabinoid CB_2 receptor. J Neurosci Methods 216:87–95.

Basavarajappa BS (2007) Critical enzymes involved in endocannabinoid metabolism. Protein Pept Lett 14:237–46.

Bass CE, Martin BR (2000) Time course for the induction and maintenance of tolerance to Delta(9)-tetrahydrocannabinol in mice. Drug Alcohol Depend 60:113–9.

Battista N, Di Tommaso M, Bari M, Maccarrone M (2012) The endocannabinoid system: an overview. Front Behav Neurosci 6:9.

Beermann S, Seifert R, Neumann D (2012) Commercially available antibodies against human and murine histamine H_4-receptor lack specificity. Naunyn Schmiedebergs Arch Pharmacol 385:125–35.

Belue RC, Howlett AC, Westlake TM, Hutchings DE (1995) The ontogeny of cannabinoid receptors in the brain of postnatal and aging rats. Neurotoxicol Teratol 17:25–30.

Bilkei-Gorzo A, Racz I, Valverde O, Otto M, Michel K, Sastre M, Sarstre M, Zimmer A (2005) Early age-related cognitive impairment in mice lacking cannabinoid CB1 receptors. Proc Natl Acad Sci U S A 102:15670–5.

Bilkei-Gorzo A (2012) The endocannabinoid system in normal and pathological brain ageing. Philos Trans R Soc Lond B Biol Sci 367:3326–41.

Bilkei-Gorzo A, Drews E, Albayram Ö, Piyanova A, Gaffal E, Tueting T, Michel K, Mauer D, Maier W, Zimmer A (2012) Early onset of aging-like changes is restricted to cognitive abilities and skin structure in $Cnr1^{-/-}$ mice. Neurobiol Aging 33:200.e11–e22.

Blankman JL, Simon GM, Cravatt BF (2007) A comprehensive profile of brain enzymes that hydrolyze the endocannabinoid 2-arachidonoylglycerol. Chem Biol 14:1347–56.

Bliss T V, Collingridge GL (1993) A synaptic model of memory: long-term potentiation in the hippocampus. Nature 361:31–9.

Bossong MG, Niesink RJM (2010) Adolescent brain maturation, the endogenous cannabinoid system and the neurobiology of cannabis-induced schizophrenia. Prog Neurobiol 92:370–85.

Boyce A, McArdle P (2008) Long-term effects of cannabis. Paediatr Child Health (Oxford) 18:37–41.

Bradford MM (1976) A rapid and sensitive method for the quantitation of microgram quantities of protein utilizing the principle of protein–dye binding. Anal Biochem 72:248–54.

Breivogel CS, Griffin G, Di Marzo V, Martin BR (2001) Evidence for a new G protein-coupled cannabinoid receptor in mouse brain. Mol Pharmacol 60:155–63.

Breivogel CS (2006) Cannabinoid receptor binding to membrane homogenates and cannabinoid-stimulated [35S]GTPgammaS binding to membrane homogenates or intact cultured cells. Methods Mol Med 123:149–62.

Centonze D, Finazzi-Agrò A, Bernardi G, Maccarrone M (2007) The endocannabinoid system in targeting inflammatory neurodegenerative diseases. Trends Pharmacol Sci 28:180–7.

Cha YM, White AM, Kuhn CM, Wilson W a, Swartzwelder HS (2006) Differential effects of delta9-THC on learning in adolescent and adult rats. Pharmacol Biochem Behav 83:448–55.

Chanda PK, Gao Y, Mark L, Btesh J, Strassle BW, Lu P, Piesla MJ, Zhang M-Y, Bingham B, Uveges A, Kowal D, Garbe D, Kouranova E V, Ring RH, Bates B, Pangalos MN, Kennedy JD, Whiteside GT, Samad TA (2010) Monoacylglycerol lipase activity is a critical modulator of the tone and integrity of the endocannabinoid system. Mol Pharmacol 78:996–1003.

Chaperon F, Thiébot MH (1999) Behavioral effects of cannabinoid agents in animals. Crit Rev Neurobiol 13:243–81.

Chen R, Zhang J, Wu Y, Wang D, Feng G, Tang Y, Teng Z (2012) Monoacylglycerol lipase is a therapeutic target for Alzheimer's disease. 1:1329–39.

Childers SR, Breivogel CS (1998) Cannabis and endogenous cannabinoid systems. Drug Alcohol Depend 51:173–87.

Childers SR (2006) Activation of G-proteins in brain by endogenous and exogenous cannabinoids. AAPS J 8:E112–7.

Choleris E, Thomas AW, Kavaliers M, Prato FS (2001) A detailed ethological analysis of the mouse open field test: effects of diazepam, chlordiazepoxide and an extremely low frequency pulsed magnetic field. Neurosci Biobehav Rev 25:235–60.

Compton SJ, Jones CG (1985) Mechanism of dye response and interference in the Bradford protein assay. Anal Biochem 151:369–74.

Connelly WM, Shenton FC, Lethbridge N, Leurs R, Waldvogel HJ, Faull RLM, Lees G, Chazot PL (2009) The histamine H4 receptor is functionally expressed on neurons in the mammalian CNS. Br J Pharmacol 157:55–63.

Cravatt BF, Demarest K, Patricelli MP, Bracey MH, Giang DK, Martin BR, Lichtman AH (2001) Supersensitivity to anandamide and enhanced endogenous cannabinoid signaling in mice lacking fatty acid amide hydrolase. Proc Natl Acad Sci U S A 98:9371–6.

Curtin F, Schulz P (1998) Multiple correlations and Bonferroni's correction. Biol Psychiatry 44:775–7.

D'Addario C, Micioni Di Bonaventura MV, Pucci M, Romano A, Gaetani S, Ciccocioppo R, Cifani C, Maccarrone M (2014) Endocannabinoid signaling and food addiction. Neurosci Biobehav Rev 47:203–24.

Daskalakis NP, Enthoven L, Schoonheere E, de Kloet ER, Oitzl MS (2014) Immediate effects of maternal deprivation on the (re)activity of the HPA-axis differ in CD1 and C57Bl/6J mouse pups. Front Endocrinol (Lausanne) 5:Article 190.

Dauvilliers Y, Bassetti C, Lammers GJ, Arnulf I, Mayer G, Rodenbeck A, Lehert P, Ding C-L, Lecomte J-M, Schwartz J-C (2013) Pitolisant versus placebo or modafinil in patients with narcolepsy: a double-blind, randomised trial. Lancet Neurol 12:1068–75.

Desmadryl G, Gaboyard-Niay S, Brugeaud A, Travo C, Broussy A, Saleur A, Dyhrfjeld-Johnsen J, Wersinger E, Chabbert C (2012) Histamine H4 receptor antagonists as potent modulators of mammalian vestibular primary neuron excitability. Br J Pharmacol 167:905–16.

Di Forti M, Morrison PD, Butt A, Murray RM (2007) Cannabis use and psychiatric and cogitive disorders: the chicken or the egg? Curr Opin Psychiatry 20:228–34.

Di Marzo V, Petrocellis DL (2006) Plant, synthetic, and endogenous cannabinoids in medicine. Annu Rev Med 57:553–74.

Di Marzo V, Bisogno T, De Petrocellis L (2007) Endocannabinoids and related compounds: walking back and forth between plant natural products and animal physiology. Chem Biol 14:741–56.

Di Marzo V (2009) The endocannabinoid system: its general strategy of action, tools for its pharmacological manipulation and potential therapeutic exploitation. Pharmacol Res 60:77–84.

Dinh TP, Freund TF, Piomelli D (2002) A role for monoglyceride lipase in 2-arachidonoylglycerol inactivation. Chem Phys Lipids 121:149–58.

Ehehalt R, Füllekrug J, Pohl J, Ring A, Herrmann T, Stremmel W (2006) Translocation of long chain fatty acids across the plasma membrane-lipid rafts and fatty acid transport proteins. Mol Cell Biochem 284:135–40.

Felder CC, Joyce KE, Briley EM, Mansouri J, Mackie K, Blond O, Lai Y, Ma AL, Mitchell RL (1995) Comparison of the pharmacology and signal transduction of the human cannabinoid CB1 and CB2 receptors. Mol Pharmacol 48:443–50.

Ferguson SS, Caron MG (1998) G protein-coupled receptor adaptation mechanisms. Semin Cell Dev Biol 9:119–27.

Fezza F, Bari M, Florio R, Talamonti E, Feole M, Maccarrone M (2014) Endocannabinoids, related compounds and their metabolic routes. Molecules 19:17078–106.

Filbey FM, Aslan S, Calhoun VD, Spence JS, Damaraju E, Caprihan A, Segall J (2014) Long-term effects of marijuana use on the brain. Proc Natl Acad Sci 111:16913–8.

Fowler CJ (2012) Monoacylglycerol lipase - a target for drug development? Br J Pharmacol 166:1568–85.

Fride E, Mechoulam R (1993) Pharmacological activity of the cannabinoid receptor agonist, anandamide, a brain constituent. Eur J Pharmacol 231:313–4.

Gao Y, Vasilyev D V, Goncalves MB, Howell F V, Hobbs C, Reisenberg M, Shen R, Zhang M-Y, Strassle BW, Lu P, Mark L, Piesla MJ, Deng K, Kouranova E V, Ring RH, Whiteside GT, Bates B, Walsh FS, Williams G et al. (2010) Loss of retrograde endocannabinoid signaling and reduced adult neurogenesis in diacylglycerol lipase knock-out mice. J Neurosci 30:2017–24.

Gemkow MJ, Davenport AJ, Harich S, Ellenbroek B a, Cesura A, Hallett D (2009) The histamine H3 receptor as a therapeutic drug target for CNS disorders. Drug Discov Today 14:509–15.

Ghosh S, Wise LE, Chen Y, Gujjar R, Mahadevan A, Cravatt BF, Lichtman AH (2013) The monoacylglycerol lipase inhibitor JZL184 suppresses inflammatory pain in the mouse carrageenan model. Life Sci 92:498–505.

Gonder JC, Laber K (2007) A renewed look at laboratory rodent housing and management. ILAR J 48:29–36.

Gong J-P, Onaivi ES, Ishiguro H, Liu Q-R, Tagliaferro P a, Brusco A, Uhl GR (2006) Cannabinoid CB2 receptors: immunohistochemical localization in rat brain. Brain Res 1071:10–23.

González S, Cebeira M, Fernández-Ruiz JJ (2005) Cannabinoid tolerance and dependence: a review of studies in laboratory animals. Pharmacol Biochem Behav 81:300–18.

Goparaju SK, Ueda N, Yamaguchi H, Yamamoto S (1998) Anandamide amidohydrolase reacting with 2-arachidonoylglycerol, another cannabinoid receptor ligand. FEBS Lett 422:69–73.

Goparaju SK, Ueda N, Taniguchi K, Yamamoto S (1999) Enzymes of porcine brain hydrolyzing 2-arachidonoylglycerol, an endogenous ligand of cannabinoid receptors. Biochem Pharmacol 57:417–23.

Greydanus DE, Hawver EK, Greydanus MM, Merrick J (2013) Marijuana: current concepts(†). Front Public Heal 1:42.

Griffin G, Atkinson PJ, Showalter VM, Martin BR, Abood ME (1998) Evaluation of cannabinoid receptor agonists and antagonists using the guanosine-5'-O-(3-[35S]thio)-triphosphate binding assay in rat cerebellar membranes. J Pharmacol Exp Ther 285:553–60.

Griffin G, Wray EJ, Tao Q, McAllister SD, Rorrer WK, Aung MM, Martin BR, Abood ME (1999) Evaluation of the cannabinoid CB2 receptor-selective antagonist, SR144528: further evidence for cannabinoid CB2 receptor absence in the rat central nervous system. Eur J Pharmacol 377:117–25.

Grotenhermen F, Müller-Vahl K (2012) The therapeutic potential of cannabis and cannabinoids. Dtsch Arztebl Int 109:495–501.

Haaksma EE, Leurs R, Timmerman H (1990) Histamine receptors: subclasses and specific ligands. Pharmacol Ther 47:73–104.

Haas HL, Sergeeva OA, Selbach O (2008) Histamine in the nervous system. Physiol Rev 88:1183–241.

Hall W, Degenhardt L (2009) Adverse health effects of non-medical cannabis use. Lancet 374:1383–91.

Hall W, Degenhardt L (2013) The adverse health effects of chronic cannabis use. Drug Test Anal 6:39–45.

Harkany T, Guzmán M, Galve-Roperh I, Berghuis P, Devi L a, Mackie K (2007) The emerging functions of endocannabinoid signaling during CNS development. Trends Pharmacol Sci 28:83–92.

Harrison C, Traynor JR (2003) The [35S]GTPγS binding assay: Approaches and applications in pharmacology. Life Sci 74:489–508.

Herkenham M, Lynn AB, Little MD, Johnson MR, Melvin LS, Costa BRDE (1990) Cannabinoid receptor localization in brain. Proc Natl Acad Sci U S A 87:1932–6.

Herkenham M, Lynn A, Johnson M, Melvin L, de Costa B, Rice K (1991) Characterization and localization of cannabinoid receptors in rat brain: a quantitative in vitro autoradiographic study. J Neurosci 11:563–83.

Hill MN, Froc DJ, Fox CJ, Gorzalka BB, Christie BR (2004) Prolonged cannabinoid treatment results in spatial working memory deficits and impaired long-term potentiation in the CA1 region of the hippocampus in vivo. Eur J Neurosci 20:859–63.

Hoffman AF, Oz M, Yang R, Lichtman AH, Lupica CR (2007) Opposing actions of chronic Delta9-tetrahydrocannabinol and cannabinoid antagonists on hippocampal long-term potentiation. Learn Mem 14:63–74.

Hollister LE (1986) Health aspects of cannabis. Pharmacol Rev 38:1–20.

Hotchkiss AK, Pyter LM, Neigh GN, Nelson RJ (2004) Nycthemeral differences in response to restraint stress in CD-1 and C57BL/6 mice. Physiol Behav 80:441–7.

Howlett AC, Barth F, Bonner TI (2002) International Union of Pharmacology. XXVII. Classification of cannabinoid receptors. Pharmacol Rev 54:161–202.

Howlett AC (2002) The cannabinoid receptors. Prostaglandins Other Lipid Mediat 68-69:619–31.

INCB (2013) International Narcotics Control Board - Yellow List - List of Narcotic Drugs under International Control.

Jablonowski JA, Grice CA, Chai W, Dvorak CA, Venable JD, Kwok AK, Ly KS, Wei J, Baker SM, Desai PJ, Jiang W, Wilson SJ, Thurmond RL, Karlsson L, Edwards JP, Lovenberg TW, Carruthers NI (2003) The first potent and selective non-imidazole human histamine H4 receptor antagonists. J Med Chem 46:3957–60.

Jähkel M, Rilke O, Koch R, Oehler J (2000) Open field locomotion and neurotransmission in mice evaluated by principal component factor analysis - Effects of housing condition, individual activity disposition and psychotropic drugs. Prog Neuro-Psychopharmacology Biol Psychiatry 24:61–84.

Kasteleijn-Nolst Trenité D, Parain D, Genton P, Masnou P, Schwartz J-C, Hirsch E (2013) Efficacy of the histamine 3 receptor (H3R) antagonist pitolisant (formerly known as tiprolisant; BF2.649) in epilepsy: dose-dependent effects in the human photosensitivity model. Epilepsy Behav 28:66–70.

Katz PS, Sulzer JK, Impastato RA, Teng SX, Rogers EK (2014) Endocannabinoid degradation inhibition improves neurobehavioral function, blood brain barrier integrity and neuroinflammation following mild traumatic brain injury. J Neurotrauma 1–38.

Kinsey SG, Long JZ, O'Neal ST, Abdullah RA, Poklis JL, Boger DL, Cravatt BF, Lichtman AH (2009) Blockade of endocannabinoid-degrading enzymes attenuates neuropathic pain. J Pharmacol Exp Ther 330:902–10.

Kinsey SG, Long JZ, Cravatt BF, Lichtman AH (2010) Fatty acid amide hydrolase and monoacylglycerol lipase inhibitors produce anti-allodynic effects in mice through distinct cannabinoid receptor mechanisms. J Pain 11:1420–8.

Kinsey SG, Wise LE, Ramesh D, Abdullah R, Selley DE, Cravatt BF, Lichtman AH (2013) Repeated low-dose administration of the monoacylglycerol lipase inhibitor JZL184 retains cannabinoid receptor type 1-mediated antinociceptive and gastroprotective effects. J Pharmacol Exp Ther 345:492–501.

Klein TW (2005) Cannabinoid-based drugs as anti-inflammatory therapeutics. Nat Rev Immunol 5:400–11.

Lazareno S (1999) Measurement of agonist-stimulated [35S]GTP gamma S binding to cell membranes. Methods Mol Biol 106:231–45.

Leslie CA, Robertson MW, Cutler AJ, Bennett JP (1991) Postnatal development of D 1 dopamine receptors in the medial prefrontal cortex, striatum and nucleus accumbens of normal and neonatal 6-hydroxydopamine treated rats: a quantitative autoradiographic analysis. Dev Brain Res 62:109–14.

Lethbridge N, Chazot PL (2009) Immunological identification of the mouse H4 histamine receptor on spinal cord motor neurons using a novel anti-mouse H4R antibody. Inflamm Res 59 (Suppl.:197–8.

Leurs R, Smit MJ, Timmerman H (1995) Molecular pharmacological aspects of histamine receptors. Pharmacol Ther 66:413–63.

Lichtman AH, Hawkins EG, Griffin G, Cravatt BF (2002) Pharmacological activity of fatty acid amides is regulated, but not mediated, by fatty acid amide hydrolase in vivo. J Pharmacol Exp Ther 302:73–9.

Lim HD, van Rijn RM, Ling P, Bakker R a, Thurmond RL, Leurs R (2005) Evaluation of histamine H1-, H2-, and H3-receptor ligands at the human histamine H4 receptor: identification of 4-methylhistamine as the first potent and selective H4 receptor agonist. J Pharmacol Exp Ther 314:1310–21.

Lim HD, de Graaf C, Jiang W, Sadek P, McGovern PM, Istyastono EP, Bakker R a, de Esch IJP, Thurmond RL, Leurs R (2010) Molecular determinants of ligand binding to H4R species variants. Mol Pharmacol 77:734–43.

Liu C, Wilson SJ, Kuei C, Lovenberg TW (2001) Comparison of human, mouse, rat, and guinea pig histamine H4 receptors reveals substantial pharmacological species variation. J Pharmacol Exp Ther 299:121–30.

Long JZ, Li W, Booker L, Burston JJ, Kinsey SG, Schlosburg JE, Pavón FJ, Serrano AM, Selley DE, Parsons LH, Lichtman AH, Cravatt BF (2009b) Selective blockade of 2-arachidonoylglycerol hydrolysis produces cannabinoid behavioral effects. Nat Chem Biol 5:37–44.

Long JZ, Nomura DK, Cravatt BF (2009a) Characterization of monoacylglycerol lipase inhibition reveals differences in central and peripheral endocannabinoid metabolism. Chem Biol 16:744–53.

Lubman DI, Cheetham A, Yücel M (2015) Cannabis and adolescent brain development. Pharmacol Ther 148:1–16.

Maccarrone M, Dainese E, Oddi S (2010) Intracellular trafficking of anandamide: new concepts for signaling. Trends Biochem Sci 35:601–8.

Makara JK, Mor M, Fegley D, Szabó SI, Kathuria S, Astarita G, Duranti A, Tontini A, Tarzia G, Rivara S, Freund TF, Piomelli D (2005) Selective inhibition of 2-AG hydrolysis enhances endocannabinoid signaling in hippocampus. Nat Neurosci 8:1139–41.

Malfitano AM, Basu S, Maresz K, Bifulco M, Dittel BN (2014) What we know and do not know about the cannabinoid receptor 2 (CB2). Semin Immunol 2:1–11.

Marchalant Y, Baranger K, Wenk GL, Khrestchatisky M, Rivera S (2012) Can the benefits of cannabinoid receptor stimulation on neuroinflammation, neurogenesis and memory during normal aging be useful in AD prevention? J Neuroinflammation 9:10.

Marchese A, George SR, Kolakowski LF, Lynch KR, O'Dowd BF (1999) Novel GPCRs and their endogenous ligands: expanding the boundaries of physiology and pharmacology. Trends Pharmacol Sci 20:370–5.

Marson CM (2011) Targeting the histamine H4 receptor. Chem Rev 111:7121–56.

Martin BR, Compton DR, Thomas BF, Prescott WR, Little PJ, Razdan RK, Johnson MR, Melvin LS, Mechoulam R, Ward SJ (1991) Behavioral, biochemical, and molecular modeling evaluations of cannabinoid analogs. Pharmacol Biochem Behav 40:471–8.

Martin BR, Sim-Selley LJ, Selley DE (2004) Signaling pathways involved in the development of cannabinoid tolerance. Trends Pharmacol Sci 25:325–30.

Matsuda L, Lolait SJ, Brownstein MJ, Young AC, Bonner TI (1990) Structure of a cannabinoid receptor and functional expression of the cloned cDNA. Nature 346:561–4.

McKinney DL, Cassidy MP, Collier LM, Martin BR, Wiley JL, Selley DE, Sim-Selley LJ (2008) Dose-related differences in the regional pattern of cannabinoid receptor adaptation and in vivo tolerance development to delta9-tetrahydrocannabinol. J Pharmacol Exp Ther 324:664–73.

Mechoulam R, Fride E, Di Marzo V (1998) Endocannabinoids. Eur J Pharmacol 359:1–18.

Mechoulam R, Parker LA (2013) The endocannabinoid system and the brain. Annu Rev Psychol 64:21–47.

Michel MC, Wieland T, Tsujimoto G (2009) How reliable are G-protein-coupled receptor antibodies? Naunyn Schmiedebergs Arch Pharmacol 379:385–8.

Min R, Di Marzo V, Mansvelder HD (2010) DAG lipase involvement in depolarization-induced suppression of inhibition: does endocannabinoid biosynthesis always meet the demand? Neuroscientist 16:608–13.

Moore NLT, Greenleaf ALR, Acheson SK, Wilson W a, Swartzwelder HS, Kuhn CM (2010) Role of cannabinoid receptor type 1 desensitization in greater tetrahydrocannabinol impairment of memory in adolescent rats. J Pharmacol Exp Ther 335:294–301.

Moore RJ, Xiao R, Sim-Selley LJ, Childers SR (2000) Agonist-stimulated [35S]GTPyS binding in brain - Modulation by endogenous adenosine. Neuropharmacology 39:282–9.

Mülhardt C (2003) Die Polymerase-Kettenreaktion, Der Experimentator: Molekularbiologie / Genomics, 4th edn. Spektrum Akademischer Verlag, Berlin

Mulvihill MM, Nomura DK (2013) Therapeutic potential of monoacylglycerol lipase inhibitors. Life Sci 92:492–7.

Munro S, Thomas K, Abu-Shaar M (1993) Molecular characterization of a peripheral receptor for cannabinoids. Nature 365:61–5.

Murataeva N, Straiker A, Mackie K (2014) Parsing the players: 2-arachidonoylglycerol synthesis and degradation in the CNS. Br J Pharmacol 171:1379–91.

Nickel T, Bauer U, Schlicker E, Kathmann M, Go M, Sasse A, Stark H, Schunack W (2001) Novel histamine H 3 -receptor antagonists and partial agonists with a non-aminergic structure. Br J Pharmacol 132:1665–72.

Obernier JA, Baldwin RL (2006) Establishing an appropriate period of acclimatization following transportation of laboratory animals. ILAR J 47:364–9.

Onaivi ES (2011) Commentary: Functional neuronal CB2 cannabinoid receptors in the CNS. Curr Neuropharmacol 9:205–8.

Onaivi ES, Ishiguro H, Gu S, Liu Q-R (2012) CNS effects of CB2 cannabinoid receptors: beyond neuro-immuno-cannabinoid activity. J Psychopharmacol 26:92–103.

Pan B, Wang W, Zhong P, Blankman JL, Cravatt BF, Liu Q (2011) Alterations of endocannabinoid signaling, synaptic plasticity, learning, and memory in monoacylglycerol lipase knock-out mice. J Neurosci 31:13420–30.

Parolaro D, Realini N, Viganò D, Guidali C, Rubino T (2010) The endocannabinoid system and psychiatric disorders. Exp Neurol 224:3–14.

Parsons ME, Ganellin CR (2006) Histamine and its receptors. Br J Pharmacol 147 Suppl:S127–35.

Pertwee RG, Ross RA (2002) Cannabinoid receptors and their ligands. Prostaglandins Leukot Essent Fatty Acids 66:101–21.

Pertwee RG, Howlett AC, Abood ME, Alexander SPH, Di Marzo V, Elphick MR, Greasley PJ, Hansen HS, Kunos G (2010) International Union of Basic and Clinical Pharmacology. LXXIX. Cannabinoid receptors and their ligands: Beyond CB1 and CB2. Pharmacol Rev 62:588–631.

Pertwee RG (2014) Elevating endocannabinoid levels: pharmacological strategies and potential therapeutic applications. Proc Nutr Soc 73:96–105.

Piomelli D (2003) The molecular logic of endocannabinoid signalling. Nat Rev Neurosci 4:873–84.

Prut L, Belzung C (2003) The open field as a paradigm to measure the effects of drugs on anxiety-like behaviors: a review. Eur J Pharmacol 463:3–33.

Ramesh D, Schlosburg JE, Wiebelhaus JM, Lichtman AH (2011) Marijuana dependence: not just smoke and mirrors. ILAR J 52:295–308.

Realini N, Rubino T, Parolaro D (2009) Neurobiological alterations at adult age triggered by adolescent exposure to cannabinoids. Pharmacol Res 60:132–8.

Renard J, Krebs M-O, Le Pen G, Jay TM (2014) Long-term consequences of adolescent cannabinoid exposure in adult psychopathology. Front Neurosci 8:361.

Rivera C, Voipio J, Payne JA, Ruusuvuori E, Lahtinen H, Lamsa K, Pirvola U, Saarma M, Kaila K (1999) The K+/Cl- co-transporter KCC2 renders GABA hyperpolarizing during neuronal maturation. Nature 397:251–5.

Robson PJ (2014) Therapeutic potential of cannabinoid medicines. Drug Test Anal 6:24–30.

Rodríguez de Fonseca F, Ramos JA, Bonnin A, Fernández-Ruiz JJ (1993) Presence of cannabinoid binding sites in the brain from early postnatal ages. Neuroreport 4:135–8.

Roth BL, Willins DL, Kroeze WK (1998) G protein-coupled receptor (GPCR) trafficking in the central nervous system: relevance for drugs of abuse. Drug Alcohol Depend 51:73–85.

Rubino T, Parolaro D (2008) Long lasting consequences of cannabis exposure in adolescence. Mol Cell Endocrinol 286:S108–13.

Rubino T, Realini N, Braida D, Guidi S, Capurro V, Viganò D, Guidali C, Pinter M, Sala M, Bartesaghi R, Parolaro D (2009) Changes in hippocampal morphology and neuroplasticity induced by adolescent THC treatment are associated with cognitive impairment in adulthood. Hippocampus 19:763–72.

Rubino T, Zamberletti E, Parolaro D (2012) Adolescent exposure to cannabis as a risk factor for psychiatric disorders. J Psychopharmacol 26:177–88.

Ryberg E, Larsson N, Sjögren S, Hjorth S, Hermansson N-O, Leonova J, Elebring T, Nilsson K, Drmota T, Greasley PJ (2007) The orphan receptor GPR55 is a novel cannabinoid receptor. Br J Pharmacol 152:1092–101.

Sánchez AJ, García-Merino A (2012) Neuroprotective agents: cannabinoids. Clin Immunol 142:57–67.

Sander K, Kottke T, Tanrikulu Y, Proschak E, Weizel L, Schneider EH, Seifert R, Schneider G, Stark H (2009) 2,4-Diaminopyrimidines as histamine H4 receptor ligands--Scaffold optimization and pharmacological characterization. Bioorg Med Chem 17:7186–96.

Sarne Y, Asaf F, Fishbein M, Gafni M, Keren O (2011) The dual neuroprotective-neurotoxic profile of cannabinoid drugs. Br J Pharmacol 163:1391–401.

Sawzdargo M, Nguyen T, Lee DK, Lynch KR, Cheng R, Heng HH, George SR, O'Dowd BF (1999) Identification and cloning of three novel human G protein-coupled receptor genes GPR52, PsiGPR53 and GPR55: GPR55 is extensively expressed in human brain. Brain Res Mol Brain Res 64:193–8.

Schlicker E, Behling A, Lümmen G, Göthert M (1992) Histamine H3 receptor-mediated inhibition of noradrenaline release in the mouse brain cortex. Naunyn Schmiedebergs Arch Pharmacol 345:489–93.

Schlicker E, Malinowska B, Kathmann M, Göthert M (1994) Modulation of neurotransmitter release via histamine H3 heteroreceptors. Fundam Clin Pharmacol 8:128–37.

Schlicker E, Kathmann M (2001) Modulation of transmitter release via presynaptic cannabinoid receptors. Trends Pharmacol Sci 22:565–72.

Schlosburg JE, Blankman JL, Long JZ, Nomura DK, Pan B, Kinsey SG, Nguyen PT, Ramesh D, Booker L, Burston JJ, Thomas E a, Selley DE, Sim-Selley LJ, Liu Q, Lichtman AH, Cravatt BF (2010) Chronic monoacylglycerol lipase blockade causes functional antagonism of the endocannabinoid system. Nat Neurosci 13:1113–9.

Schneider EH, Neumann D, Seifert R (2015) Histamine H4-receptor expression in the brain? Naunyn Schmiedebergs Arch Pharmacol 388:5–9.

Schramm-Sapyta NL, Cha YM, Chaudhry S, Wilson W a, Swartzwelder HS, Kuhn CM (2007) Differential anxiogenic, aversive, and locomotor effects of THC in adolescent and adult rats. Psychopharmacology (Berl) 191:867–77.

Schulte K (2011) Modulation der Neurotransmitterfreisetzung durch präsynaptische Cannabinoid-CB1-Rezeptoren und andere Rezeptoren. PhD Thesis. University of Bonn

Schwartz J-C (1975) Histamine as a transmitter in brain. Life Sci 17:503–17.

Schwartz J-C (2011) The histamine H3 receptor: from discovery to clinical trials with pitolisant. Br J Pharmacol 163:713–21.

Sciolino NR, Zhou W, Hohmann AG (2011) Enhancement of endocannabinoid signaling with JZL184, an inhibitor of the 2-arachidonoylglycerol hydrolyzing enzyme monoacylglycerol lipase, produces anxiolytic effects under conditions of high environmental aversiveness in rats. Pharmacol Res 64:226–34.

Seifert R, Strasser A, Schneider EH, Neumann D, Dove S, Buschauer A (2013) Molecular and cellular analysis of human histamine receptor subtypes. Trends Pharmacol Sci 34:33–58.

Silvestri C, Di Marzo V (2013) The endocannabinoid system in energy homeostasis and the etiopathology of metabolic disorders. Cell Metab 17:475–90.

Simons FER, Simons KJ (2011) Histamine and H1-antihistamines: celebrating a century of progress. J Allergy Clin Immunol 128:1139–50.e4.

Skosnik PD, Ranganathan M, D'Souza DC (2012) Cannabinoids, working memory, and schizophrenia. Biol Psychiatry 71:662–3.

Spear LP (2000) The adolescent brain and age-related behavioral manifestations. Neurosci Biobehav Rev 24:417–463.

Strakhova MI, Nikkel AL, Manelli AM, Hsieh GC, Esbenshade T a, Brioni JD, Bitner RS (2009) Localization of histamine H4 receptors in the central nervous system of human and rat. Brain Res 1250:41–8.

Strange PG (2010) Use of the GTPγS ([35S]GTPγS and Eu-GTPγS) binding assay for analysis of ligand potency and efficacy at G protein-coupled receptors. Br J Pharmacol 161:1238–49.

Sugiura T, Kobayashi Y, Oka S, Waku K (2002) Biosynthesis and degradation of anandamide and 2-arachidonoylglycerol and their possible physiological significance. Prostaglandins Leukot Essent Fatty Acids 66:173–92.

Sugiura T, Kishimoto S, Oka S, Gokoh M (2006) Biochemistry, pharmacology and physiology of 2-arachidonoylglycerol, an endogenous cannabinoid receptor ligand. Prog Lipid Res 45:405–46.

Svízenská I, Dubový P, Sulcová A (2008) Cannabinoid receptors 1 and 2 (CB1 and CB2), their distribution, ligands and functional involvement in nervous system structures--a short review. Pharmacol Biochem Behav 90:501–11.

Swartzwelder NA, Risher ML, Abdelwahab SH, D'Abo A, Rezvani AH, Levin ED, Wilson W a, Swartzwelder HS, Acheson SK (2012) Effects of ethanol, Δ(9)-tetrahydrocannabinol, or their combination on object recognition memory and object preference in adolescent and adult male rats. Neurosci Lett 527:11–5.

Szabo B, Schlicker E (2005) Effects of cannabinoids on neurotransmission. Handb Exp Pharmacol 327–65.

Tanimura A, Yamazaki M, Hashimotodani Y, Uchigashima M, Kawata S, Abe M, Kita Y, Hashimoto K, Shimizu T, Watanabe M, Sakimura K, Kano M (2010) The endocannabinoid 2-arachidonoylglycerol produced by diacylglycerol lipase alpha mediates retrograde suppression of synaptic transmission. Neuron 65:320–7.

Tchantchou F, Tucker LB, Fu AH, Bluett RJ, McCabe JT, Patel S, Zhang Y (2014) The fatty acid amide hydrolase inhibitor PF-3845 promotes neuronal survival, attenuates inflammation and improves functional recovery in mice with traumatic brain injury. Neuropharmacology 85:427–39.

Teicher MH, Andersen SL, Hostetter JC (1995) Evidence for dopamine receptor pruning between adolescence and adulthood in striatum but not nucleus accumbens. Dev Brain Res 89:167–72.

Tiligada E, Zampeli E, Sander K, Stark H (2009) Histamine H3 and H4 receptors as novel drug targets. Expert Opin Investig Drugs 18:1519–31.

Timm J, Marr I, Werthwein S, Elz S, Schunack W, Schlicker E (1998) H2 receptor-mediated facilitation and H3 receptor-mediated inhibition of noradrenaline release in the guinea-pig brain. Naunyn Schmiedebergs Arch Pharmacol 357:232–9.

Trezza V, Cuomo V, Vanderschuren LJMJ (2008) Cannabis and the developing brain: insights from behavior. Eur J Pharmacol 585:441–52.

Tsao P, von Zastrow M (2000) Downregulation of G protein-coupled receptors. Curr Opin Neurobiol 10:365–69.

Tsou K, Brown S, Sañudo-Peña M., Mackie K, Walker J. (1998) Immunohistochemical distribution of cannabinoid CB1 receptors in the rat central nervous system. Neuroscience 83:393–411.

Turner JG, Parrish JL, Hughes LF, Toth LA, Caspary DM (2005) Hearing in laboratory animals: strain differences and nonauditory effects of noise. Comp Med 55:12–23.

Turner P V, Brabb T, Pekow C, Vasbinder MA (2011) Administration of substances to laboratory animals: routes of administration and factors to consider. J Am Assoc Lab Anim Sci 50:600–13.

Ueda N, Tsuboi K, Uyama T (2010) N-acylethanolamine metabolism with special reference to N-acylethanolamine-hydrolyzing acid amidase (NAAA). Prog Lipid Res 49:299–315.

Ulugöl A (2014) The endocannabinoid system as a potential therapeutic target for pain modulation. Balkan Med J 31:115–20.

Verdurand M, Nguyen V, Stark D, Zahra D, Gregoire M-C, Greguric I, Zavitsanou K (2011) Comparison of cannabinoid CB(1) receptor binding in adolescent and adult rats: A positron emission tomography study using [F]MK-9470. Int J Mol Imaging 2011:548123.

Vermersch P (2011) Sativex(®) (tetrahydrocannabinol + cannabidiol), an endocannabinoid system modulator: basic features and main clinical data. Expert Rev Neurother 11:15–9.

Vogeser M, Schelling G (2007) Pitfalls in measuring the endocannabinoid 2-arachidonoyl glycerol in biological samples. Clin Chem Lab Med 45:1023–5.

Vogeser M, Seger C (2010) Pitfalls associated with the use of liquid chromatography-tandem mass spectrometry in the clinical laboratory. Clin Chem 56:1234–44.

Volkow ND, Baler RD, Compton WM, Weiss SRB (2014) Adverse health effects of marijuana use. N Engl J Med 370:2219–27.

Walsh RN, Cummins RA (1976) The Open-Field Test: a critical review. Psychol Bull 83:482–504.

Walter M, Kottke T, Stark H (2011) The histamine H_4 receptor: targeting inflammatory disorders. Eur J Pharmacol 668:1–5.

Wang J, Ueda N (2009) Biology of endocannabinoid synthesis system. Prostaglandins Other Lipid Mediat 89:112–9.

Wenzel D, Matthey M, Bindila L, Lerner R, Lutz B, Zimmer A, Fleischmann BK (2013) Endocannabinoid anandamide mediates hypoxic pulmonary vasoconstriction. Proc Natl Acad Sci U S A 110:18710–5.

Wiley J, Martin BR (2003) Cannabinoid pharmacological properties common to other centrally acting drugs. Eur J Pharmacol 471:185–93.

Wiley JL, Martin BR (2002) Cannabinoid pharmacology: implications for additional cannabinoid receptor subtypes. Chem Phys Lipids 121:57–63.

Würbel H (2002) Behavioral phenotyping enhanced--beyond (environmental) standardization. Genes Brain Behav 1:3–8.

Zanettini C, Panlilio L V, Alicki M, Goldberg SR, Haller J, Yasar S (2011) Effects of endocannabinoid system modulation on cognitive and emotional behavior. Front Behav Neurosci 5:57.

Zhang M, Venable JD, Thurmond RL (2006) The histamine H4 receptor in autoimmune disease. Expert Opin Investig Drugs 15:1443–52.

Zhuang S, Kittler J, Grigorenko E V, Kirby MT, Sim LJ, Hampson RE, Childers SR, Deadwyler SA (1998) Effects of long-term exposure to delta9-THC on expression of cannabinoid receptor (CB1) mRNA in different rat brain regions. Brain Res Mol Brain Res 62:141–9.

G. Publications and Conference Abstracts

Publications

Feliszek M, Speckmann V, Schacht D, von Lehe M, Stark H, Schlicker E (2015) A search for functional histamine H_4 receptors in the human, guinea pig and mouse brain. *Naunyn-Schmiedeberg´s Arch Pharmacol* 388: 11-17

Conference Abstracts

Feliszek M, Bilkei-Gorzo A, Schlicker E (2014) Does aging influence the tolerance development after chronic Δ^9- tetrahydrocannabinol treatment in mice? *Naunyn-Schmiedeberg´s Arch Pharmacol* 387 (Suppl 1): 39. Deutsche Gesellschaft für experimentelle und klinische Pharmakologie und Toxikologie (DGPT), 80. Jahrestagung, Hannover - Poster

Feliszek M, Bilkei-Gorzo A (2014) Does aging influence the tolerance development after chronic Δ^9- tetrahydrocannabinol treatment in mice? - Cannabinoid Workshop: The Endocannabinoid System: from Physiology to Pathophysiology, Life & Brain Center, Bonn – Talk

Feliszek M (2013) Effect of Δ^9-tetrahydrocannabinol treatment on CB_1 receptor-mediated [^{35}S]GTPγS binding in young adult and aged mice. 4th THEME Annual Symposium – Talk

Ilayan E, Feliszek M, Schlicker E (2013) Do cannabinoids exhibit a tyramine-like effect? *Naunyn-Schmiedeberg´s Arch Pharmacol* 386 (Suppl 1): 21. DGPT, 79. Jahrestagung, Halle – Poster

Feliszek M, Schlicker E (2012) The [^{35}S]GTPγS binding method as a powerful instrument to quantify genetic and drug-induced alterations of cannabinoid receptors. Man & Environment - Societas Humboldiana Polonorum, Krakow, Poland – Poster

Feliszek M, Schacht D, Schulte K, Jergas B, von Lehe M, Schlicker E (2012) Do histamine H_2 and H_4 receptors affect noradrenaline release in the human cerebral cortex? *Naunyn-Schmiedeberg´s Arch Pharmacol* 385 (Suppl 1):25. DGPT, 78. Jahrestagung, Dresden – Poster